



PETRECON AUSTRALIA PTY. LTD.

Petroleum Exploration Consultants

499001

11 Midland Highway
Brighton, Tasmania 7030
Australia

Phone: 61 (0) 02 68 1222
Fax: 61 (0) 02 68 1349

CONFIDENTIAL

ASSESSMENT
OF THE
RECOVERABLE GAS RESERVES
BASS BASIN
TASMANIA

J.K. Davidson
April 1991

TPR
OR-399

CONTENTS

	Page
SUMMARY	1
INTRODUCTION	1
GEOLOGICAL CONTROLS OF GAS ACCUMULATIONS IN BASS BASIN	2
YOLLA-1 GAS/CONDENSATE/OIL	4
Structure	5
Source/Seal	7
Reservoir	8
Gas/Water Contacts	9
Porosity and Water Saturation	11
Gas Expansion Factor	11
In-Place Gas Reserves	11
Reservoir Fluids & Recovery Factor	13
Conclusions	13
PIPIPA	13
DUROON AREA	16
IBIS	17
PELICAN AREA	17
CORMORANT-1	18
OTHER	18
CONCLUSIONS	18
REFERENCES	20

FIGURES

1. Bass Basin / Gas Assessment - Gas, Condensate, Oil Shows & Tests
2. No. of Wells drilled per year
3. Bass Basin / Gas Assessment - Major Structural Trends
4. Bass Basin - NE-SW Cross Section
- 4a. Stratigraphic Column
5. Bass Basin / Gas Assessment - Post Eastern View Isopach
6. Bass Basin / Gas Assessment - Upper Eastern View Isopach (Mid *M.diversus* to Low *N.asperus*)
7. Bass Basin / Gas Assessment - Lower Eastern View ("Pelican Zone") Isopach (Upp. *L.balmei* to Low *M.diversus*)
8. Top EVCM: Time Structure
9. Yolla - Structure Map (Lower *M.diversus* marker)
10. Top Palaeocene: Time Structure
11. Top Palaeocene: Time Structure
- 11a. Top EVCM: Time Structure (transparency overlay)
- 11b. Structure Map (lower *M. Diversus* Marker) (transparency overlay)
12. Base Map
- 12a. Top Palaeocene: Time Structure (transparency overlay)
13. Core Lab Preliminary – Compositional Analysis
14. Section of Log - 2600 to 3100
15. Yolla #1 RFT Pressures
16. Yolla Pressure Data – *L.balmei* Gas Zones
17. Yolla Pressure Data – *L.balmei* Gas Zones – Probability 100%
18. Yolla Pressure Data – *L.balmei* Gas Zones – Probability 90%
19. Yolla #1 RFT Pressures
20. Yolla Pressure Data – *L.balmei* Gas Zones – Probability 60%
21. Yolla Pressure Data – *L.balmei* Gas Zones – Probability 15%
22. Yolla Pressure Data – *L.balmei* Gas Zones – Probability 1%
23. Yolla #1 – Results Summary
24. Yolla #1 – Reservoir Sand
25. Yolla #1 – Reservoir Sand 1
26. Yolla #1 – Reservoir Sand 2a
27. Yolla #1 – Reservoir Sand 2b

FIGURES (cont.)

28. Yolla #1 – Reservoir Sand 2c
29. Yolla #1 – Reservoir Sand 2 other
30. Yolla #1 – Reservoir Sand 3
31. Yolla #1 – Reservoir Sand 3 other
32. Yolla #1 – Reservoir Sand 4a
33. Yolla #1 – Reservoir Sand 4b
34. Yolla #1 – Reservoir Sand 4c
35. Yolla #1 – Reservoir Sand 4 other
36. Reservoir Sand – Probability Master
37. Reservoir Sand – Probability 100%
38. Reservoir Sand – Probability 90%
39. Reservoir Sand – Probability 60%
40. Reservoir Sand – Probability 15%
41. Missing
42. Yolla – Probability of Gas In-Place
43. Yolla #1 – DST Summary
44. Well Stream Gas
45. Yolla – Probability of Recoverable Sales Gas
46. T-22-P Block / Pipipa Deep Prospect - Top Seismic Amplitude Anomaly-Depth Structure
47. Section of Log – 2250 to 3000
48. Seismic Section – Amplitude Anomaly
49. Seismic Section – Top of Gas sand
50. Seismic Section – Top of High Velocity Intrusion
51. Pipipa – Probability of Recoverable Sales Gas
52. Seismic Section – Durroon#1
53. Seismic Section – Phase Change
54. Seismic Section – Horizontal Terminations/ Dipping Multiple Interference
55. Seismic Section – Top Eastern View Group (M.diversus unconformity)
56. Durroon – Probability of Recoverable Sales Gas
57. Ibis #1 - Base Upper M.diversus – Top Upper L.balmei
58. Location of Bass 3 & Proposed Ibis 1
59. Location of Bass 3 & Proposed Ibis 1
60. Bass Basin – Probability of Recoverable Sales Gas

SUMMARY

This assessment concentrates on the *L. balmei* (2700m-3030m) zone in Yolla-1 in which probabilities of 100%, 50% and 1% are assigned to recoverable sales gas reserves of 250 BCF, 660 BCF and 2.35 TCF respectively. Other units in the basin are highlighted but not treated as rigorously due to the more subjective assumptions associated with undiscovered accumulations. The Pipipa and Durroon areas have been assigned 0, 360 BCF, 2.4 TCF and 0, 210 BCF and 4 TCF to the above probabilities, respectively.

Initial encouragement at Pelican-Cormorant spurred the early seventies drilling "boom", which finally lost momentum in 1982 (Pipipa-1). The lack of commercial oil at Yolla resulted in an abrupt end to the Yolla led "mini boom". It is apparent that if oil alone was the only prize in Bass Basin, there would probably be no more drilling. Yet, if there was a gas market, considerable quantities of gas and liquids would be produced over decades of intermittent drilling for gas/condensate reservoirs.

INTRODUCTION

In March 1991, the Tasmanian Development Authority (TDA) requested an assessment of the potentially commercial gas reserves of Bass Basin as part of their study of the possible use of gas as both a future electricity generator and industrial/domestic fuel.

A reserves estimate has been undertaken by Sagasco (Stock, 1989) as part of a strategy to develop the Yolla-1 discovery as a source of gas and liquids for Tasmania. The general thrust of the Sagasco paper was for conversion of the Bell Bay oil-fired electricity generating station from a peak generator to base-load, gas-fired, and for an increasing northern Tasmanian industrial gas usage. Sagasco suggested a reserve of 285 petajoules (approximately 270 billion cubic of gas (BCFG)). The Bureau of Mineral Resources (BMR) (Morrison, *et. al.*, 1989) undertook a study of the Yolla petroleum reserves and concluded deliverable sales gas reserves of 213 BCFG comprising proven and probable (88 BCFG), possible (210 BCFG) and "hypothetical" (2.7 BCFG).

This paper again addresses the Yolla gas reserves and adds an estimate of potentially recoverable, as yet

undiscovered, gas reserves in other parts of the basin. Substantial hydrocarbon liquids are present in the basin, but, for the purpose of this report, have been ignored.

Petrecon has a long history of exploration in Bass Basin and has drawn on the experience so gained to undertake this assessment. The exploration data file at the Tasmanian Division of Mines and Mineral Resources was made available, and Mr. Peter Baillie extended every support in making all relevant data available. The writer was also brought up to date on the exploration currently being undertaken by Bridge in the southeastern part of the basin (T15P). This was kindly done by Mr Keith Skipper in early April at the APEA Conference in Melbourne. Immediately after the Conference, Richard Suttill of Sagasco, in Adelaide, reviewed the most recent work undertaken by Sagasco on T14 and 18P.

The Yolla section of this report follows the format of the BMR report (Morrison, *et. al.*, 1989). Indeed, some of the reservoir engineering tables and diagrams have been copied directly from that report and Amoco's Drill Stem Test (DST) report (Amoco, February 1986). This was done due to Petrecon's April time constraint for completion of this report and Petrecon apologises for parts of the presentation. However, the report is as rigorous as the data allow and adds further geological data to the above two reports.

Apart from Yolla, there are other potential gas/condensate fields in Bass Basin some of which lie in operating permits and some in areas which are about to be granted. In both cases confidential data have been generated and were made available to Petrecon. Substantial undiscovered potential exists in these areas. Thus this report is confidential.

The report, by its very nature, is technical and would be difficult for an educated layman to totally digest. However, some explanation which a geologist or reservoir engineer might find trivial, is included.

GEOLOGICAL CONTROLS OF GAS ACCUMULATIONS IN BASS BASIN

Bass Basin is a northwest trending structural depression (Figure 1) formed in the Jurassic about 150 million years ago (my), contemporaneously with the Gippsland and Otway Basins, as Antarctica rotated from Australia (Davidson, 1980).

Sedimentation has continued to the Recent where the current bathymetric depression (80m) is still receiving sediment.

The basin is in excess of 14km deep making it considerably deeper than the prolific oil and gas producing Gippsland Basin on the northeastern side of the Flinders Island basement high. The greater thinning of the Earth's crust under Bass explains the more extensive, continuous and intense volcanism. Twenty-seven wells have been drilled in the basin (Figures 1 & 2). These wells have established a major period of volcanic activity in the Late Cretaceous/earliest Paleocene (100 to 60 my) whereas, in Gippsland, this was the time of source rock accumulation. Bass is a much less prolific oil source but a substantial gas/condensate source.

Figure 3 shows the major basin and structure-forming faults. Although the northwest trends of many of these faults parallels the basin margin defined by the edge of the reservoir/source Eastern View Group, there is a significant northerly cross-trend which has not only controlled local features like Yolla, but also major segments of the basin which exhibit differing periods of sedimentation. These segments also offer differing potential for gas accumulation.

Figure 4 is a 1982 cross-section which illustrates the basin geometry. The youngest event, the post Eastern View (44 to 0 my.; the Torquay and Demons Bluff units of Figure 4a) has a simple geometry which is translated to a basinal depression on the isopach (thickness) map of this unit (Figure 5). All wells have penetrated this shaley and volcanic unit. The unit is basically a seal but a fault breached this section at Yolla and allowed the passage of oil and gas into porous volcanics.

The Upper Eastern View (52-44 my) is a less simple depression with Figure 6 showing the closing stages of the Pelican-Cormorant Trough. The sediments in the trough, although immature, generated small quantities of oil at Cormorant and significant oil at Yolla.

The Lower Eastern View Isopach (Figure 7) shows the dominance of the Pelican-Cormorant Trough at this time (60-52 my). No oil has been recovered from this unit but significant quantities of gas/condensate were expelled, probably mainly in the last 5 to 10 million years. Although several wells, both within the trough and on its margins, have encountered gas/condensate, the real extent of the shows and the

prospectivity of this unit comprises barely a quarter of the basin area.

The Lower Eastern View includes two major zones. The upper is the "Pelican Zone" (54-52 my and comprises the palynological zones Lower *M. diversus* to the lowest part of the Middle *M. diversus*) and the lower could be referred to as the "Yolla Zone" (60-54 my, and comprises the palynological zone Upper *L. balmei*). Both units are self-sourcing and reservoiring. Below the *L. balmei*, the basal Tertiary (65-60 my) becomes increasingly volcanic with both basalt flows and volcanically derived sandstones (Figure 4a).

Few wells have penetrated the pre-Tertiary (65 my), Cretaceous section. The evidence from the Pelican, Koorkah and Yolla areas is one of tight, generally volcanic sandstones, more widespread and probably thicker than the above Lower Tertiary part of the Eastern View. The Pelican-Cormorant Trough was not the only major depression, with the Upper Cretaceous preserved. In the Durroon area to the southeast is a thick Cretaceous section within an area of minimal post-Cretaceous subsidence. In fact, this area is the only one where the Lower Cretaceous (135-100 my) Otway Group has been penetrated and where the earliest rocks in the basin, the Jurassic, can at least be seen seismically. The oil potential of the Lower Cretaceous, hence of the Durroon area, is low, but Petrecon thinks the dominantly non-marine section which contains substantial amounts of organic matter should have generated quite significant volumes of gas. Trapping the gas is the problem.

YOLLA-1 GAS/CONDENSATE/OIL

Amoco as Operator, and SAOG (now Sagasco), farmed into the T14P permit, held by a group of small explorers, in 1984 and the Yolla discovery was made in June 1985. Oil and gas/condensate was production tested at the top of the Eastern View Group and gas/condensate was similarly tested within the Lower Eastern View, *L. balmei*.

It is misleading to quote a reserve of gas as a single number. Many variables are not known precisely so it is more accurate to present a range of reserves, each with an assigned probability. For example, the BMR (Morrison, *et. al.*, 1989) reported deliverable sales gas at Yolla as 88 BCFG proven and

probable, 210 BCFG possible and 2.7 BCFG "hypothetical". These data might be interpreted as:

Probability	Reserve
100%	30 BCFG
50%	88 BCFG
1%	210 BCFG

(The 2.7 BCFG "hypothetical" is included in the event the upper, Top Eastern View zone, was produced). This report includes a graph of probability versus reserve and thus offers a full range of reserve probabilities, from which drilling/investment decisions can be assigned a chance of success.

There are three basic requirements for calculating a gas reserve: (a) gross gas-bearing rock volume; (b) nett gas reservoir and (c) the recoverable proportion. Thus:

$$\text{Volume} = (\text{Area} \times \text{Reservoir Thickness}) \times \text{(a)}$$

$$(\text{Porosity} \times \text{Hydrocarbon Saturation}) \times \text{(Recovery Factor)}$$

(b) (c)

$$\text{or } V = A.h (1-S_w) E.R$$

Structure

In determining the area of reservoirs, a map is required of the structure. Amoco has produced three maps. The shallowest is at the Top of the Eastern View Coal Measures (Figure 8). The map is contoured in seismic two-way travel time. Yolla-1 intersected this horizon at 1490 milliseconds (msec) which is approximately 1835m drill-depth (1835 mKB). This map is quite accurate and shows Yolla to be a triangular block formed by the intersection of two sets of north and northwest trending faults. The closing contour, or spill point of the structure, is at 1520 msec or approximately 1860 mKB. Later compressional wrench movement on the north trending fault has created two smaller, separate culminations, north of the well location.

The Lower *M. diversus* map (Figure 9) shows the area and form of the structure at the closing contour to be quite different from the Figure 8. This problem has no doubt arisen because the *M. diversus* event is notoriously difficult to pick on seismic and, in the Yolla area, is made even more difficult because of an igneous intrusion. The map is almost certainly incorrect and it was an error by the BMR to use this map in reserve calculations.

Figure 10 is the time structure map at the top of the Paleocene, i.e., the top of the *L. balmei* gas/condensate bearing interval. It was incorrect of the BMR to dismiss this map as being on "basement". Presumably it was thought that the volcanics immediately below the reservoir constituted basement and this map was on that unit. The volcanics are not basement and they are well below the top Paleocene. The closing contour on the map is 2180 msec. If a line is drawn on the 2230 msec contour, the feature is more regular. It is then surrounded by a number of countoured "lows" at approximately 2240 msec and the structure appears more strongly controlled by the faults which form it. In selecting 2230 msec, the only contours being "ignored" are in the far north and south of the structure and in areas under volcanics where mapping is difficult.

Again, the Paleocene structure is triangular, formed by the intersection of north and northwest trending faults. The similarity of the structural geometry is better illustrated by Figure 11 in which Figure 8 is overlain on Figure 10. The reason for the area of closure being less on the overlay is that the gentle post-Eastern View dip into the basin (Figure 5) caused the structure to tilt and thus lose dip (and closure) to the northeast. The compatibility of the two structure maps, together with the known accuracy of the Top EVCM map, means the deeper map is quite accurate. Similarly, the overlay of Figure 9 on Figure 11 demonstrates the incompatibility, hence inaccuracy, of the *M. diversus* mapping.

Before forming Petrecon, the writer used to take structural geology courses for Exxon which included field trips to the Sierra Diablo Mountain region of West Texas. The geological map of the mountain (Figure 12) shows a large, triangular topographic high bounded by north and northwest trending normal faults. If Figure 10 is overlain on Figure 12, the similarity is quite apparent. Although the Yolla map is about half the scale of the Sierra Diablo map, the parallels are clear to relatively fine points of detail, e.g.,

the normal faults have tapped the upper mantle and formed the Black Mountain volcanic neck in the far northwest of Figure 12 and on the overlay. On the overlay, Bass-1, located a large volcanic pile, demonstrates the same activity.

Source and Seal

The main source of the gas/condensate in the *L. balmei* is almost certainly the same unit as it is underlain by volcanics. The effects of the carbonate charged waters, often associated with volcanics, is probably evidenced in the unusual quantity of carbon dioxide in the gas (19%; Figure 13 from Amoco after Core Lab 1986). On the other hand, it is highly unlikely any carbon dioxide would have been present in the Upper Eastern View oil source. This unit is known to source only oil at Cormorant. Therefore, the 7.5% carbon dioxide in the gas condensate is clear evidence of mixing of the two source units, i.e., the *L. balmei*, yellow, carbon dioxide rich gas/condensate, has and is, passing upwards and mixing with with Upper Eastern View crude which in turn is escaping into the post-Eastern View volcanics. It is little wonder that the sophisticated liquid analysis reported by Baillie (1987) concluded the sources to be "similar", the "deeper sample... indicating a higher maturity level". Had the analysis included the carbon dioxide content, it is doubtful the word "similar" would have been attached to the sources. The gases are from very different sources but are similar in their current reservoirs due to mixing.

The sealing capacity of the thick marine to marginal marine shales over each of the deeper gas/condensate reservoirs, and over the upper reservoir, are not in question. However, the effectiveness of the seal is only partial due to fault movement. Not only have the faults been extensional and acted as conduits for hydrocarbons, but also for upper mantle fluids (!); as evidenced by the Bass-1/Black Mountain example in Figure 12 and the "area of thick Miocene volcanics" on Figure 10. As mentioned above, the faults have been conduits for igneous activity on several occasions. The northwest extensional faults have moved intermittently and leaked and so have the northerly set. This is most unusual as their last movement was wrenched and should have been dominantly compressional under northwesterly directed compression (see inset on Figure 8 from Davidson, *et. al.*, 1984).

There can be little argument that the faults do not seal. If they did, Yolla would have been a 30 to 50 million

barrel oilfield, producing today. Thus in calculating the area of the reservoir, fault sealing effects are so local that they can be ignored and the structural contours are the reservoir area determinents.

Reservoir

The BMR identified eight potential reservoirs within the *L. balmei* between 2700m and 3000m and these are labelled 1, 2a,b,c, 3 & 4a,b,c on the left hand side under the gamma ray curve on Figure 14. It was zones 2b & c which produced 15.1 million cubic feet of gas per day (MCFGPD) over a 23 foot interval with the remarkably high permeability of 308 millidarcies (md). It has been the general experience in Bass Basin that around 3000m it is very difficult to encounter such high production rates; a few 10's of md's is the norm. It is the environment of deposition of the sands that holds the key to this. The gamma ray curve indicates coarsening upwards sandstones, typical of a near-shore/beach environment. Beach sands are well sorted and cleaned by wave action as opposed to non-marine sands deposited in a delta plain environment, as is typical for most of Bass Basin. Also, beach sands form very extensive reservoirs and would probably be present, more or less as at Yolla-1, over the entire structure.

Marine sand units can be correlated using the electrical resistivity of the intervening shales. The shales deposited during a single depositional cycle will tend to be of a similar composition, as will the interstitial water. Even if not similar, a trend in the variation will be apparent. As an example, the reservoirs 4a, b and c are contained in a "shale resistivity package" which falls from left at 2890m to right at 3033m as shown by the black bar to the right of the depth-line (Figure 14). This unit is referred to as Zone 4. The figure also shows a brief but marked departure over Zone 3 and over the whole of Zones 1 and 2 (i.e., BMR sands 1, 2a, b and c) which form a single zone.

The recognition of these depositional units is most important because it shows that reservoir sands 1 to 2c are in pressure communication over a high column of 160m which is sealed by a thick shale (2650-2702m). Therefore all sands, although inferior to 2b and 2c can contribute to production, i.e., probably anything in the dotted area can produce. Similarly, Zone 4 is part of a 143m column which means the sands between 4a and c, and also below 4c, can also contribute

to production. Zone 3 is of less importance but adds significantly to reserve calculations.

Gas/Water Contacts

As important as reservoir thickness and structure are, the largest variable is the location of gas/water contacts (GWC's). It is imperative that geological sense be made of the pressure data provided by (a) pre-production test, wireline, repeat formation test data (RFT's) and (b) from production tests (drill-stem tests, DST's).

There are two problems with interpretation of the RFT pressure data (Figure 15); (1) the tool can read to 4 pounds per square inch (psi) in 10,000 psi and yet two measurements at essentially the same depth (1832.5 and 1833m) have a difference of 30 psi and (2), there is no water-bearing sand within Zones 1 to 4 from which a water gradient can be calculated.

Figure 16 is the depth versus pressure plot taken from the BMR report (Morrison, *et. al.*, 1989). The reservoir sands are shown on the right and can be related to the pressure zones. Zone 4 traces the gas pressure gradient of sands 4a, b and c. It is based on fair to good pressure data, and agrees with the sedimentary sequences, Zone 4, on Figure 14. Maybe the gas gradient should be less than the 0.34 psi/ft shown, as the RFT at 2988m recovered a much lower proportion of condensate than that from 2b and 2c, also attributed the same gradient. Zone 3 is based on one point but is clearly isolated from the other zones. The BMR has separated Zones 1 and 2 based on the relative departure of the pressure at 2724m to the left. Given the variability of the data, even with the two points which define Zone 2, it seems far more likely the two zones are one as determined on Figure 14.

Amoco calculated an average water gradient of 0.45 psi/ft for the entire well. A gradient of 0.433 psi/ft (sea water) was transposed as 1.42 psi/m by the BMR onto Figure 16 (solid water gradient line). Since extrapolation of the four gas zone pressure gradients to the water gradient line caused intersection below mapped *M. diversus* (Figure 9) closure, the water gradient was dismissed and moved to a point of origin equivalent to 83.5m above mean sea level. There is absolutely no reason for doing this except that it gave a better fit for the data at the Upper Eastern View oil zone. There is likewise no reason to expect the water pressure gradient to be

constant throughout the well when water salinities vary. In fact the value of 0.433 psi/ft, which is normal 35,000 ppm NaCl brine, is ideal through the gas-bearing zone.

Figure 17 is identical to Figure 16 except that the water gradients have been removed and Zones 1 and 2 combined. From the log analysis (Figure 14) it is known that only gas sands exist between 2700 and 3030m. Therefore the water below Zone 4 can not be shallower than 3030m and not shallower than 2860m below Zones 1 and 2. Hence the three GWC's shown on Figure 17 must be proven, i.e., at the 100% probability level.

Figure 18 shows a gradient of 0.444 psi/ft "pegged" still at the Zone 4, 100% probability, GWC of 3030m. This is quite pessimistic as it generates a gradient equivalent to 70,000 ppm NaCl in these near-shore sediments which, basin-wide are generally in the range 10-20,000 ppm NaCl equivalent. These lower salinities in the nearshore might be the case at Yolla as the upper, more marine units were 30,000 ppm NaCl at 1830-35 mKB, the only water sampled by DST in the well. The calculated GWC's for Zones 1 and 2, and 3 must therefore be conservative and a 90% probability has been assigned.

The best way to approach a reasonable water gradient in the gas zone is to use the water-wet reservoir pressure data immediately above the zone. Amoco plotted these five points which are shown as Figure 19. A line of "best fit" through the data generates a gradient of 0.4275 psi/ft. That gradient might be tending to the lighter end of actuality but is reasonable given two points depart by 10 to 15 psi. A pressure of 4000 psi is equivalent to a depth of 2775m and this has been transposed to Figure 20. To keep the generated GWC's conservatively shallow, the 0.4275 psi/ft gradient was extrapolated to depth. The three GWC's generated have a probability of 60%, being a little more probable than most likely.

It is possible the two lower water points on Figure 19 are also inaccurate and the Amoco water gradient extrapolated from above 6500ft has validity. Taking the conservative intercept at 4000 psi of 2820m and transposing to Figure 21 as in Figure 20, and using a normal brine salinity, gives three much deeper GWC's (2972, 3020 and 3126m) which have been assigned a 15% probability.

The same procedure using the 2864m intercept on Figure 19 generates Figure 22 which gives the deepest GWC's at the

lowest probability of 1%. (As unlikely as this possibility is, it may not be a coincidence that the 3030m GWC for Zones 1 and 2 fills the structure to the maximum spill point).

Porosity and Water Saturation

Log-interpretted sandstone porosities and water saturations were calculated by both Amoco and the BMR (Figure 23). Comparison of the two data sets indicates no significant differences and the BMR data are used in this report.

It is interesting to note that sands with porosities of 14-15% have water saturations of approximately 33% which validates Petrecon's assertion that with such long hydrocarbon columns, such sands could be anticipated to contribute to production.

The similarity of the data sets also supports the BMR's choice of nett reservoir thicknesses.

Gas Expansion Factor

On producing gas, it will expand depending on the depth and temperature of the reservoir and the composition of the gas. The gas expansion factor E, is determined by the equation:

$$E = 35.37P/(ZT)$$

where:

P = average reservoir pressure

Z = gas deviation factor

T = reservoir temperature

The BMR calculated values of E varying from 237 in reservoir unit 1 to 248 in reservoir unit 4c.

In-Place Gas Reserves

To assist in the understanding of the calculation of in-place gas reserves when multiple sands constitute a single pressure zone, a graph which plots structure area (area of the reservoir) versus depth was constructed (Figure 24). Yolla-1 was drilled at a position equivalent to 2075 msec on the Top Paleocene *L. balmei* structure map. As this is essentially the crest of the structure at this horizon, the top of Zones 1 and 2 can be placed at this point using the well log (right side

of the figure). The area at this point is zero. The area at any depth can then be planimeted off the structure map to form the graph. The area at the mapped closing contour of 2180 msec is 40 sq.km., while the maximum possible area of closure at 2230 msec is 96 sq.km.

The GWC's calculated at the various probabilities for reservoir sand, in Figures 16 to 22 can be plotted on Figure 24 as Figure 25. The base of Zone 1 and 2 at 2860m is the shallowest possible GWC (100% probability) at which depth reservoir unit 1 has an area of approximately 20 sq.km., an area of 27 sq.km. at GWC 2890 (90% probability) and so on, out to the maximum possible area of 96sq.km at the deepest GWC of approximately 3030m.

By moving the GWC upwards a distance equal to the separation of reservoir sands 1 and 2a, a similar depth versus area map is constructed for each GWC for reservoir sand 2a (Figure 26). This process is repeated for reservoir sands 2b and 2c. The effect is to graphically demonstrate that for each GWC the area of gas-filled sand decreases with depth when the sands are in pressure communication.

There are some sands below 2c which could contribute to reserves and they have been plotted as Figure 29. The above process was repeated for Zones 3 and 4 and are presented as Figures 30 through 35.

The BMR calculated in-place reserves and the resulting table has been rearranged and presented in this report as Figure 36. Figure 37 shows the in-place reserves for all reservoir units with a probability of 100%. (The tight timing of this report did not allow for the latter to be typed. Actually, the hand written numbers serve to indicate that the main difference between this report and the BMR's is in the area of each reservoir unit and the addition of three groups of "other", lower porosity (15%) reservoir sands). The same process was repeated for the other probability categories and presented as Figures 38 through 41.

Figure 42 is a probability versus gas reserve graph which was derived from Figures 37 through 41. Figure 42 has to be reduced by the amounts of carbon dioxide, hydrocarbon liquids, and adjusted for a recovery factor.

Reservoir Fluids and Recovery Factor

Figure 43 is taken from the Yolla-1 well completion report and records the basic physical data derived from the DST's. The BMR has tabulated the physical and chemical properties of the well-stream gas derived during the flow of DST-1. From this table (Figure 44), it can be seen in calculating sales gas proportions of the well-stream gas, 18.9% and 10.4% must be subtracted for carbon dioxide and hydrocarbon liquids, respectively.

The recovery factor RF, for a water-drive gas reservoir can be calculated from:

$$RF = \frac{VSE \text{ Sgr } E_a - E_a(1-VSE)}{(1-S_{wi})E_i \quad E_i}$$

where VSE = volumetric sweep efficiency

Sgr = residual gas saturation

S_{wi} = initial water saturation

E_i = initial gas expansion factor

E_a = abandonment gas expansion factor

The BMR calculated RF to be 85%.

Taking 60% of Figure 42 (71.5% for carbon dioxide and liquid hydrocarbons multiplied by 85% for recovery factor), a graph of recoverable gas reserves has been constructed (Figure 45).

Conclusions

A second well on the Yolla structure some 3km to the northwest of Yolla-1 would have the potential to lift proven reserves into the 600 BCF - 1 TCF range at probabilities of 60% to 20%.

PIPIPA

Sagasco has undertaken a major mapping and seismic modelling study in the Pipipa area of the previous T22P licence. As this area is about to be gazetted, Sagasco's study, which although circulated widely within the industry, was subject to a letter of confidentiality, and should be treated in this report as confidential.

Pipipa-1 was drilled by BHP in 1982 and was terminated in the *M. diversus* above the Middle *M. diversus* - Lower *M. diversus* "Pelican Zone". Shows were encountered over a few hundred metres prior to total depth. Indications of liquids were good due to the presence of C_6 in the drill cuttings/mud.

Sagasco has mapped an horizon (Figure 46) which ties to the top of the "F" sand in Pelican-5 (Figure 47). The seismic event was noted to have a high amplitude reflector at this level, which became more pronounced when the line was reprocessed by Shell (Figure 48). Indeed, not only was the amplitude increased, but a seismic flat spot was noted at 2000 msec (centred on shot point 700) and which could be interpreted as a fluid contact within the "F" sand. A small gas saturation is required to generate a velocity gradient associated with such events which are often found to be a GWC; in this case, possibly a rich-condensate/water contact or condensate/oil contact.

Sagasco modelled the same section of the line and again produced a flat spot (Figure 49). The right hand side of the flat spot shows signs of a weak diffraction pattern generated by a point source at the extremity of the gas filled sand. A very pronounced diffraction pattern was formed (Figure 50) when the opposite model was undertaken i.e., a high velocity igneous rock was inserted instead of the low velocity gas sand. So there must be a caution about elevating the seismic indicators of gas to the "certain" category. Note also that the high amplitude event at 1500 msec (1.5 seconds) at shot point 900 on Figure 48 diminishes abruptly at shot point 715 to the right, and yet there was no gas-sand in Pipipa-1 at this level.

A table which assigns a range of possibilities to various reserve categories is presented overleaf. These data are presented on a graph of probability versus recoverable sales gas (Figure 51). Note that the curve is similar in upside potential to Yolla (Figure 45) but lacks the "shoulder" at 100% created by the confirmation of gas. A 50% probability has been assigned to the validity of the seismic indications of gas over the area of 28 sq.km. The structure is normal fault bounded and thus requires a shale seal across the 100msec (approx. 180m) fault. Figure 47 indicates there is a 200m shale section above the "F" sand which probably would form the seal. Seal probability is assigned 80%, which means an overall chance of 40% (50% x 80%) of 490BCF recoverable.

PROBABILITY (%)	AREA (SQ. KM.)	RESERVOIR THICKNESS	POROSITY (%)	HYDROCARBON SATURATION (1-Sw)	GAS EXPANSION	GAS IN-PLACE (BCM)	CO ₂ (%)	RECOVERABLE GAS (85%) (BCF)
100	-	-	-	-	-	-	-	-
40	28	20	18	75	240	18.14	10%	490
10	28	30	21	85	240	35.98	5%	1026
1	42	45	21	85	240	80.97	0	2429

If the sand quality improves markedly toward the basin margin, the chances of fault seal similarly decrease. This is reflected in the 10% chance for the thicker, higher porosity case. The "H" Sand, if present, could be in pressure communication with the "F" sand and this would represent the upside potential at 1% chance. Carbon dioxide could be sourced from deeper in the section as volcanically derived sands were present in the *L. balmei* and Upper Cretaceous at Pelican-5.

Sagasco has mapped a larger feature north-northwest and adjacent to Pipipa but a seismic gas indicator has not been recognised. While this makes further discoveries on-trend with Pipipa less likely, it adds validity to the seismic indicators on the Pipipa structure.

DURROON

Durroon-1 is the only well in the southeastern part of the basin (Figure 1) and was a grossly invalid structural test being at least 200 msec off-structure (Figure 52). Durroon-1 was located on an old basin forming horst block under extensional conditions from the Jurassic to Early Cretaceous but was subjected to periods of wrench-induced compression intermittently from mid Late Cretaceous (Davidson *et. al.*, 1986). The compression of the thick section on the right of Figure 52 has uplifted the prospective Late Cretaceous section considerably. This is the source unit in Gippsland and the Durroon Mudstone has yielded good hydrocarbon source characteristics. Also, the higher amplitude Late Cretaceous events down-dip from Durroon might well be coal and source-prone for gas, at least.

Bridge has not completed mapping in this area (T15P) and to date has recognised four large northerly plunging noses between the major faults shown on Figure 3. Figure 53 displays a typical seismic line down a plunging nose. There are two critical factors which this line illustrates:

- (a) there is a normal fault which affords a break in the plunge and hence a possibility of creating a cross-trend with a fault throwing to the south (right).
- (b) there are indications of seismic events which might suggest the occurrence of gas. Possible gas indicators of "flat spots" and "phase changes" are, in each case,

related to a small normal fault block which might form a closed structure. Similar relationships are shown on a much larger feature (Figure 54). The termination of events possibly caused by a horizontal GWC cutting several reservoir units (like in Zones 1 and 2 or 4 at Yolla) are distinguishable from the dipping multiples generated off high velocity contrasting units higher in the section. The horizontal terminations can be compared with those on Figure 55 which shows similar events at the *L. balmei* level (2100 msec) on a 1982 seismic line and which was confirmed by drilling in 1985 (Yolla-1).

Without mapping the structurally complex Durroon area and looking very carefully for indications of hydrocarbons on the numerous seismic lines, it is not possible to reasonably quantify the potentially recoverable gas reserves. However, the similarity in seismic signature with Yolla must indicate an upside at least as high as Yolla and, given the much greater area for potential structures, Petrecon suggests an upside potential approximately twice that of Yolla (Figure 56).

The Durroon area data are confidential to Bridge.

IBIS

Ibis is a prospect on the Bass-3 block in T18P which has been proposed by Sagasco. Bass-3 recovered a very liquid-rich condensate from a thin, 2m, *L. balmei*, "Yolla Zone" sand (Figure 57). Figure 58 is a map at the Top Eastern and shows a proposed location for Ibis in the central part of a simple, Bass-3 structure. The fault on the southwest side has had late movement up to the Torquay Group volcanics, as at Yolla, and leakage could explain the lack of shows at this top porosity level. At the *L. balmei* level, Figure 59, the structure actually divides and Ibis is a small feature, four or five times larger than Bass-3, at 4.5 sq.km. Applying a 20m sand with good porosity and water saturations generates an upside in-place reserve of 100BCF. In relation to Yolla, Pipipa and the Durroon area, this volume is insignificant and a probability graph has not been constructed.

PELICAN

Pelican-5 tested 5.5 MCFGPD and 400 BCPD from 2786-2790m while only testing 0.43 MCFGPD from only 350m deeper (3143-

3162.5m). This demonstrates the rapid deterioration in reservoir properties in the finer sands at depths greater than 3,000m. The Pelican area potential has thus been greatly reduced, leaving essentially only the western edge of this very large feature with any real potential. Although this edge is also large, it is difficult to imagine substantial areas of sealing faults and also production rates being doubled. To overcome these problems would require a lot of work which Amoco/Sagasco probably undertook prior to relinquishing T22P. No probability graph is presented here.

CORMORANT-1

The upper part of the "Pelican Zone" at Cormorant generated small quantities of gas on wireline tests. However, the deeper, thicker, although tighter sand gave no hydrocarbon response on logs. This was puzzling as there is enormous source potential in the very thick shale units, even at very low organic matter concentrates. The answer lies in the post Eastern View compression (Davidson, 1980). As mentioned above, Cormorant was a very deep Lower Eastern View trough which, on late compression, formed an anticline in the upper horizons (oil accumulations at the top and within the Eastern View and gas in the *M. diversus*) but remained a trough, hence structureless at deeper levels. Thus Cormorant loses structural closure with depth and hence the ability to reservoir gas. The gas reserves potential at Cormorant are therefore very low; indeed negligible.

OTHER

Away from the Yolla, Pipipa, Durroon areas, reservoir quality and structural definition are difficult to combine to produce potentially large reserves of gas/condensate. As the current operators have not highlighted many features of great interest, the basin potential is currently limited to the above three areas.

CONCLUSIONS

In depth analysis of the *L. balmei* gas-bearing unit at Yolla and limited assessments on the Pelican/Pipipa and Durroon regions, suggests there is a considerable undiscovered, potentially commercial gas/condensate reserve in

Bass Basin. The Yolla, Pipipa and Durroon area assessments have been combined in Figure 60.

To date the only proven (100% probability) reserves are at Yolla (250 BCF) with 1.2 TCF at the currently 50% probability level for the total basin. The basin high-side potential is of the order of 8TCF.

REFERENCES

Amoco Australia Petroleum Company, 1986, Yolla-1 Final Well Report, unpublished.

Amoco Australia Petroleum Company, February 1986, Yolla No. 1 DST Memorandum, unpublished.

Amoco Australia Petroleum Company, 1988, Seismic Interpretation of the Yolla and Tilana Areas, T/14P, Bass Basin, Australia, unpublished.

Baillie, P.W., 1987, Petroleum Geochemistry of Crudes from Yolla and Pelican-5, Bass Basin. *Tasm. Dept. Mines Rept. 1985/13.*

Core Laboratories Inc., 1986, Reservoir Fluid Analysis, unpublished.

Davidson, J.K., 1980, Rotational Displacements in Southeastern Australia and Their Influence on Hydrocarbon Occurrence, *Tectonophysics*, 63, pp 139-153.

- Blackburn, G.J. and Morrison, K.C., 1984, Bass and Gippsland Basins: A Comparison, *APEA Journal*, 24, pp 101-109.

- and Morrison, K.C., 1986, A Comparison of Hydrocarbon Plays in the Bass, Gippsland, Otway and Taranaki Basins, in Glennie, R.C. (ed.), *Second South Eastern Australia Oil Exploration Symposium*, pp 365-374.

Morrison, G.R., Wright, D.J. and Miyazaki, S., 1989, Yolla Gas and Oil Field, Bass Basin, Tasmania - Estimated Recoverable Petroleum Reserves, as at 1 October 1988, *Bureau of Mineral Resources Record 1989/4*, pp35.

Stock, A., 1989, Natural Gas for Tasmania, *APEA Journal*, 29 Pt.1, pp35-40.

5 cm



PETRECON AUSTRALIA PTY. LTD.

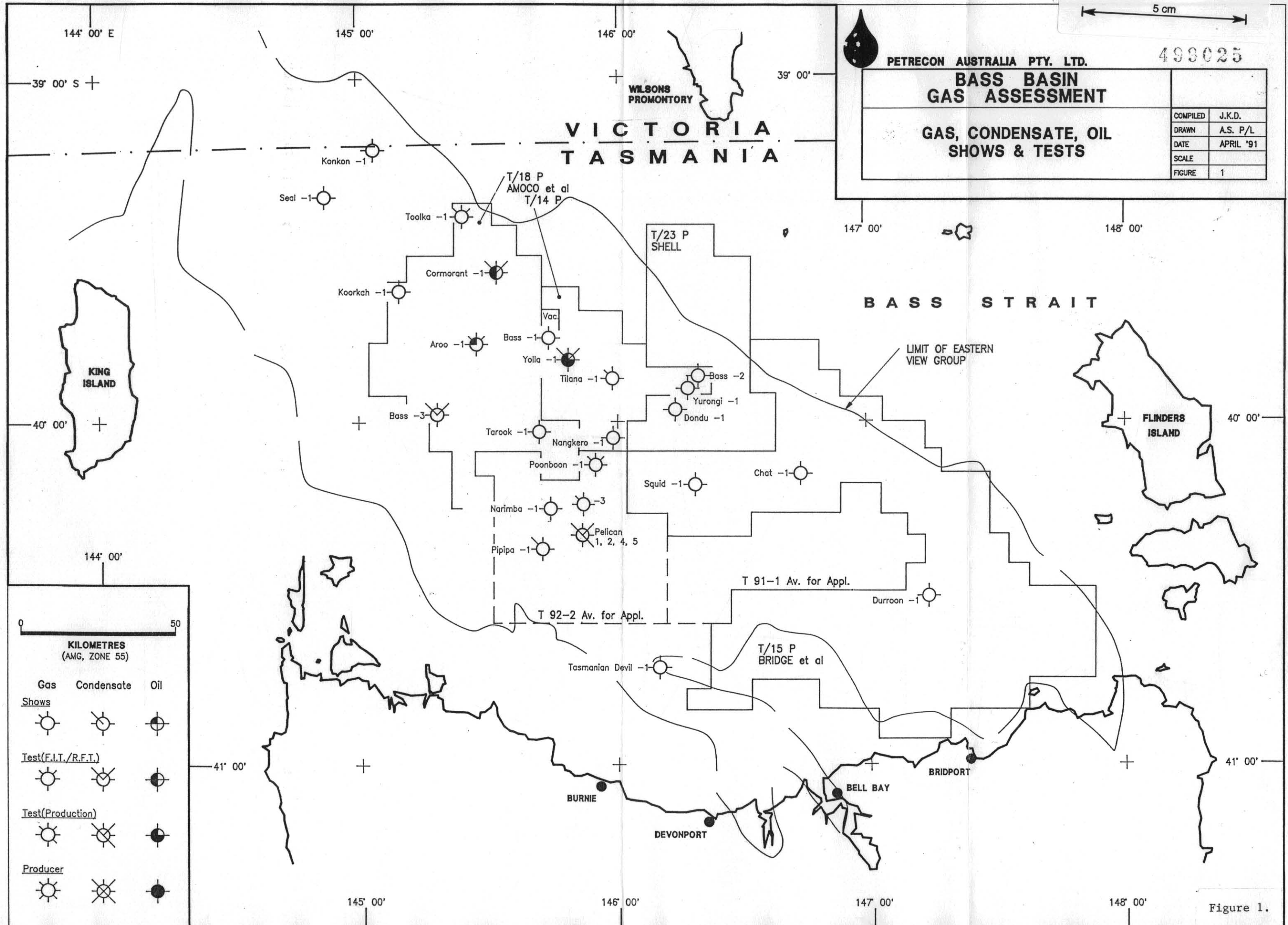
498025

**BASS BASIN
GAS ASSESSMENT**

**GAS, CONDENSATE, OIL
SHOWS & TESTS**

COMPILED	J.K.D.
DRAWN	A.S. P/L
DATE	APRIL '91
SCALE	
FIGURE	1

**VICTORIA
TASMANIA**



0 50

**KILOMETRES
(AMG, ZONE 55)**

	Gas	Condensate	Oil
<u>Shows</u>			
<u>Test(F.I.T./R.F.T.)</u>			
<u>Test(Production)</u>			
<u>Producer</u>			

Figure 1.

No. OF WELLS DRILLED PER YEAR

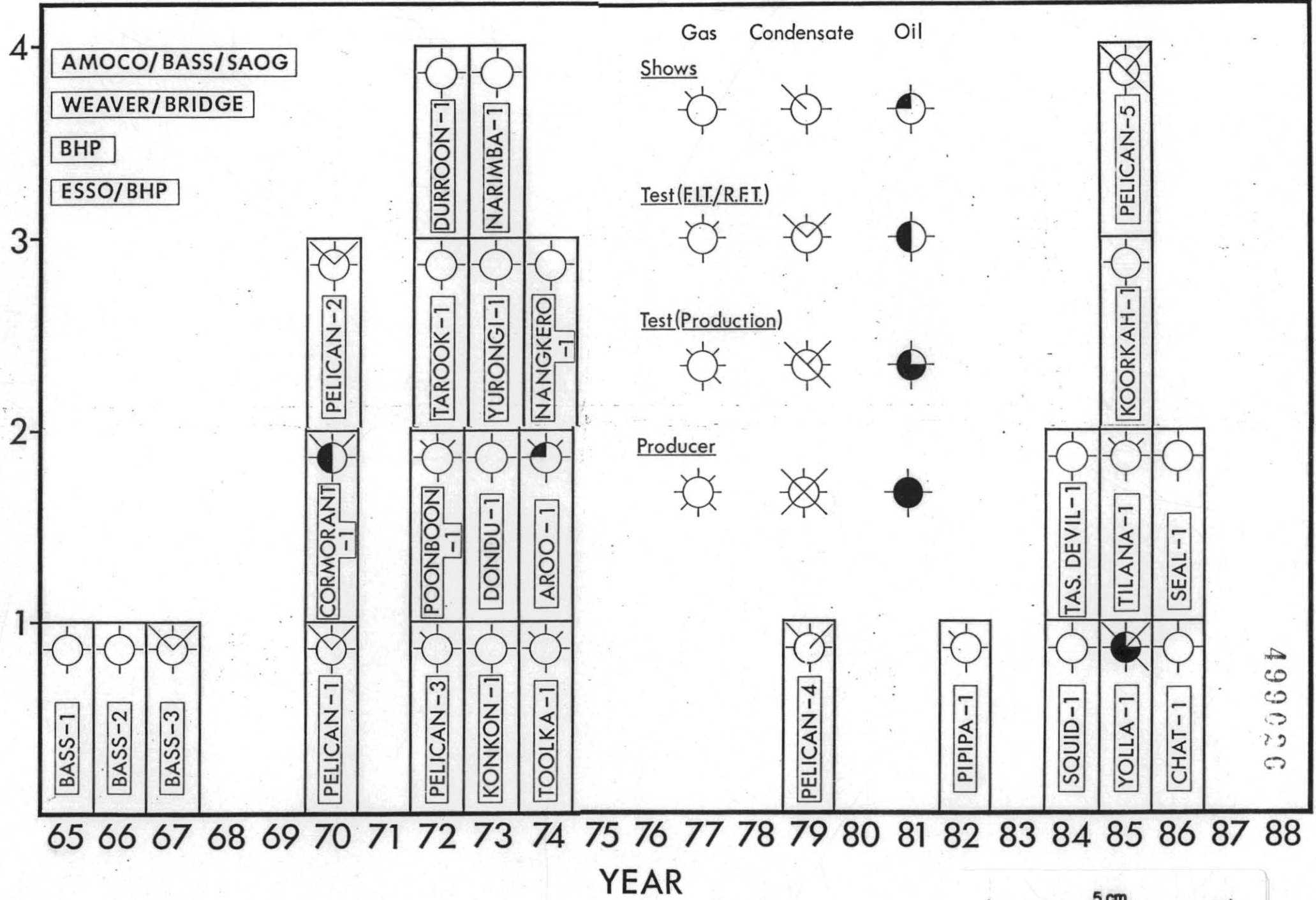
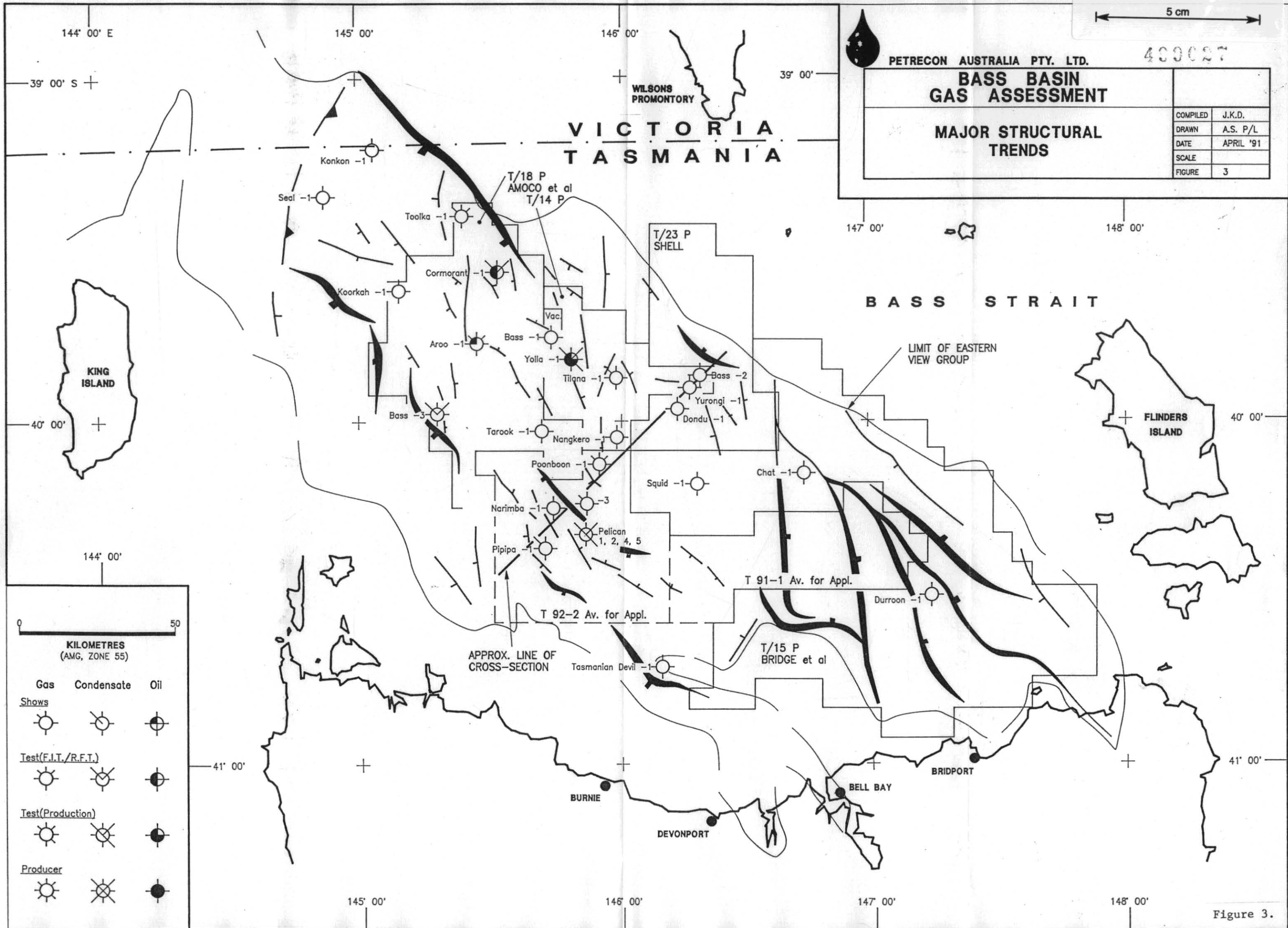


Figure 2.

499020



5 cm



PETRECON AUSTRALIA PTY. LTD.

400027

**BASS BASIN
GAS ASSESSMENT**

**MAJOR STRUCTURAL
TRENDS**

COMPILED	J.K.D.
DRAWN	A.S. P/L
DATE	APRIL '91
SCALE	
FIGURE	3

**VICTORIA
TASMANIA**

BASS STRAIT

144° 00' E

145° 00'

146° 00'

39° 00'

147° 00'

148° 00'

40° 00'

40° 00'

144° 00'

41° 00'

41° 00'

145° 00'

146° 00'

147° 00'

148° 00'

0 50
KILOMETRES
(AMG, ZONE 55)

Gas	Condensate	Oil
Shows		
Test(F.I.T./R.F.T.)		
Test(Production)		
Producer		

Figure 3.

400028

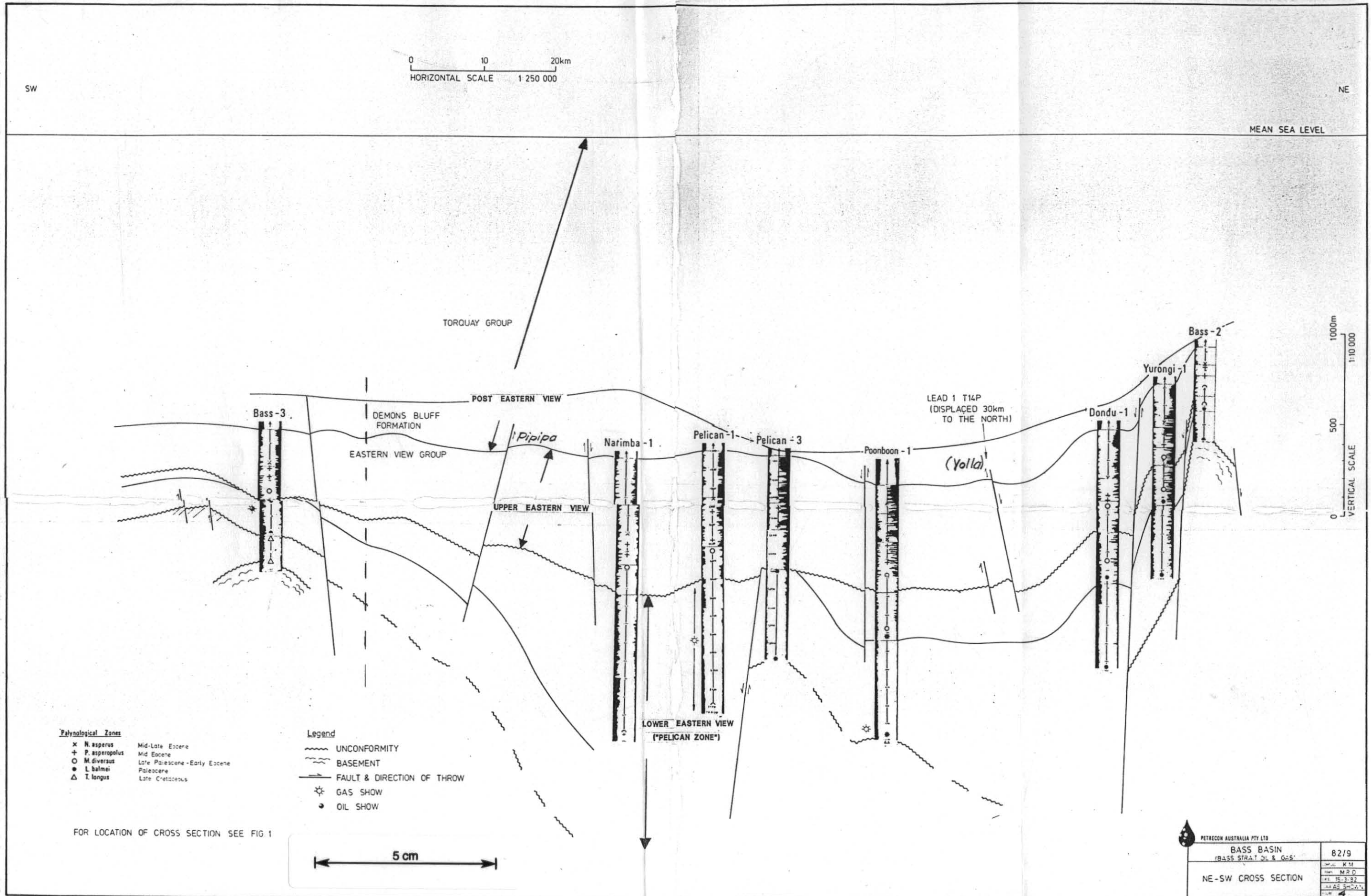
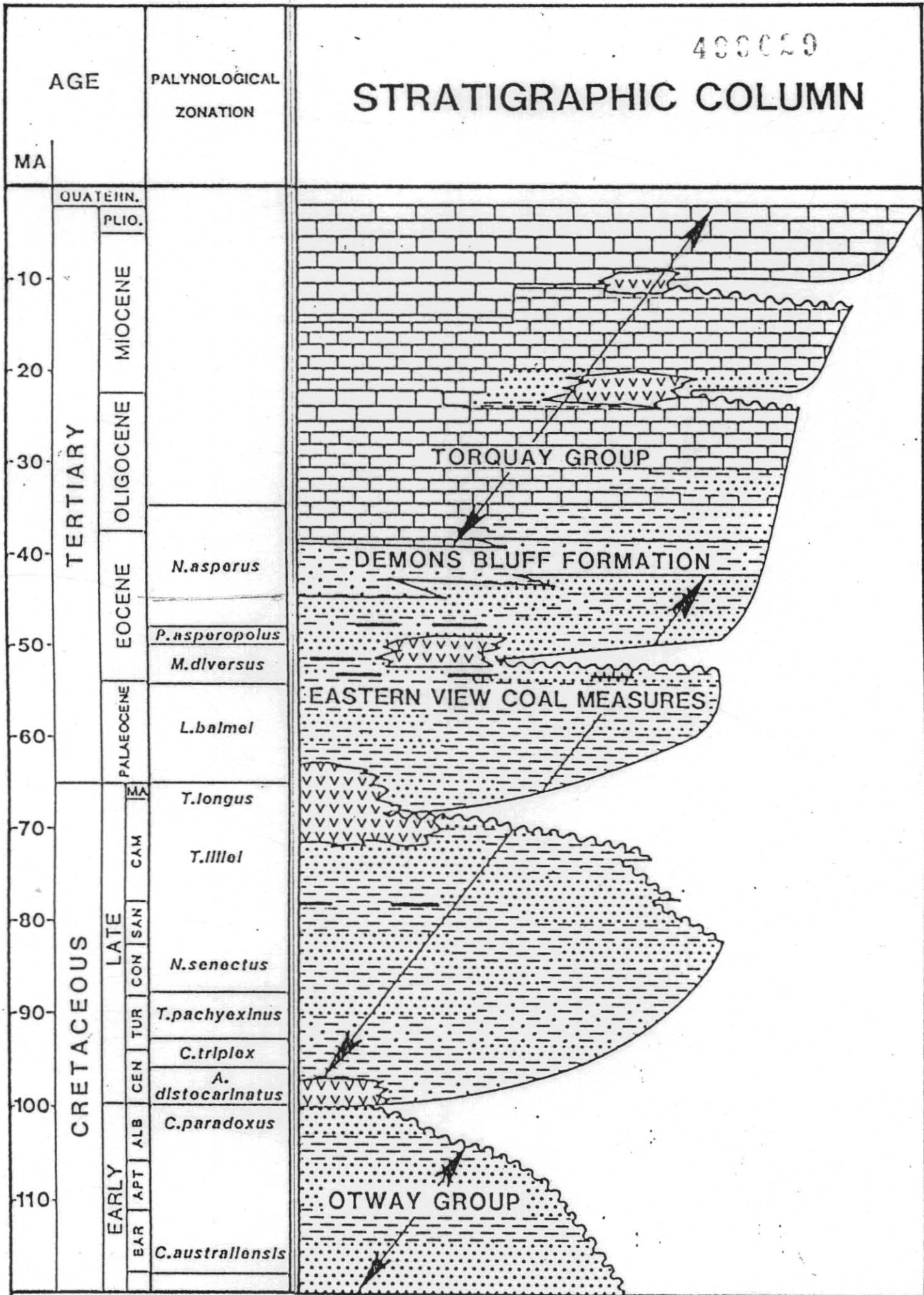


Figure 4.

488029

STRATIGRAPHIC COLUMN



5 cm

Figure 4a.

5 cm



PETRECON AUSTRALIA PTY. LTD.

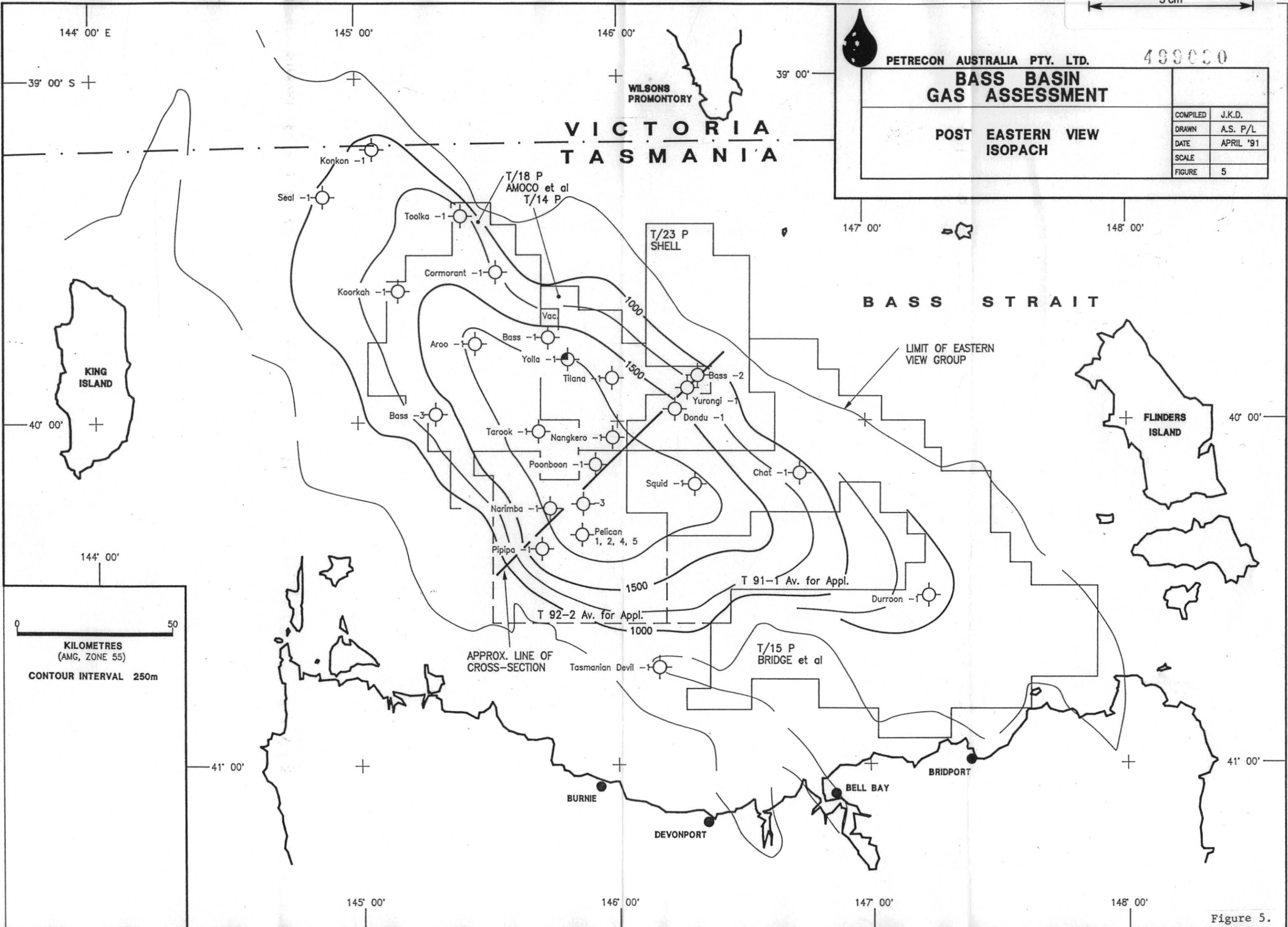
499020

BASS BASIN GAS ASSESSMENT

POST EASTERN VIEW ISOPACH

COMPILED	J.K.D.
DRAWN	A.S. P/L
DATE	APRIL '91
SCALE	
FIGURE	5

VICTORIA TASMANIA



0 50
KILOMETRES
(AMG, ZONE 55)
CONTOUR INTERVAL 250m

Figure 5.

5 cm



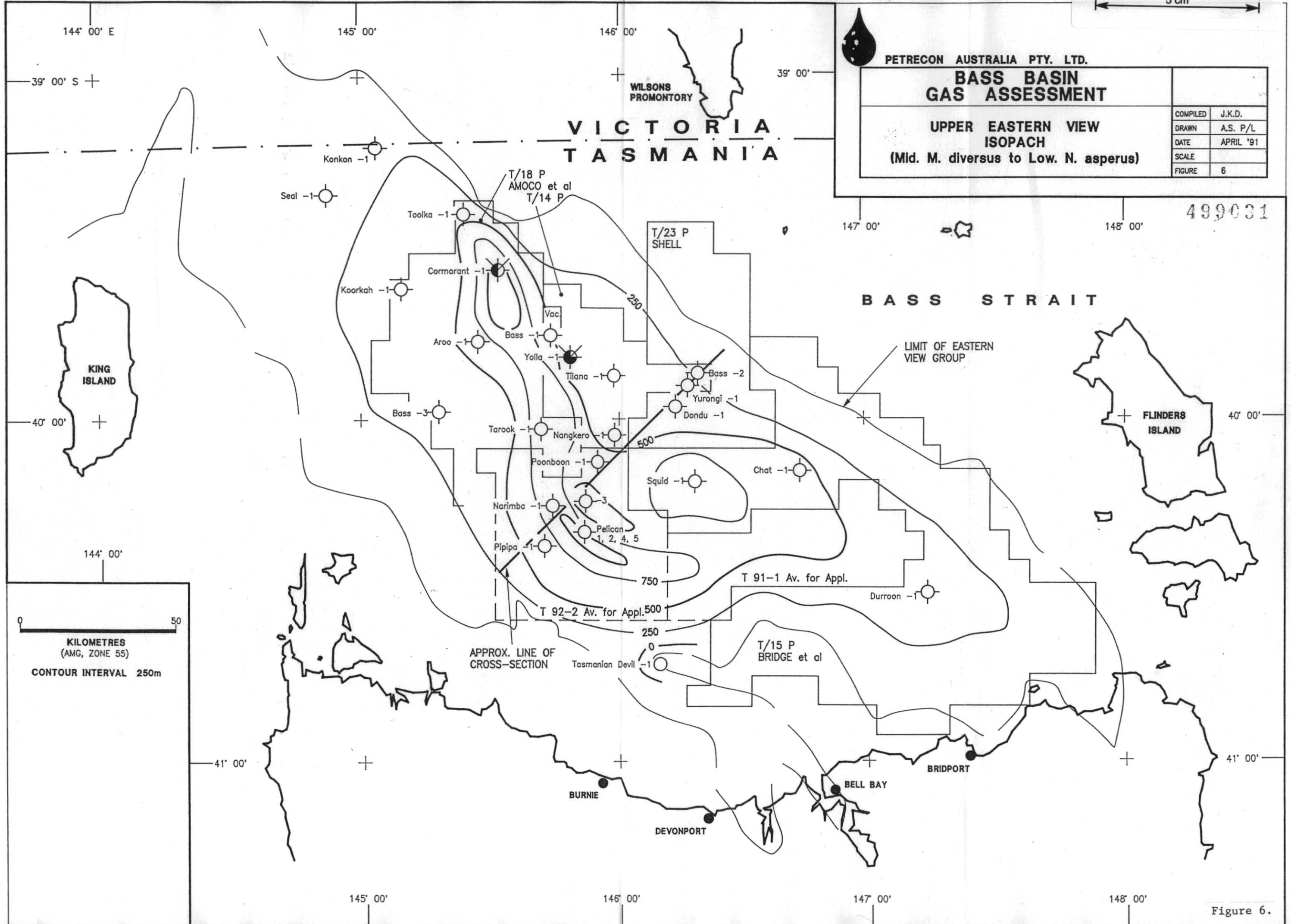
PETRECON AUSTRALIA PTY. LTD.

BASS BASIN GAS ASSESSMENT

UPPER EASTERN VIEW
ISOPACH
(Mid. M. diversus to Low. N. asperus)

COMPILED	J.K.D.
DRAWN	A.S. P/L
DATE	APRIL '91
SCALE	
FIGURE	6

499031



144° 00' E

145° 00'

146° 00'

147° 00'

148° 00'

39° 00' S

40° 00'

144° 00'

41° 00'

41° 00'

145° 00'

146° 00'

147° 00'

148° 00'

0 50
KILOMETRES
(AMG, ZONE 55)
CONTOUR INTERVAL 250m

Figure 6.

5 cm



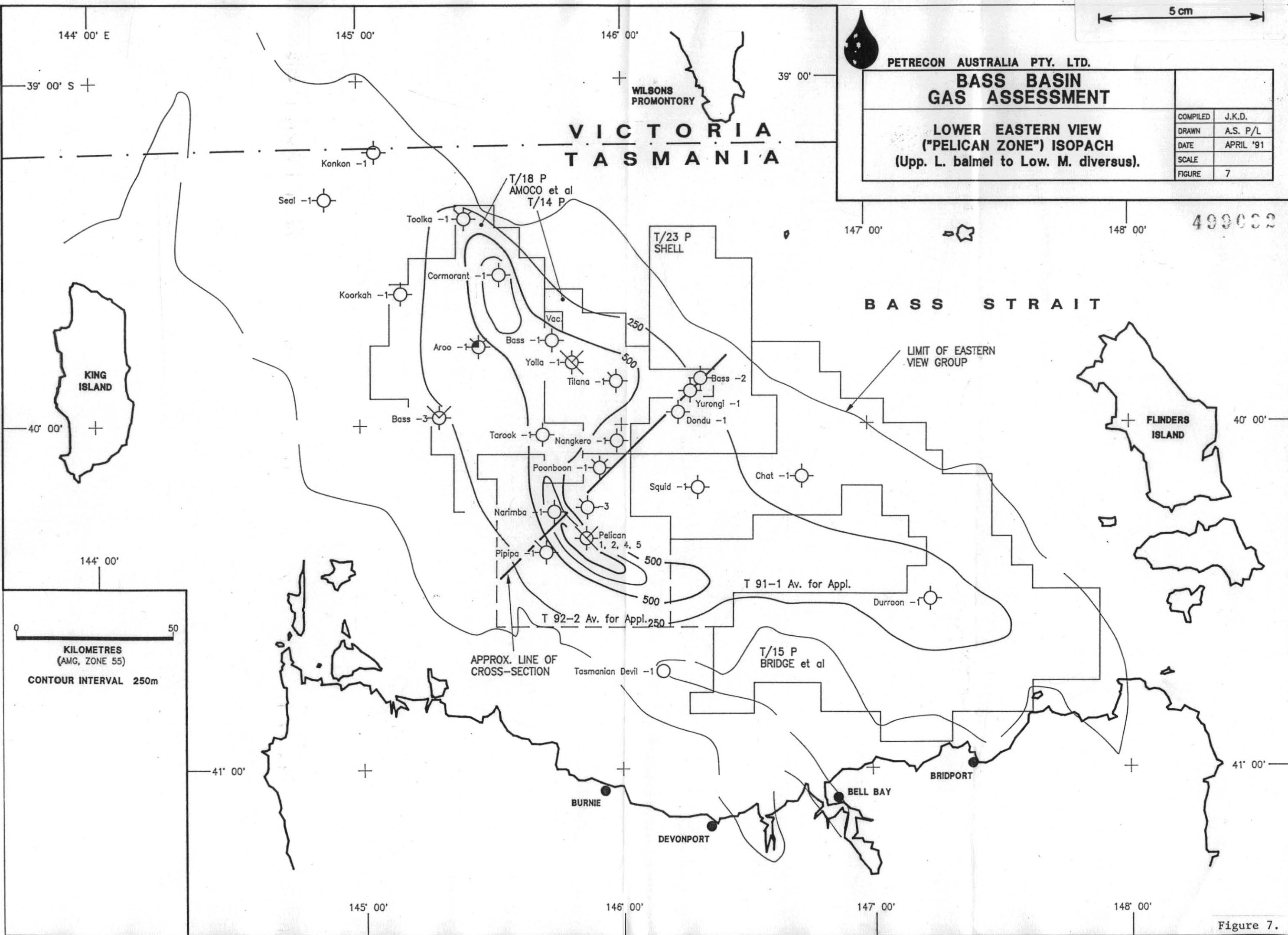
PETRECON AUSTRALIA PTY. LTD.

**BASS BASIN
GAS ASSESSMENT**

**LOWER EASTERN VIEW
("PELICAN ZONE") ISOPACH
(Upp. L. balmel to Low. M. diversus).**

COMPILED	J.K.D.
DRAWN	A.S. P/L
DATE	APRIL '91
SCALE	
FIGURE	7

**VICTORIA
TASMANIA**



499002

Figure 7.

TOP EVCM: TIME STRUCTURE

499033

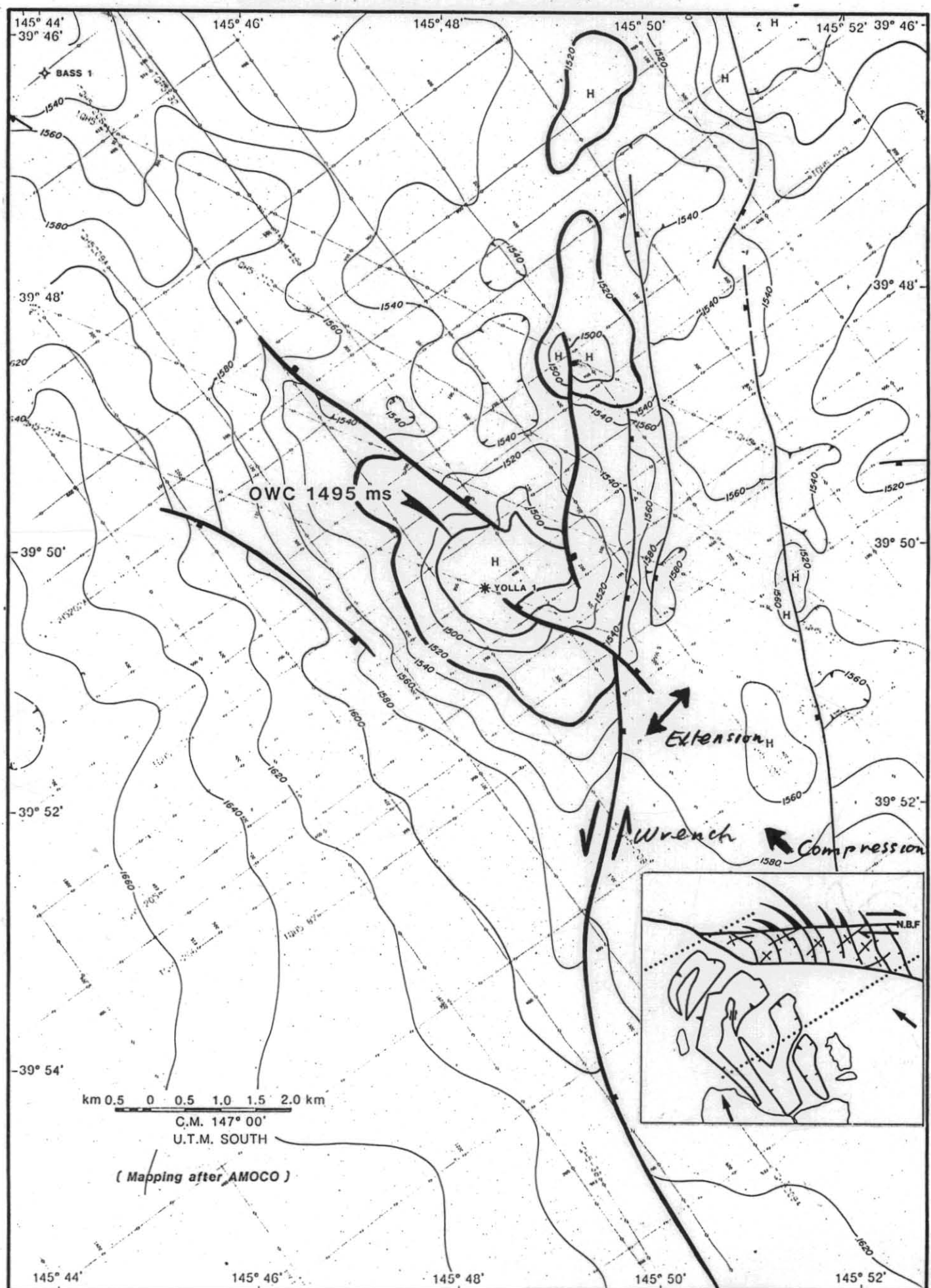
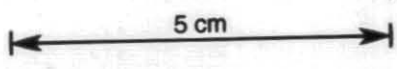
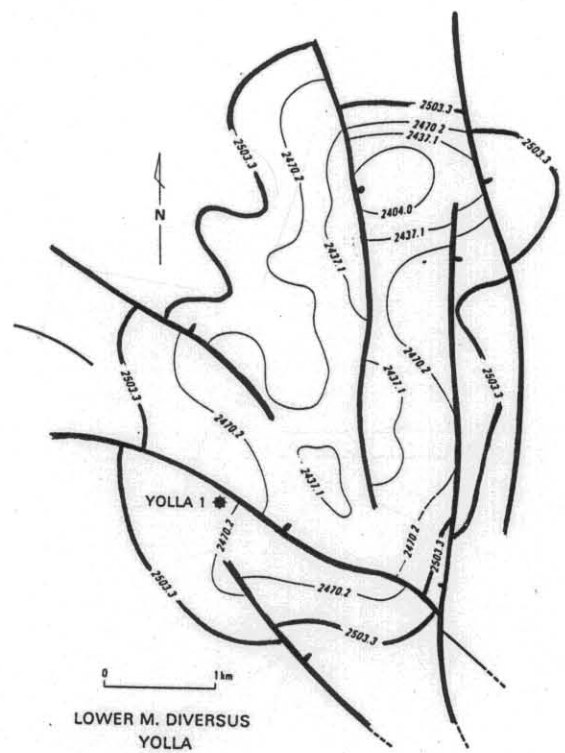


FIGURE 8



LOWER M. DIVERSUS
YOLLA

- 2503.3- Contour (in metres subsea)
- Fault
- * Oil/Gas

14/J85-14/1

Fig 5 — Structure map (lower M. diversus marker)

5 cm

TOP PALAEOCENE: TIME STRUCTURE

499025

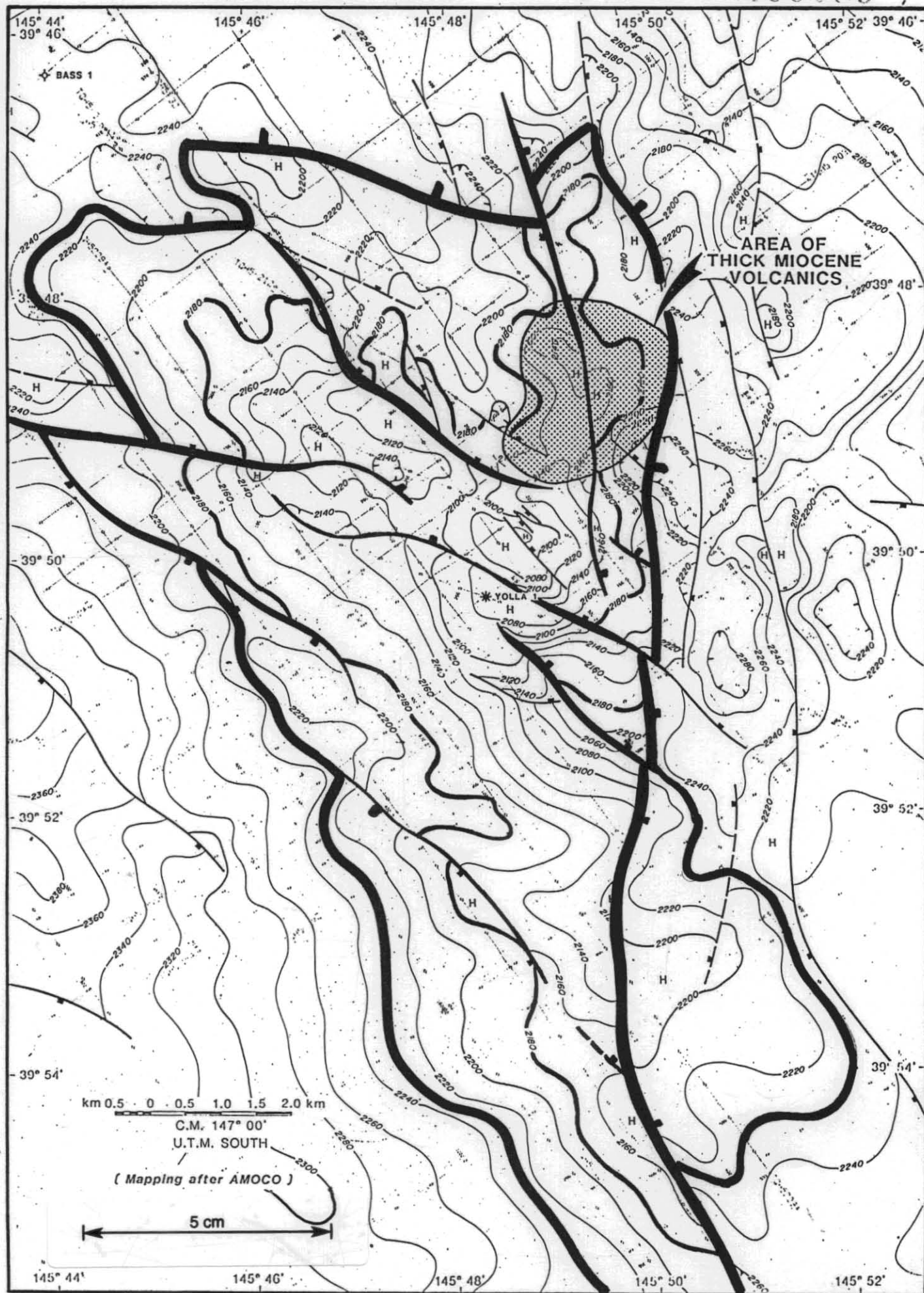


Figure 10.

499036

TOP PALAEOCENE: TIME STRUCTURE

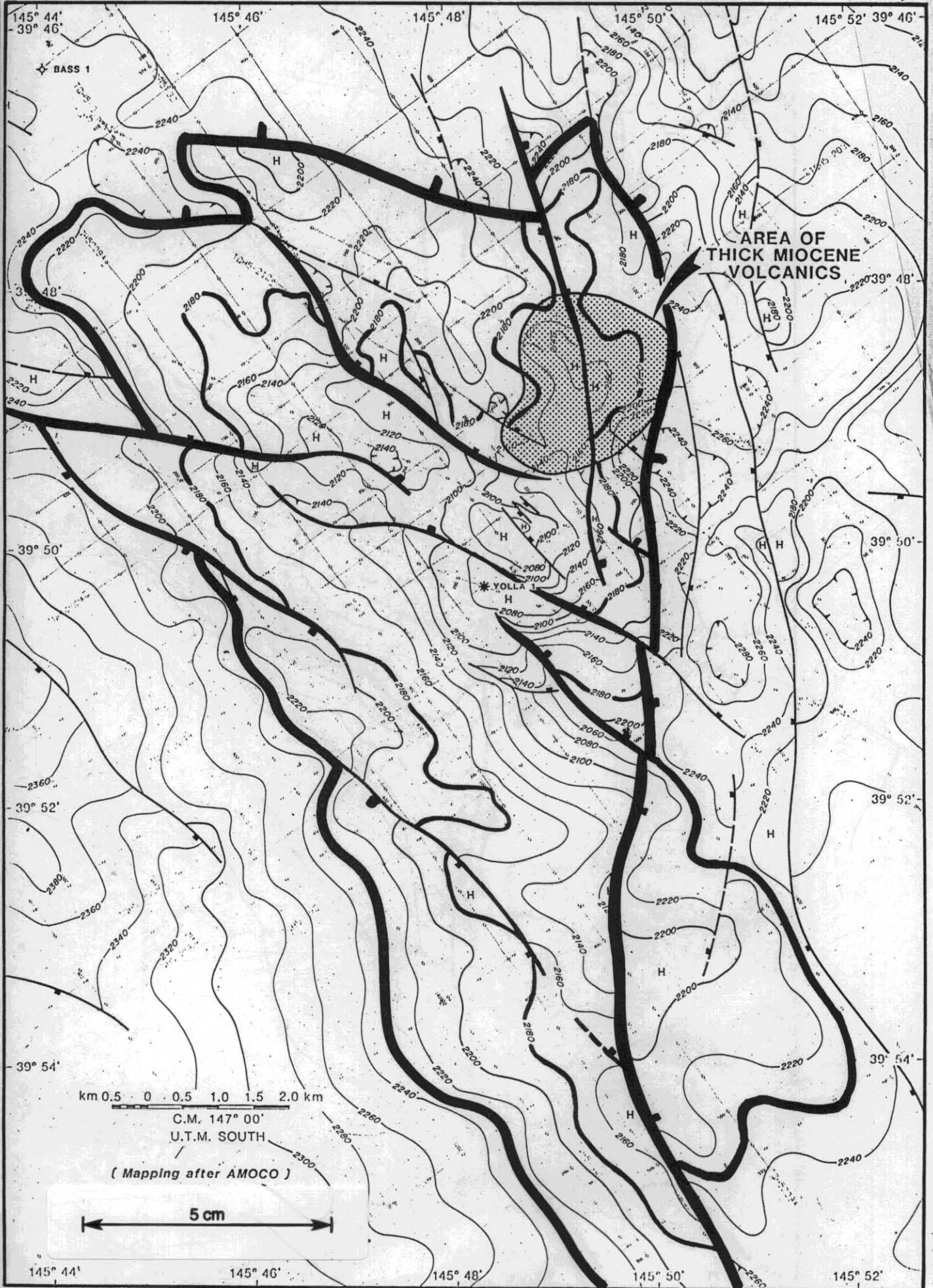


Figure 11

TOP EVCM: TIME STRUCTURE

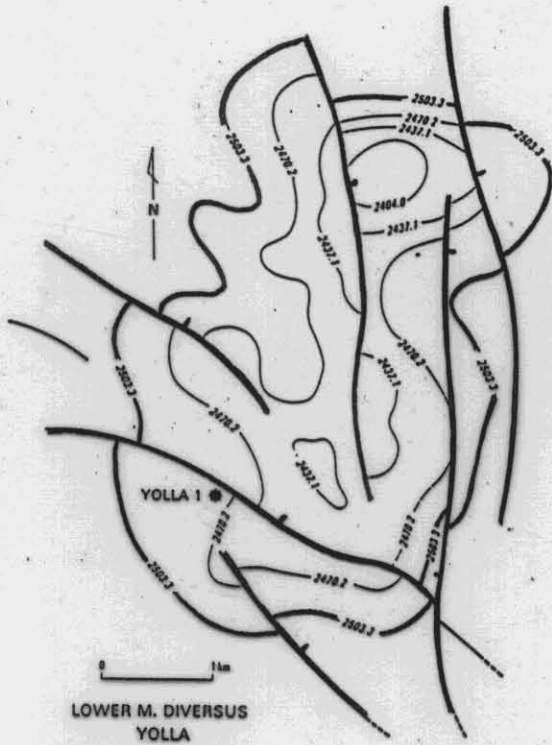


(Mapping after AMOCO)

Fig. 11a.

5 cm

Figure 11



LOWER M. DIVERSUS
YOLLA

- 2400.0- Contour (in metres above)
 - Fault
 - * Oil/Gas
- 1A/285-1A/1

Fig 5 — Structure map (lower M. diversus marker)

TOP EVCM: TIME STRUCTURE

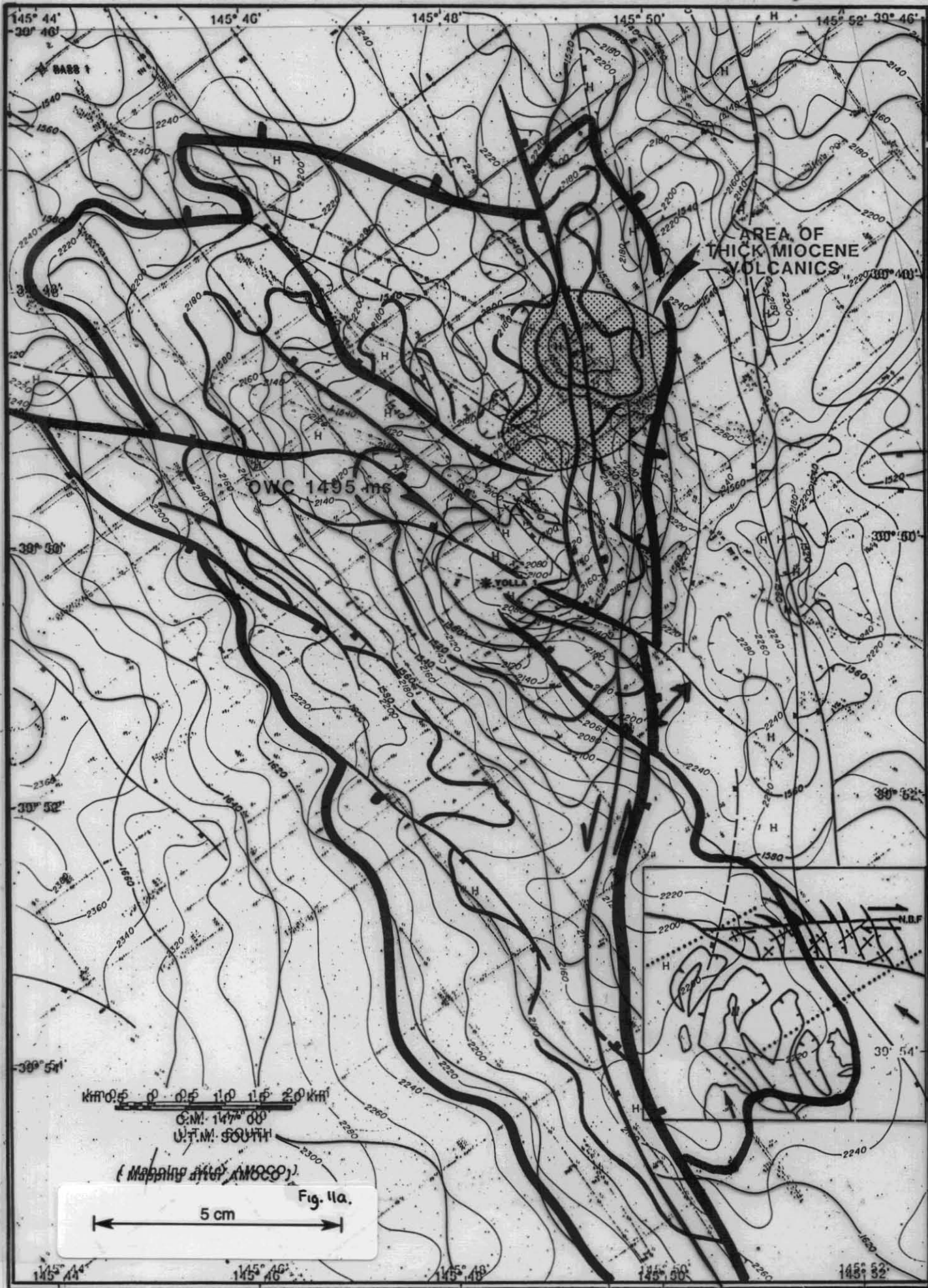


Figure 11

499038 499036

TOP PALAEOCENE: TIME STRUCTURE

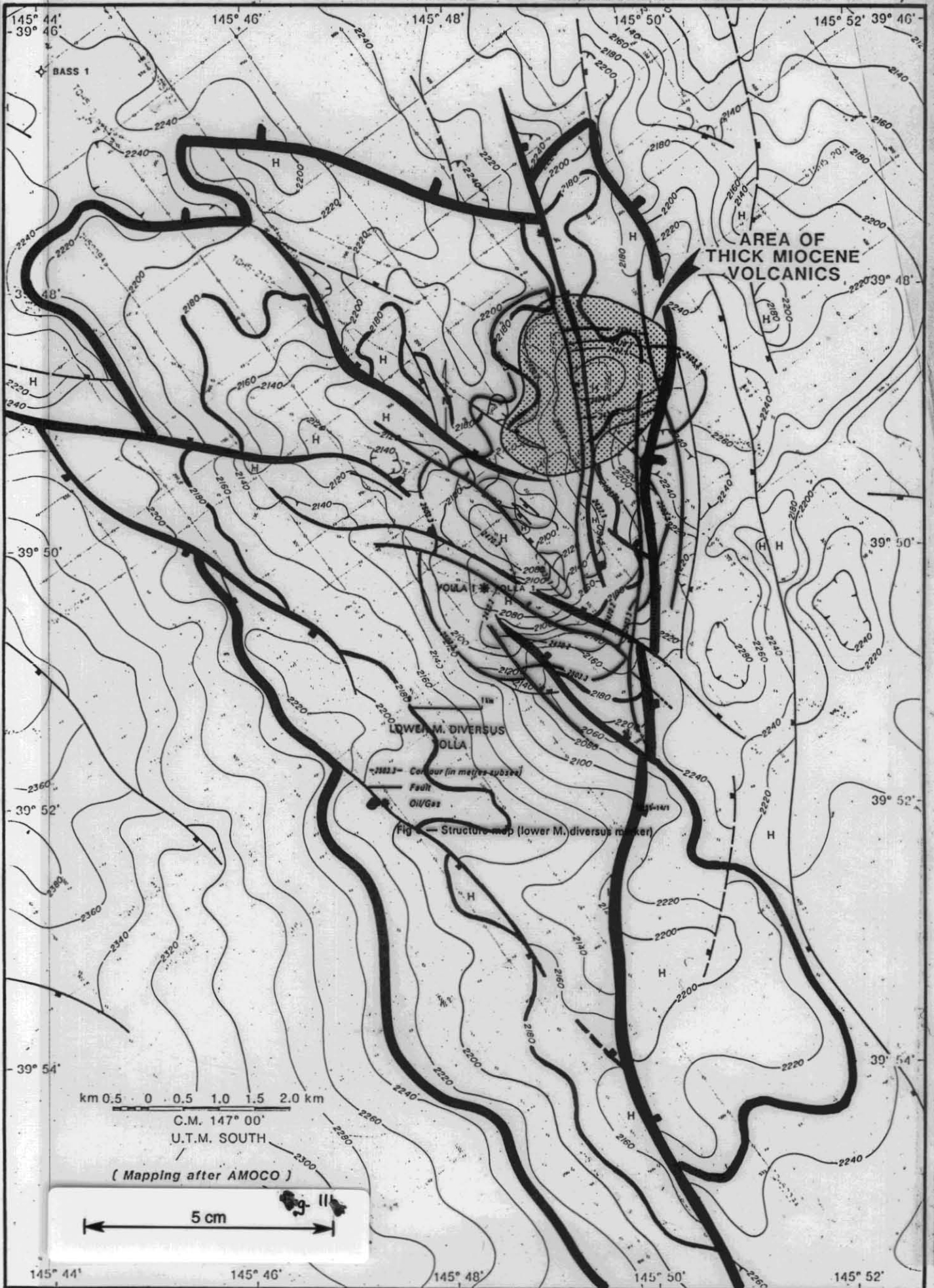
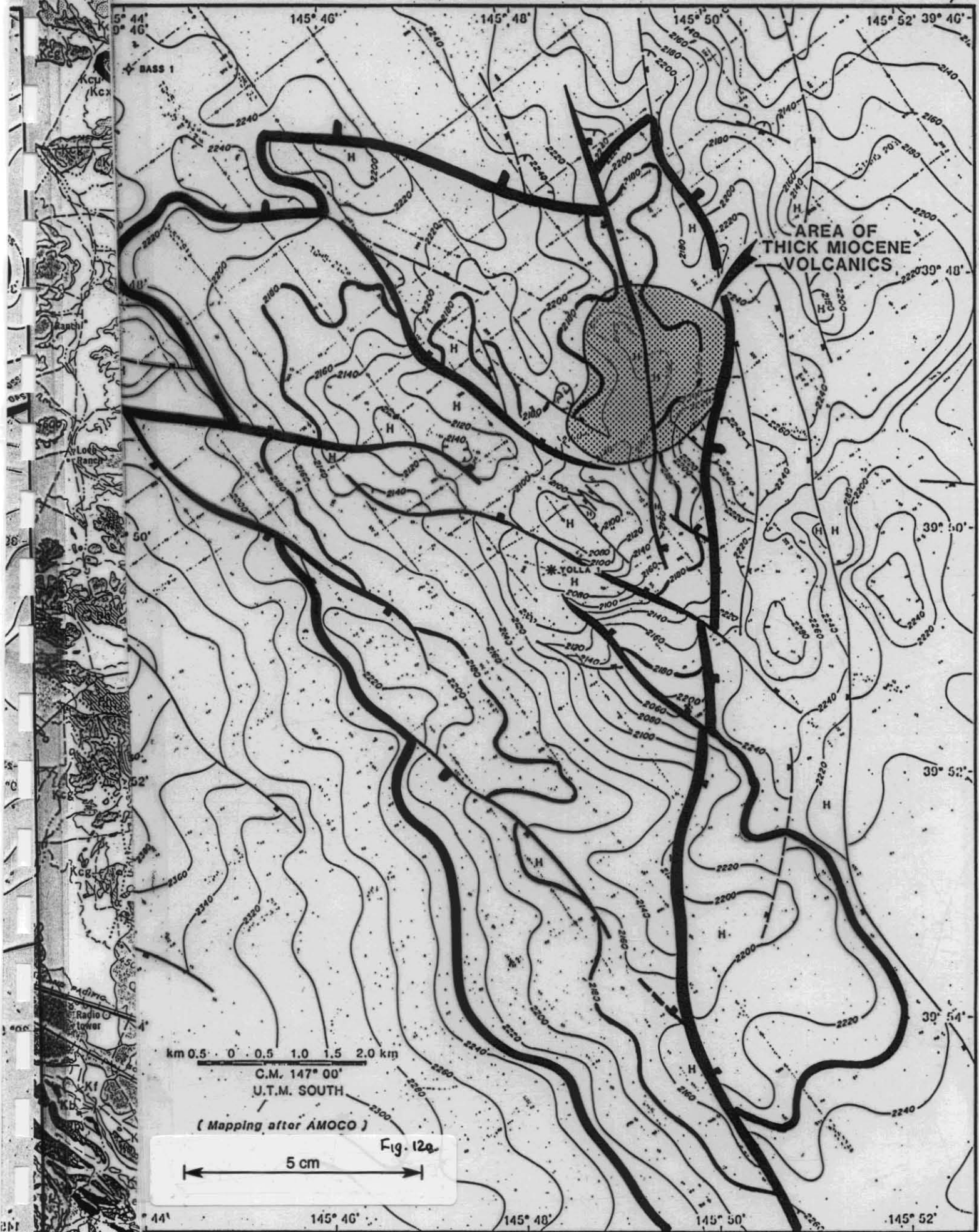


Figure 11

499040

TOP PALAEOCENE: TIME STRUCTURE



CORE LAB PRELIMINARY
COMPOSITIONAL ANALYSIS

DST CYL NO.	<u>2809-2824.5m</u>		<u>1830-35m</u>		<u>1833.1-33.7m</u>		<u>1813-33.7m.</u>	
	1		2		2A		3	
	5490	11585	A12257	A11585	A8659	011521	A8626	010691
	SEPARATOR		SEPARATOR		SEPARATOR		SEPARATOR	
	(GAS)	(LIQ)	(GAS)	(LIQ)	(GAS)	(LIQ)	(GAS)	(LIQ)
H ₂ S	0.00	0.00	0.00	0.00	0.00	0.00	0.00	0.00
CO ₂	19.30	7.89	7.43	7.91	7.61	0.60	7.49	2.59
N ₂	0.21	0.03	0.40	0.72	0.58	0.20	0.49	0.26
C1	66.71	14.08	73.83	71.72	66.78	2.50	74.66	13.32
C2	7.71	6.47	8.99	9.41	11.03	1.96	8.98	6.56
C3	3.53	7.68	5.38	5.59	7.80	4.01	5.11	9.10
IC4	0.54	2.52	1.00	1.09	1.59	1.99	0.89	3.32
NC4	0.81	5.07	1.52	1.50	2.20	3.77	1.16	5.84
IC5	0.23	2.92	0.43	0.52	0.66	2.71	0.34	3.35
NC5	0.22	3.37	0.38	0.47	0.55	2.94	0.28	3.48
C6	0.17	5.93	0.31	0.40	0.40	5.87	0.21	5.75
C7+	0.38	44.04	0.53	0.67	0.69	73.45	0.39	46.43
	100.00	100.00	100.00	100.00	100.00	100.00	100.00	100.00
	15.1 MCFGD 580 BCPD		3.4 MCFGD 2000 BCPD		1.02 CFDPD 302 BOPD		11.8 MCFPD 890 BCPD	

499042

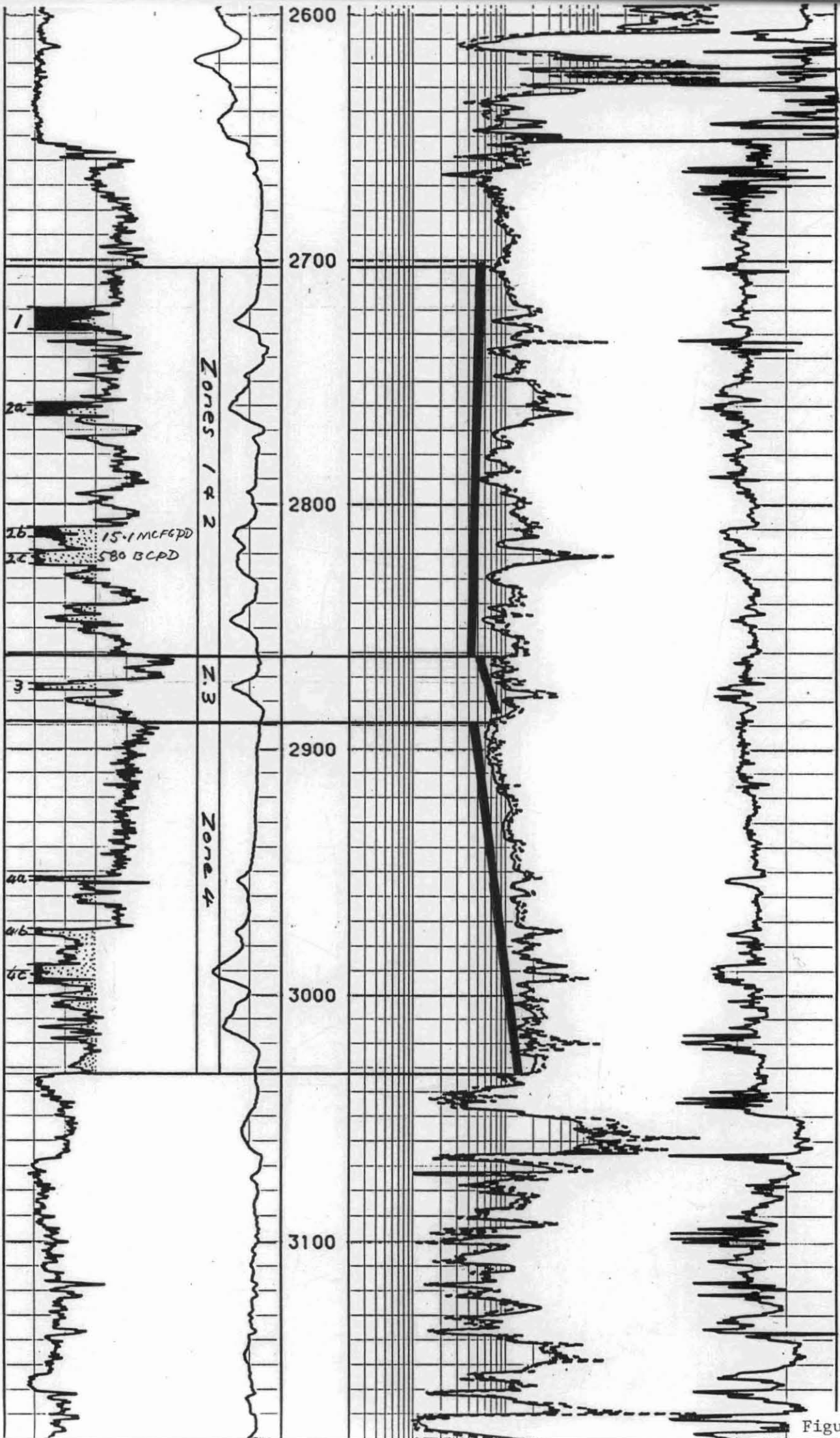


Figure 14.

YOLLA #1 RFT PRESSURES

<u>Pressure-PSIA</u>	<u>Depth-Feet</u>	<u>Meters</u>
2748	5963	1818
2752	6012.2	1833
2722	6010.6	1832.5
2731	6031.9	1839
2739	6045	1843
2742	6056.5	1846.5
2753	6087.7	1856
2763	6127	1868
2836	6248.4	1905
2850	6300.9	1921
2888	6382.9	1946
3019	6671.5	2034
3160	6970	2125
3299	7265.2	2215
3415	7632.5	2327
3555	7963.8	2428
4088	8938	2725
4135	9039.7	2756
4123	9054.4	2760.5
4120	9062.6	2763
4168	9220	2811
4162	9226.6	2813
4129	9333.2	2845.5
4152	9220	2811
4146	9252.9	2821
4142	9261	2823.5
4085	8938	2725
4114	9054.4	2760.5
4123	9063.6	2763.3

YOLLA PRESSURE DATA

499044

(mKB)
LOG
INTERVALS

L. BALMEI GAS ZONES

Yolla pressure data: L. balmei gas zones

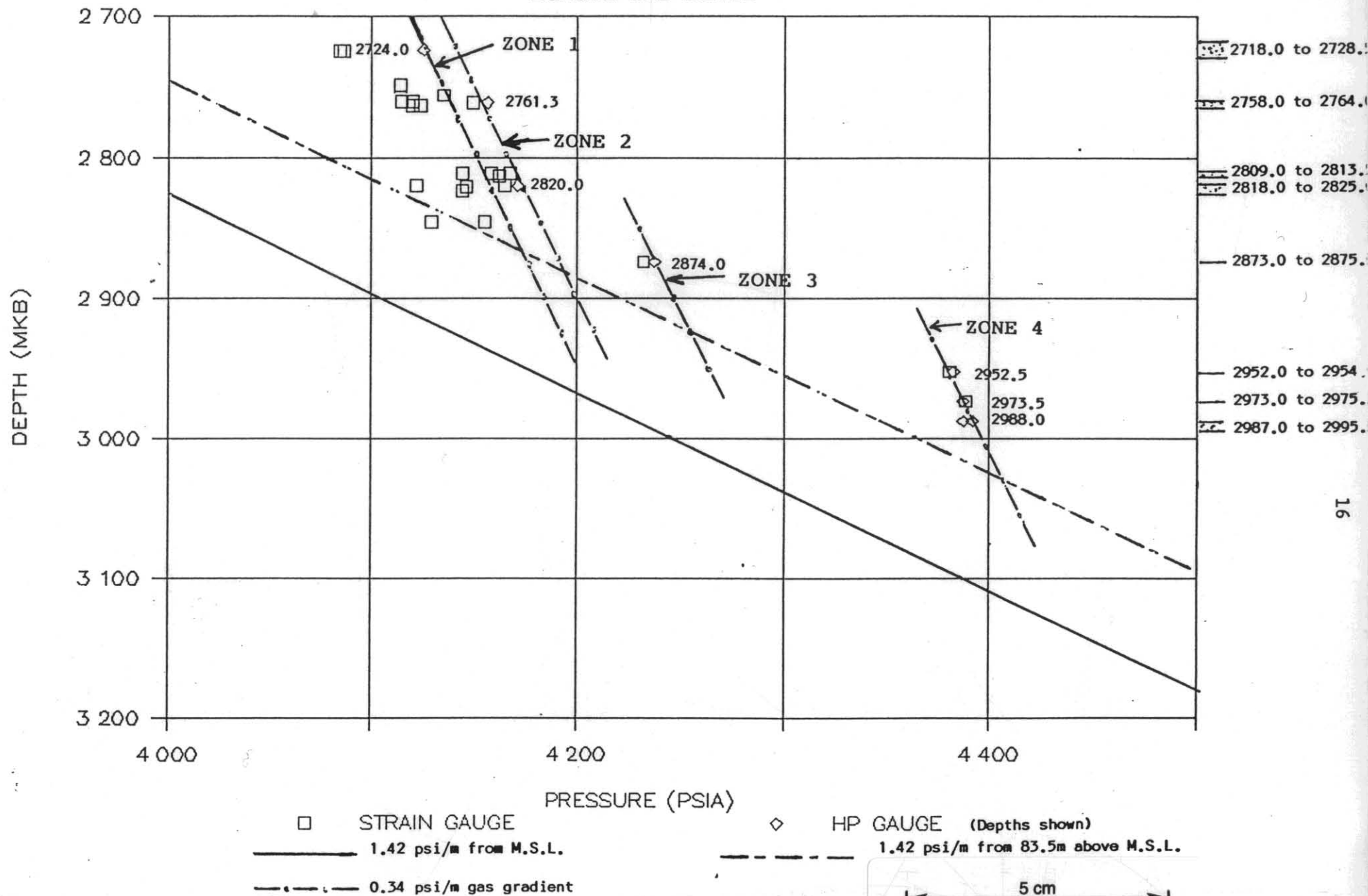


Figure 16.

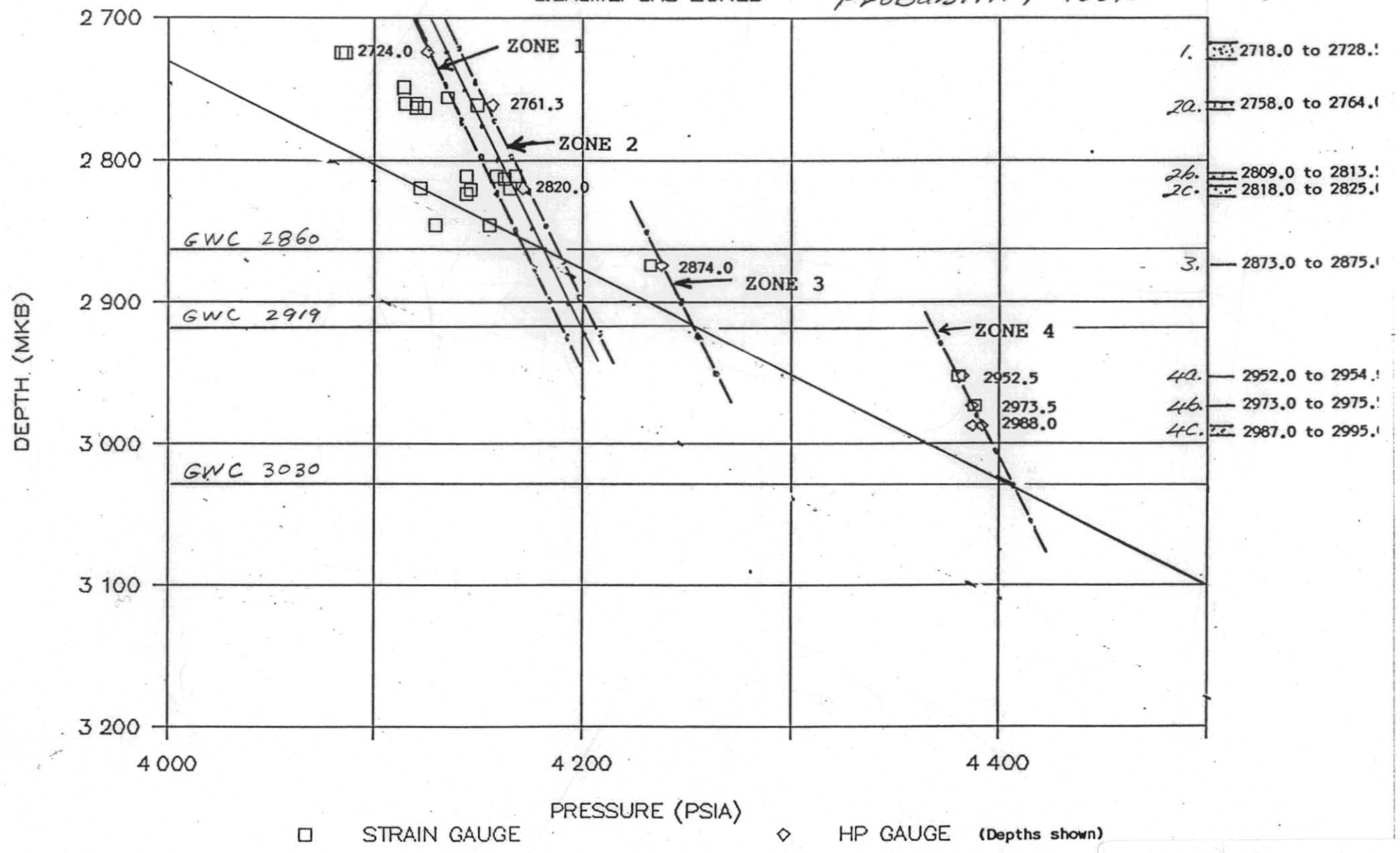
499045

YOLLA PRESSURE DATA

L. BALMEI GAS ZONES

Probability 100%

(MKB)
LOG
INTERVALS



- 1. 2718.0 to 2728.0
- 20. 2758.0 to 2764.0
- 26. 2809.0 to 2813.0
- 2C. 2818.0 to 2825.0
- 3. 2873.0 to 2875.0
- 4A. 2952.0 to 2954.0
- 4B. 2973.0 to 2975.0
- 4C. 2987.0 to 2995.0

GWC 2860

GWC 2919

GWC 3030

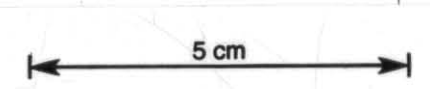


Figure 17.

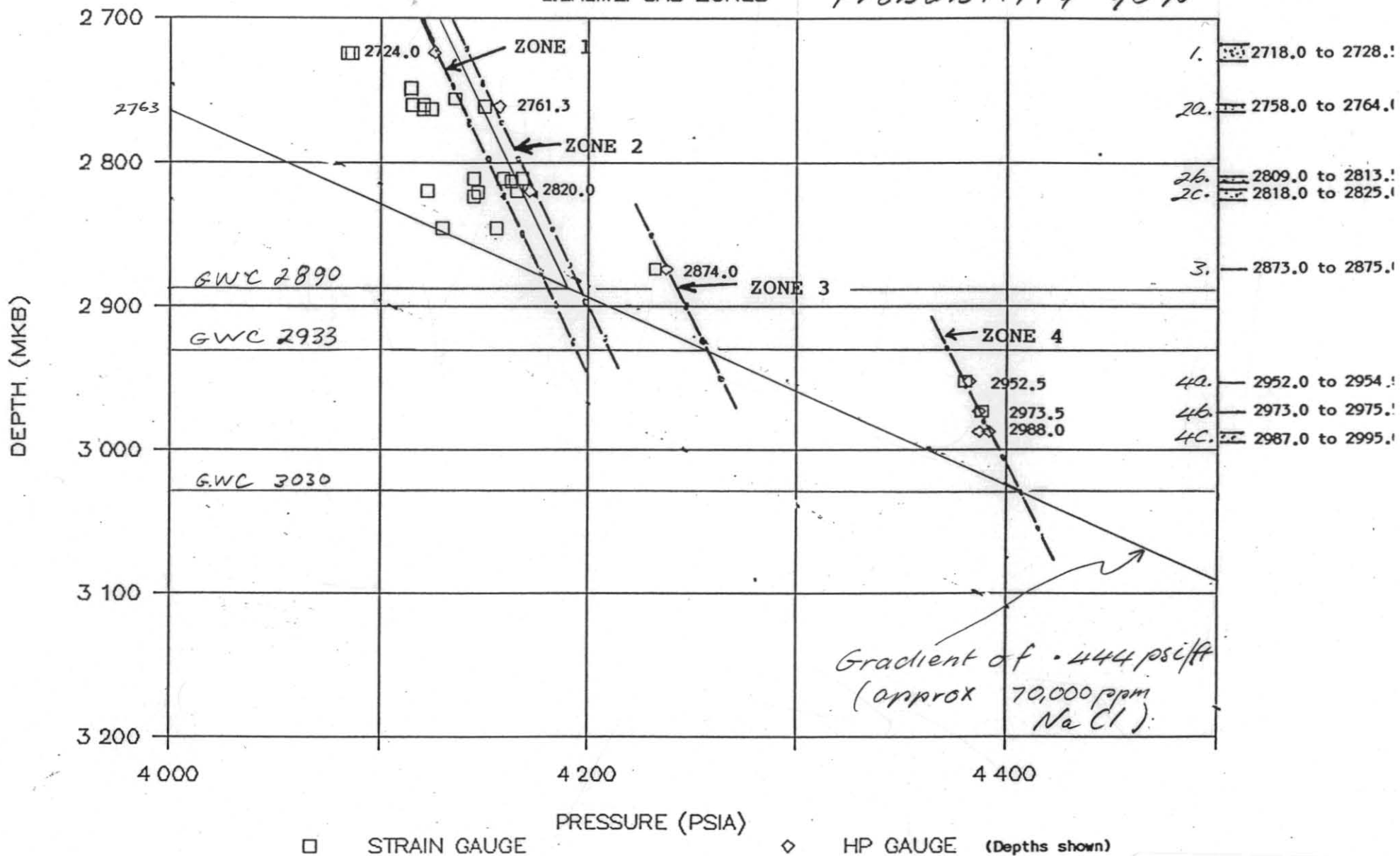
YOLLA PRESSURE DATA

499046

L. BALMEI GAS ZONES

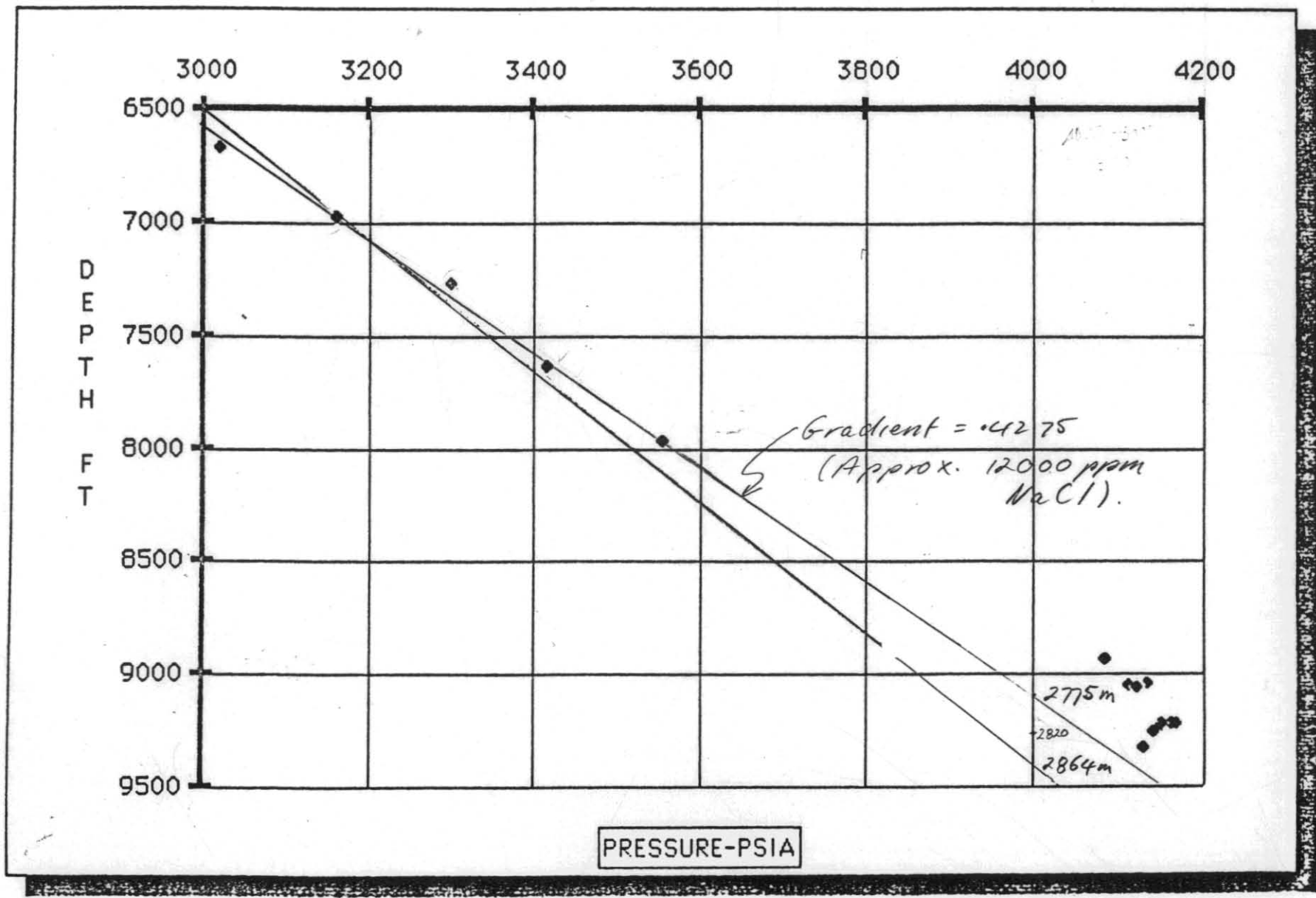
Probability 90%

(MKB)
LOG
INTERVALS



5 cm

Figure 18.



5 cm

Figure 19.

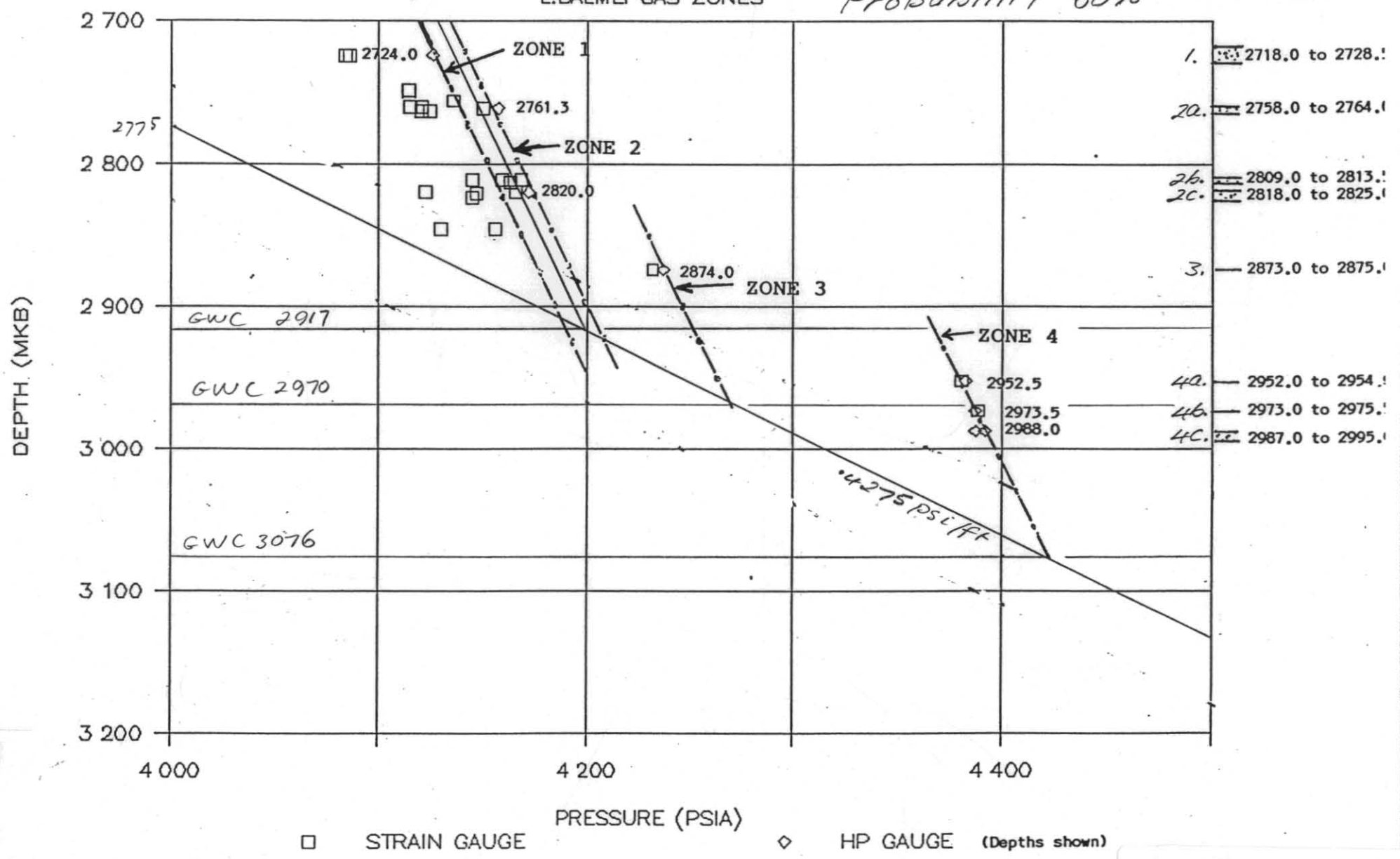
YOLLA PRESSURE DATA

499048

L. BALMEI GAS ZONES

Probability 60%

(MKB)
LOG
INTERVALS



5 cm

Figure 20.

499049

YOLLA PRESSURE DATA

L. BALMEI GAS ZONES

Probability 15%

(MKB)
LOG
INTERVALS

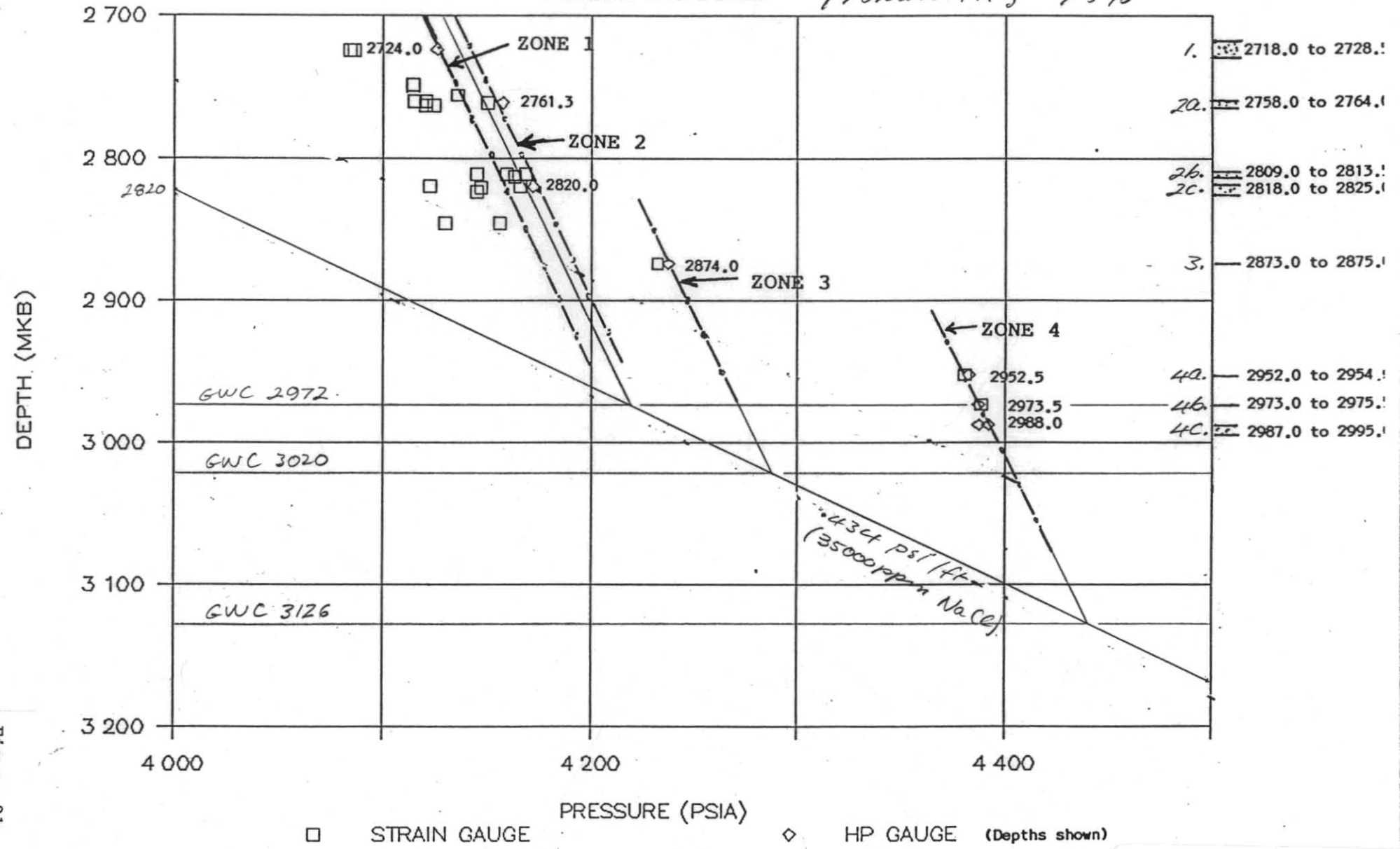
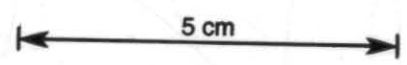


Figure 21.



YOLLA PRESSURE DATA

499050

L. BALMEI GAS ZONES

Probability 1%

(MKB)
LOG
INTERVALS

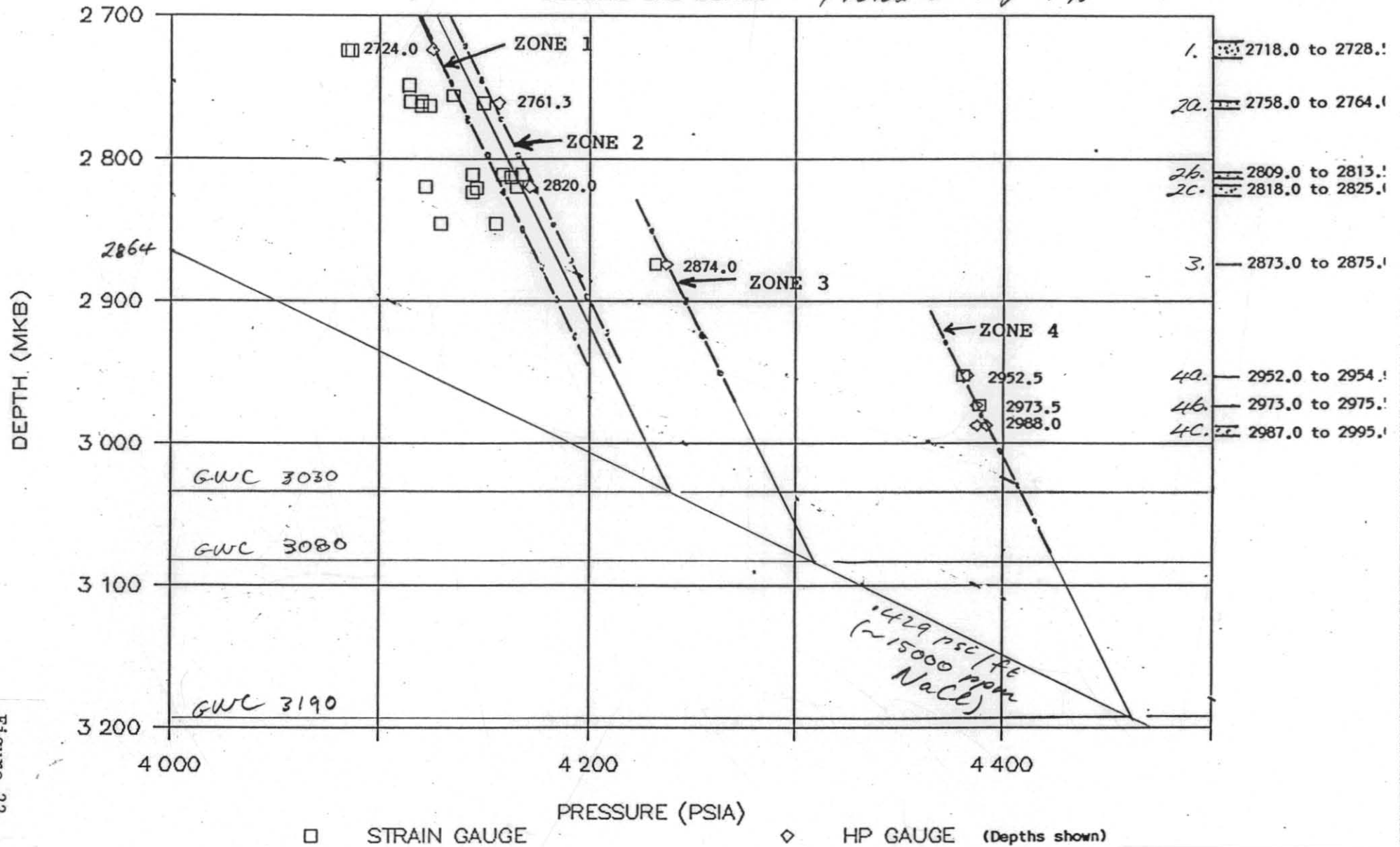


Figure 22.

5 cm

(YOLLA NO. 1, TASMANIA)

RESULTS SUMMARY

AMOCO

DEPTH	PHI	SW	VSH	RW	NEUT	RHOB	SONIC	RT		
	BMR	BMR								
1819.0	.17	.63	.29	.052	.26	2.35	96	2.8		
1833.0	.30	.40	.16	.052	.36	2.10	115	2.6		
1840.0	.21	.69	.31	.052	.32	2.25	103	1.5		
1843.0	.24	.77	.22	.052	.32	2.20	104	1.0		
1846.0	.23	.92	.28	.052	.34	2.20	110	.7		
1868.5	.26	1.00	.05	.051	.27	2.23	110	.6		
1 2725.0	.15	.33	.54	.19	.067	2.40	85	7.0		
2759.0	.16	.29	.17	.066	.20	2.38	90	21.0		
2a 2760.5	.18	.28	.25	.00	.066	2.32	95	22.0		
2762.5	.17	.21	.00	.066	.14	2.37	78	52.0		
2b 2810.0	.17	.29	.28	.10	.066	2.35	84	16.0		
2c 2820.5	.20	.18	.25	.15	.00	.065	.11	2.30	86	90.0
2845.5	.15	.63	.07	.065	.15	2.40	80	6.0		
3 2874.0	.18	.17	.39	.46	.05	.065	.17	2.40	87	10.0
4a 2952.5	.18	.15	.14	.35	.19	.063	.19	2.41	82	17.0
4b 2974.5	.17	.15	.21	.27	.02	.063	.13	2.40	84	35.0
2988.0	.20	.18	.00	.063	.14	2.27	89	50.0		
4c 2990.0	.18	.17	.21	.30	.10	.063	.18	2.37	86	20.0
2991.5	.20	.19	.00	.063	.15	2.30	90	45.0		
3012.5	.14	.46	.08	.062	.14	2.42	90	13.0		

PHI = Effective porosity
 SW = Water saturation
 VSH = Bulk volume shale
 RW = Water resistivity
 NEUT = Neutron porosity
 RHOB = Bulk density
 SONIC = Transit time
 RT = True resistivity

Reservoir Sand.

Depth
(msec.)

Yolla-1 2075 msec

2080

2130

2180

96

2230
60

Area (km²)

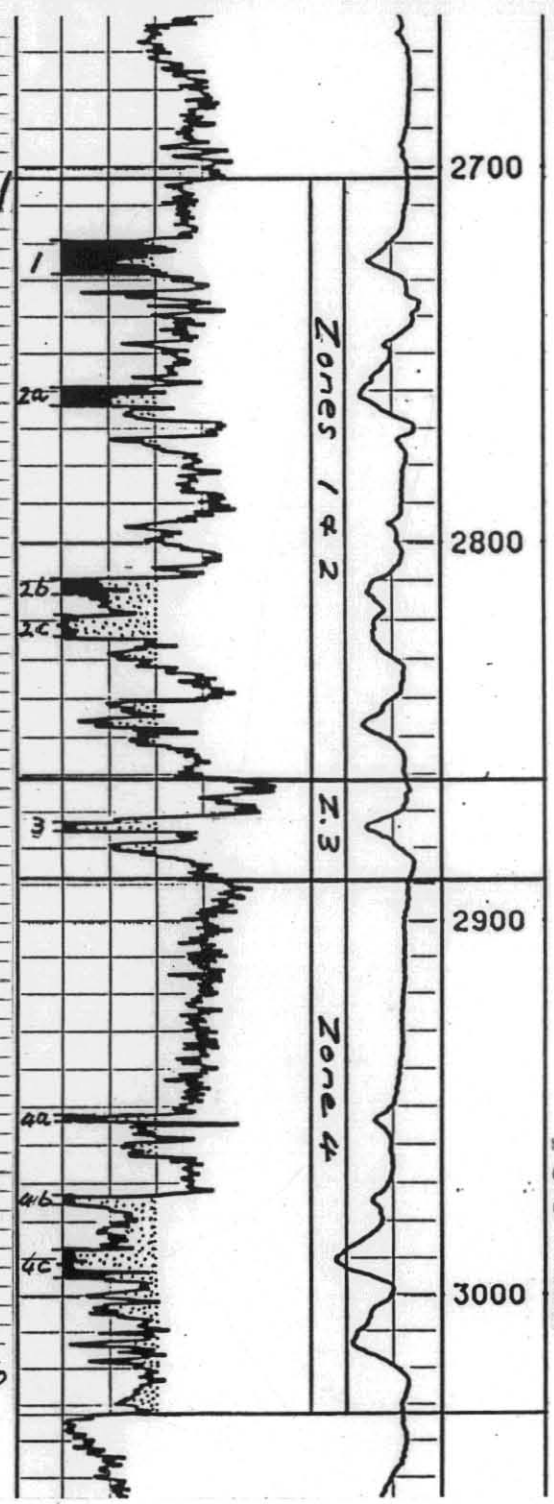
80

40

20

0

5 cm



499052

Figure 24.

Reservoir Sand 1.

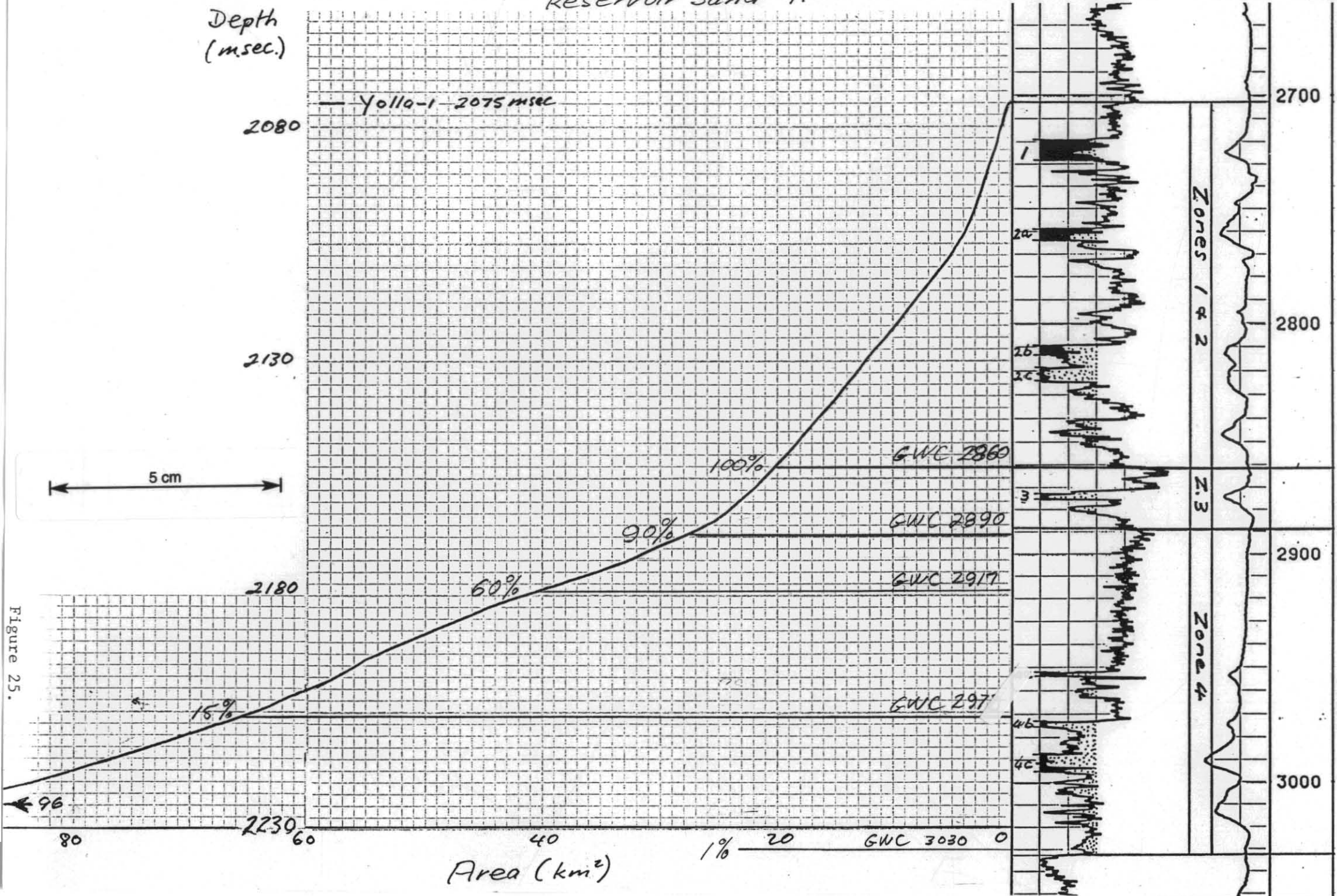


Figure 25.

499053

Reservoir Sand 2a.

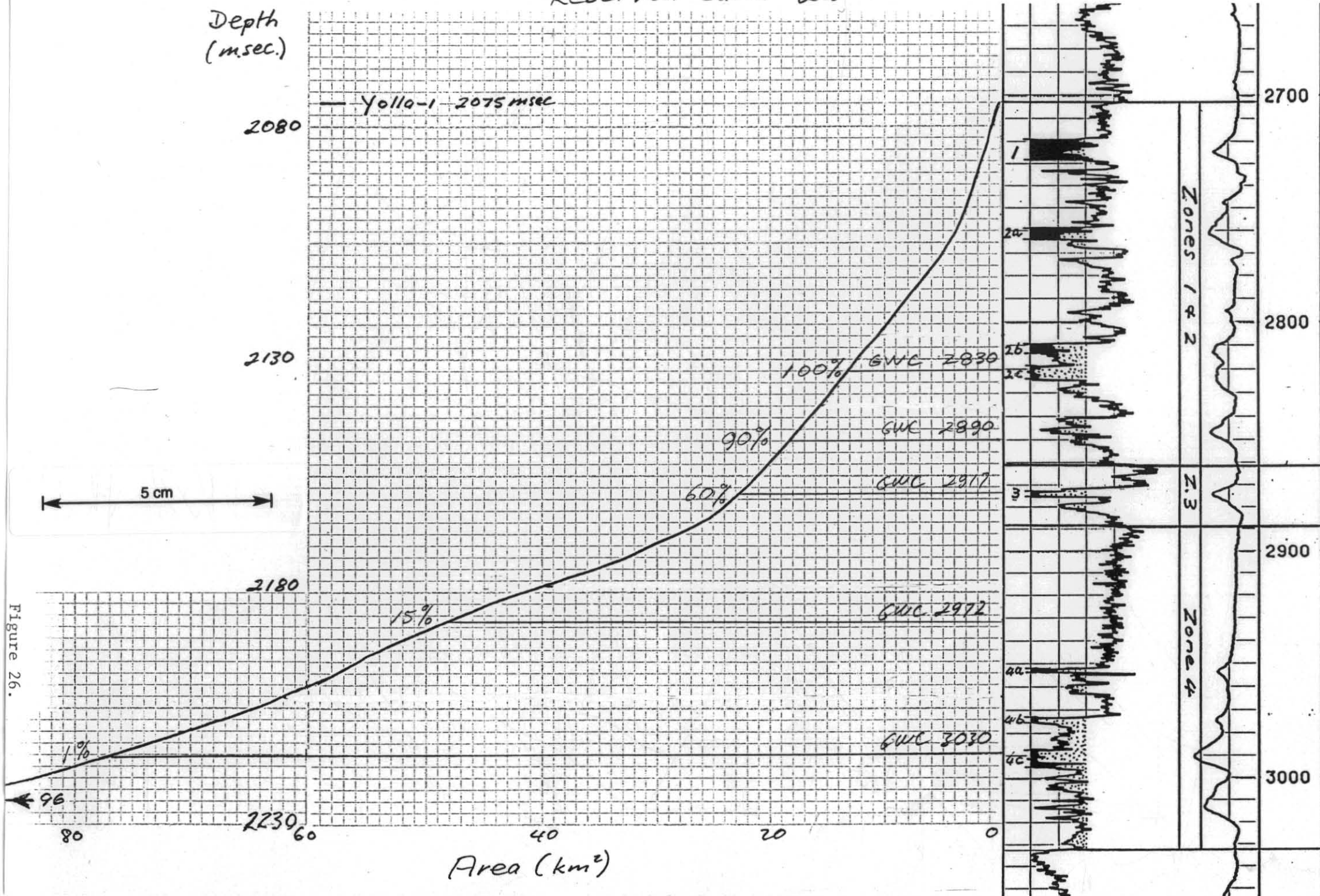


Figure 26.

499054

Reservoir Sand 2b.

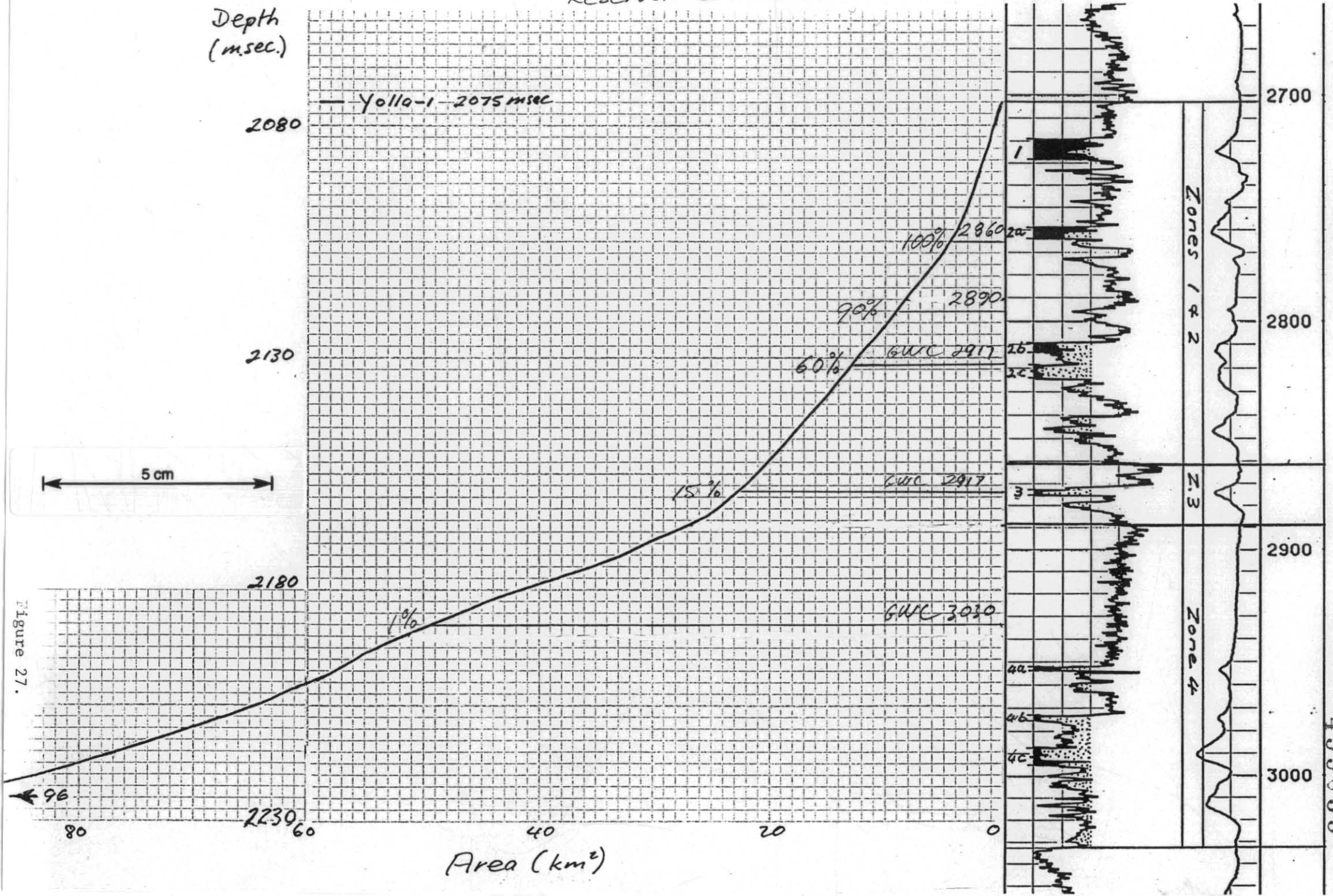


Figure 27.

499055

Reservoir Sand 2c.

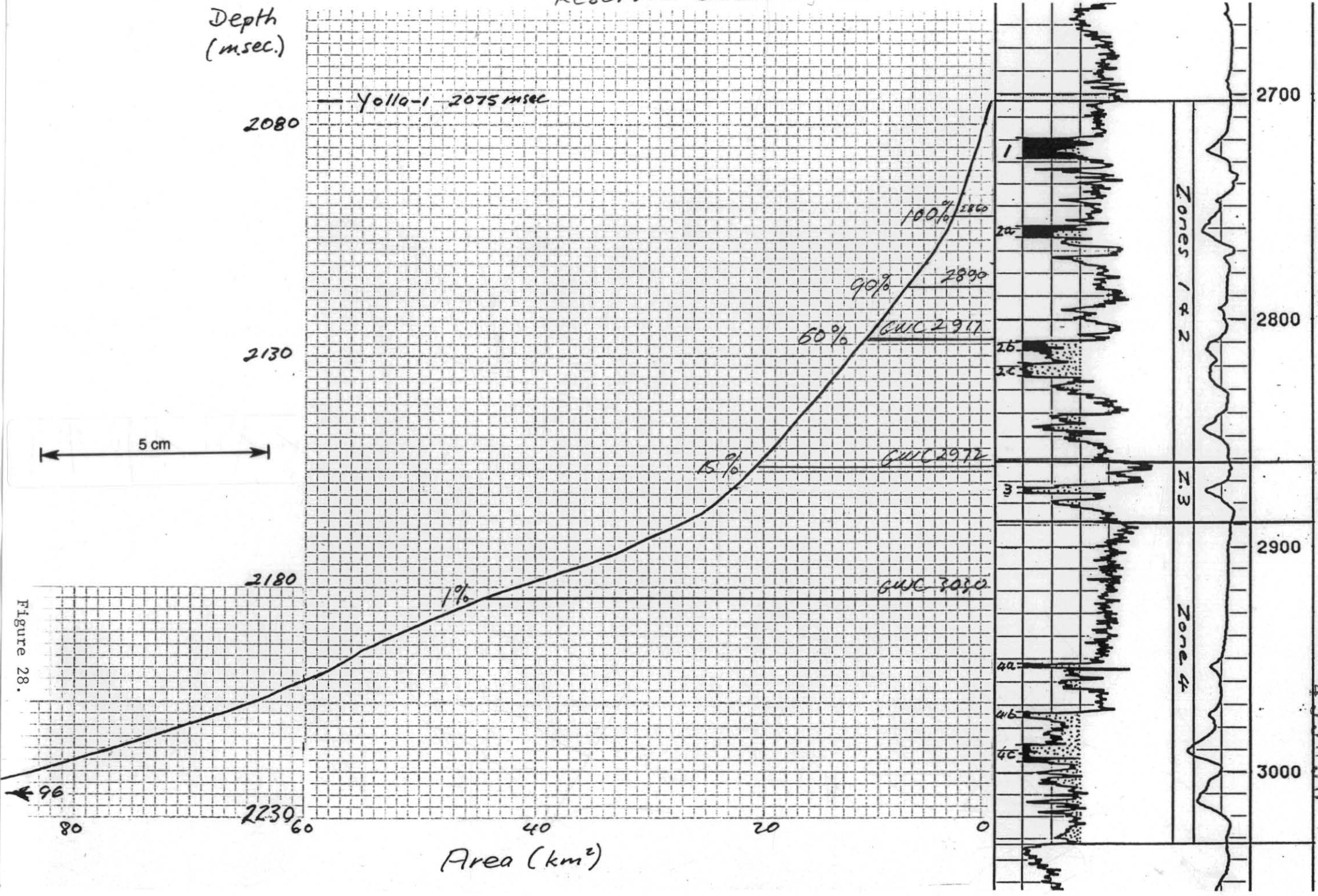


Figure 28.

Reservoir Sands 2 other.

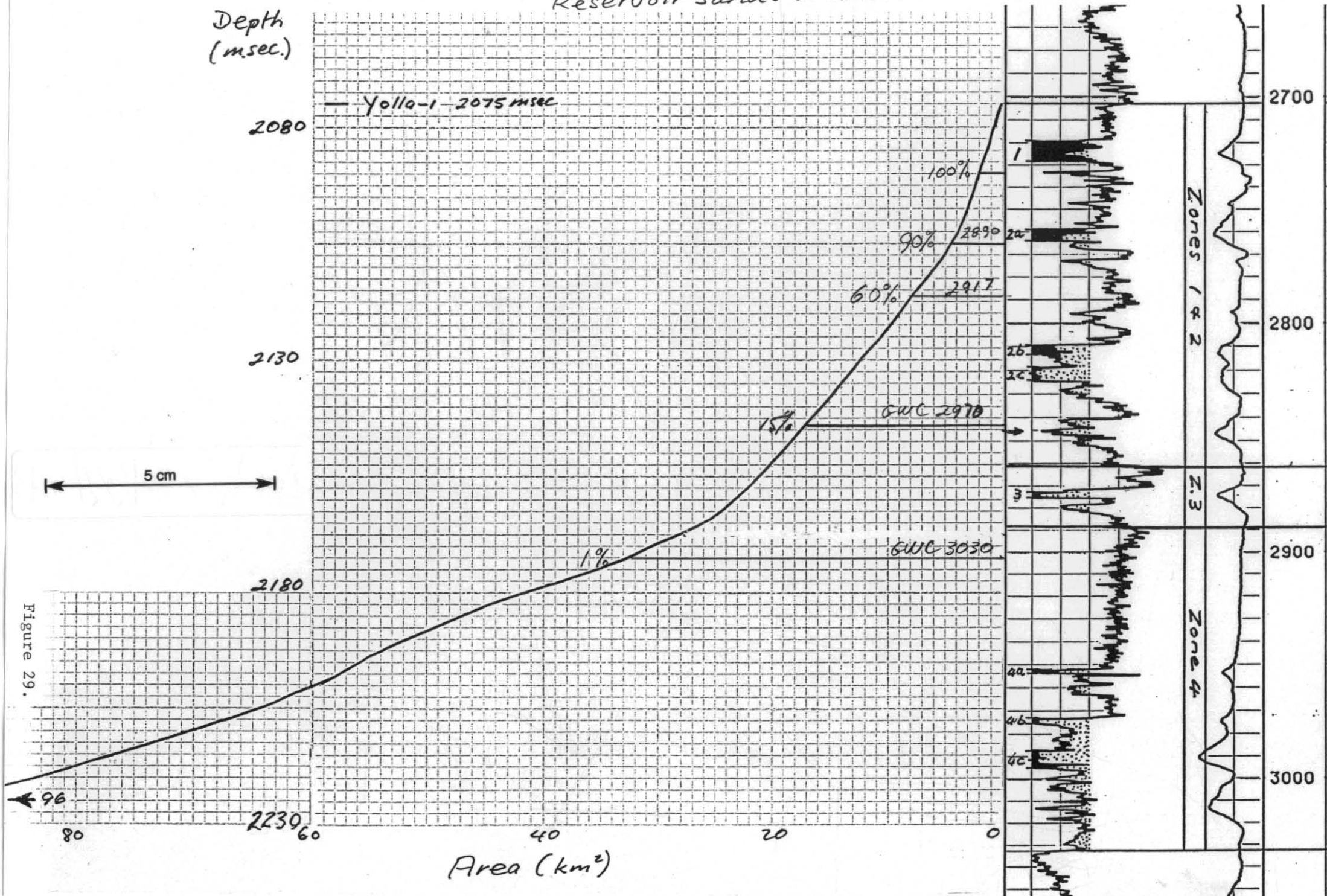


Figure 29.

499057

Reservoir Sand 3

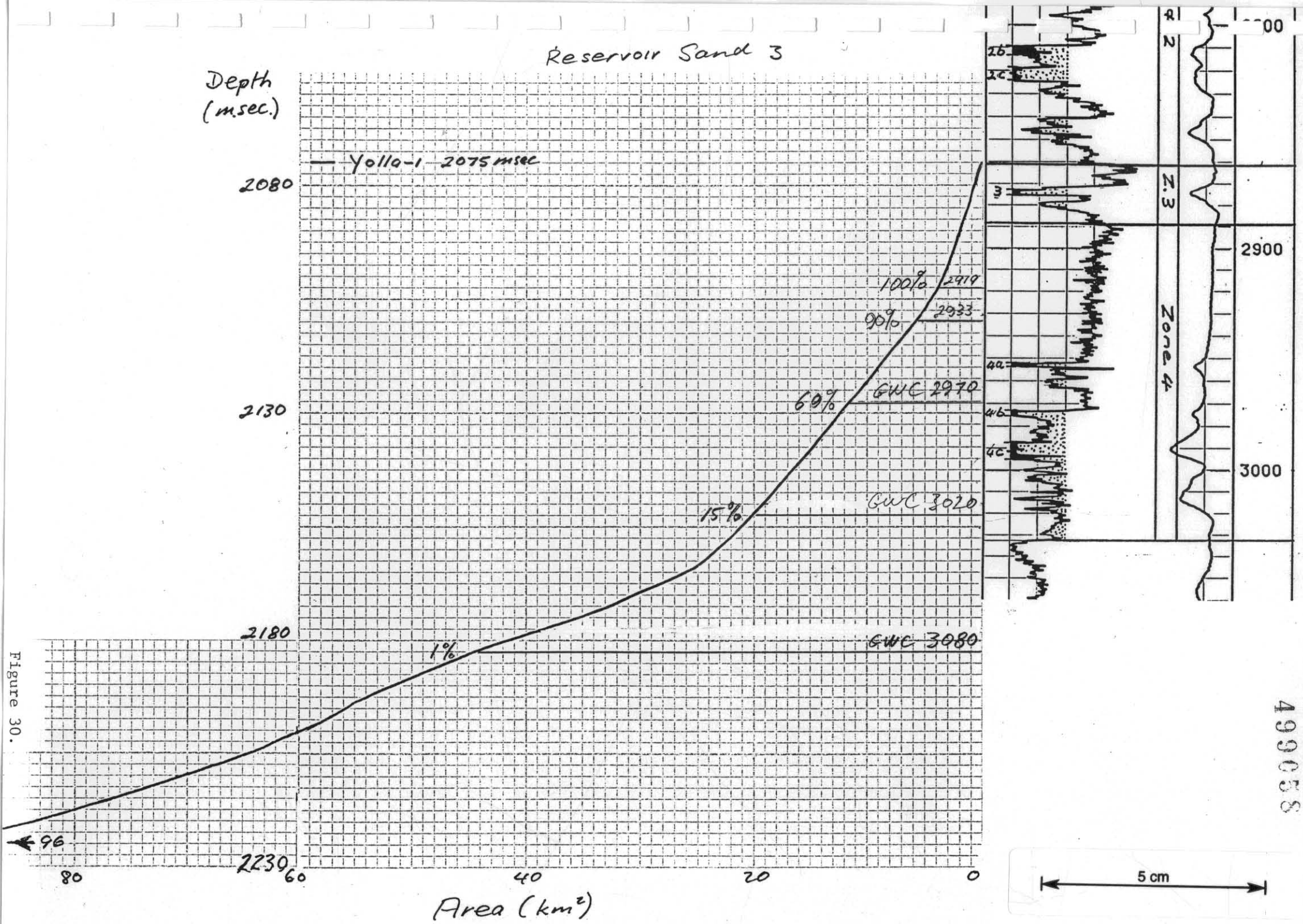


Figure 30.

499058

Reservoir Sands 3 other.

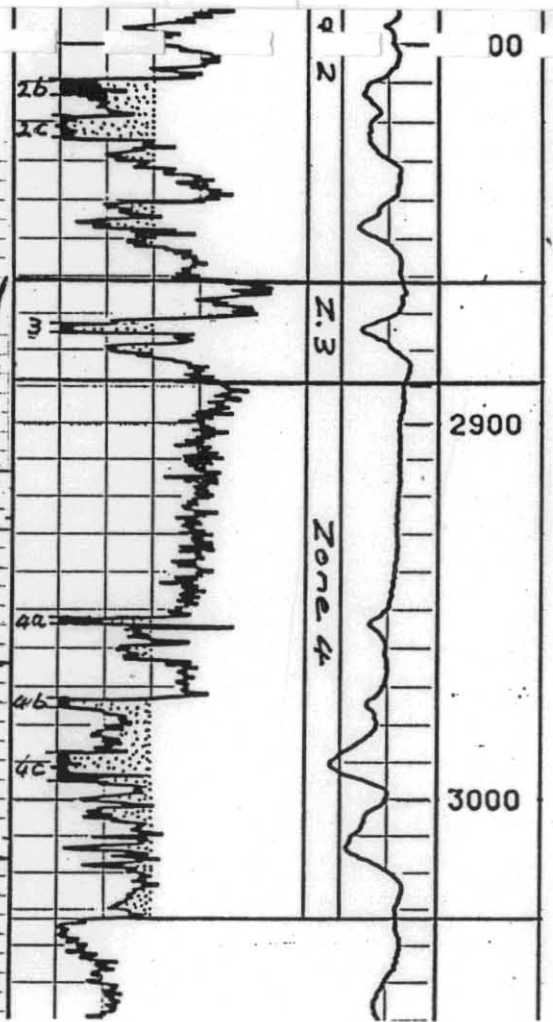
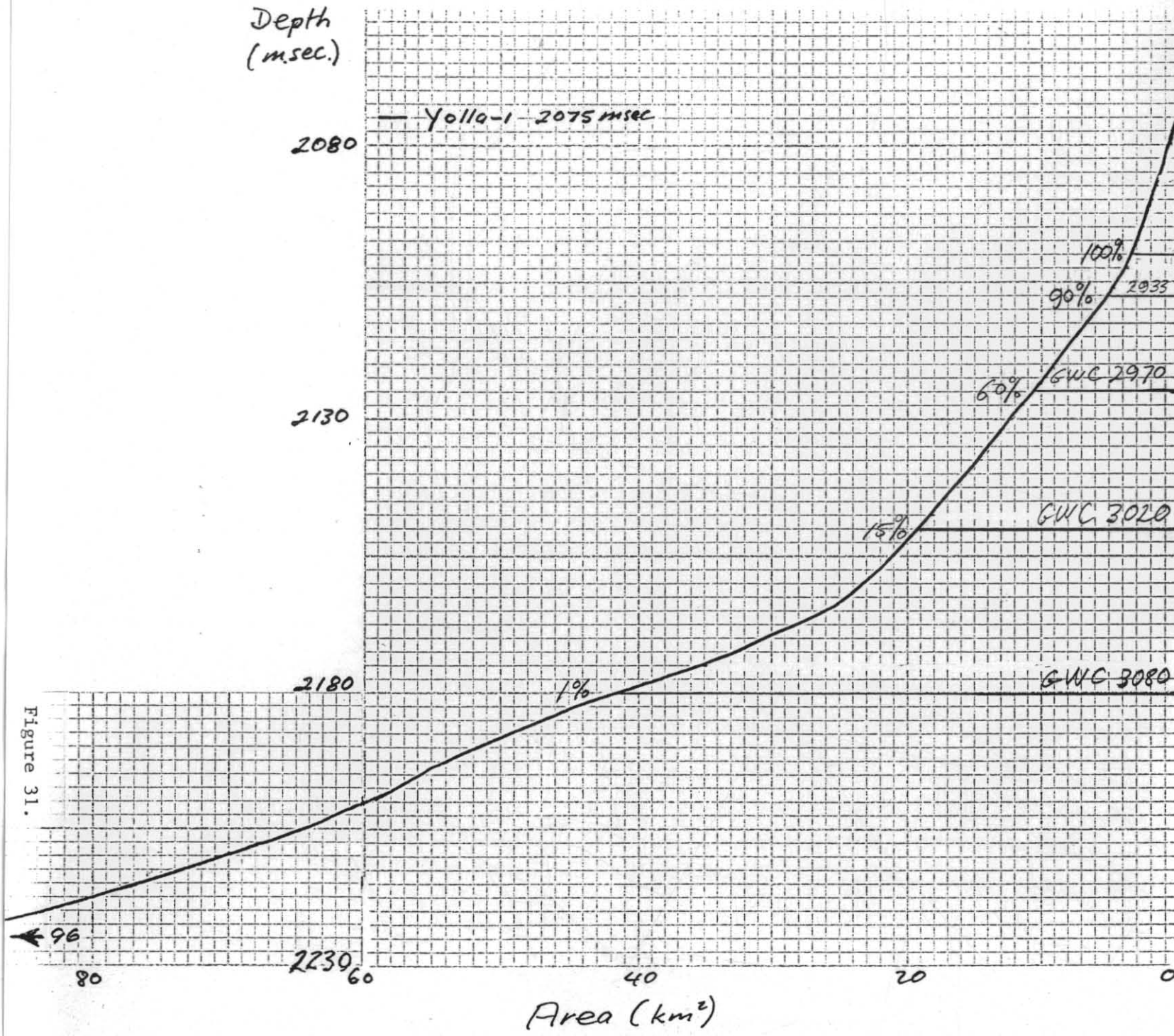


Figure 31.

499059

Reservoir Sand 4a

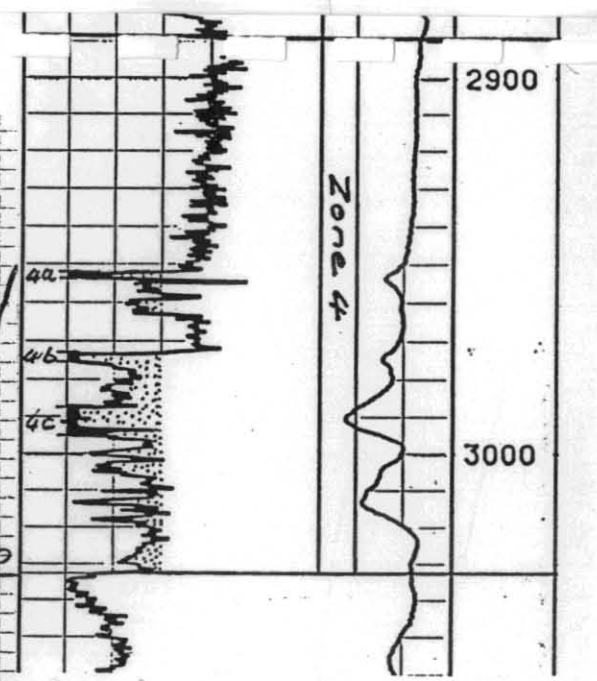
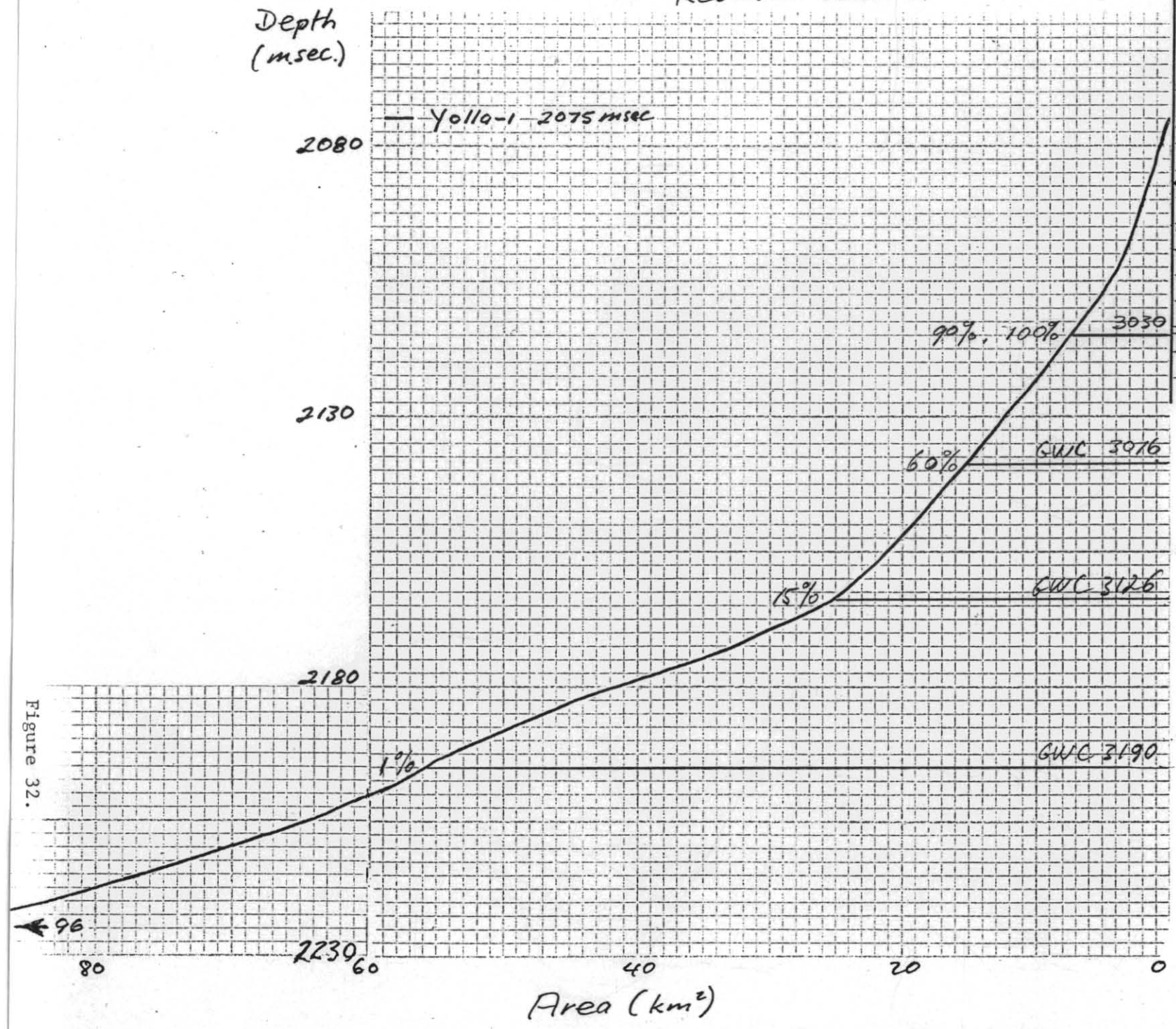
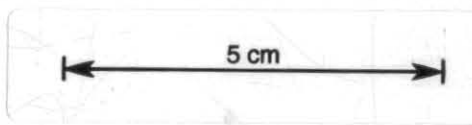


Figure 32.

499060



Reservoir Sand 4b.

Depth (msec.)

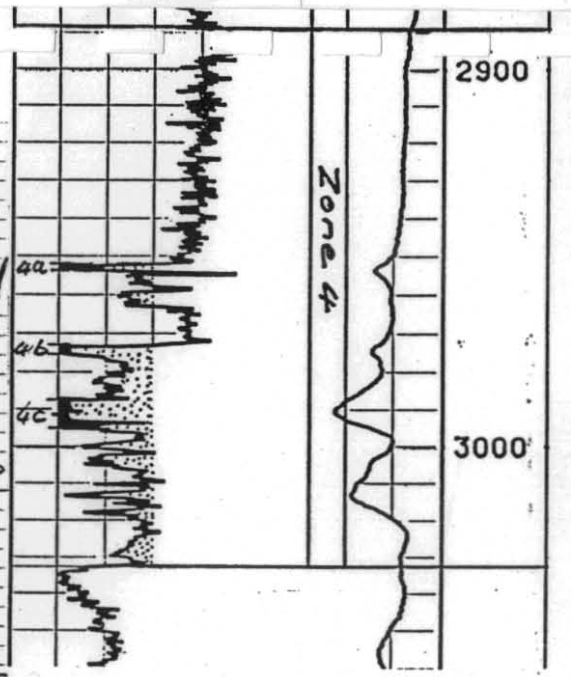
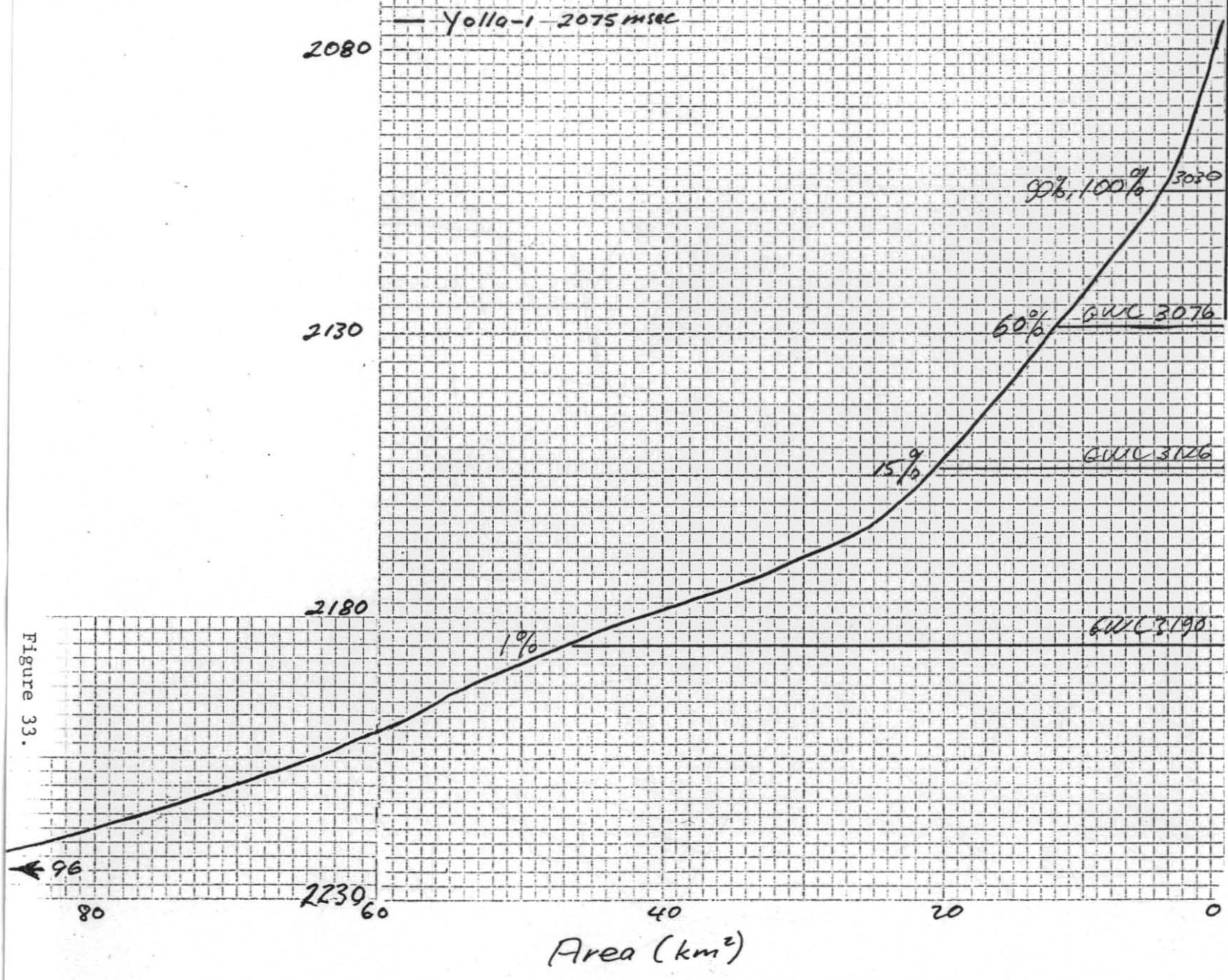
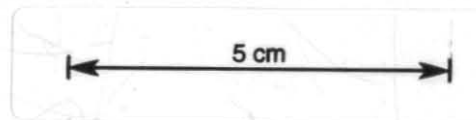


Figure 33.



499061

Reservoir Sand 4c

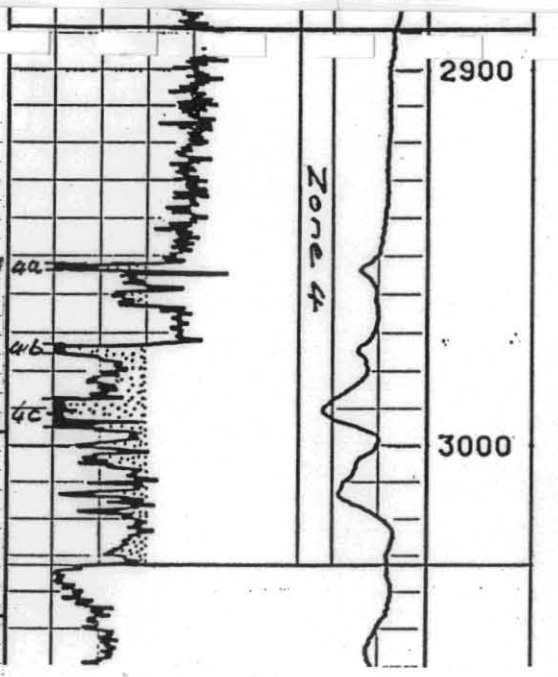
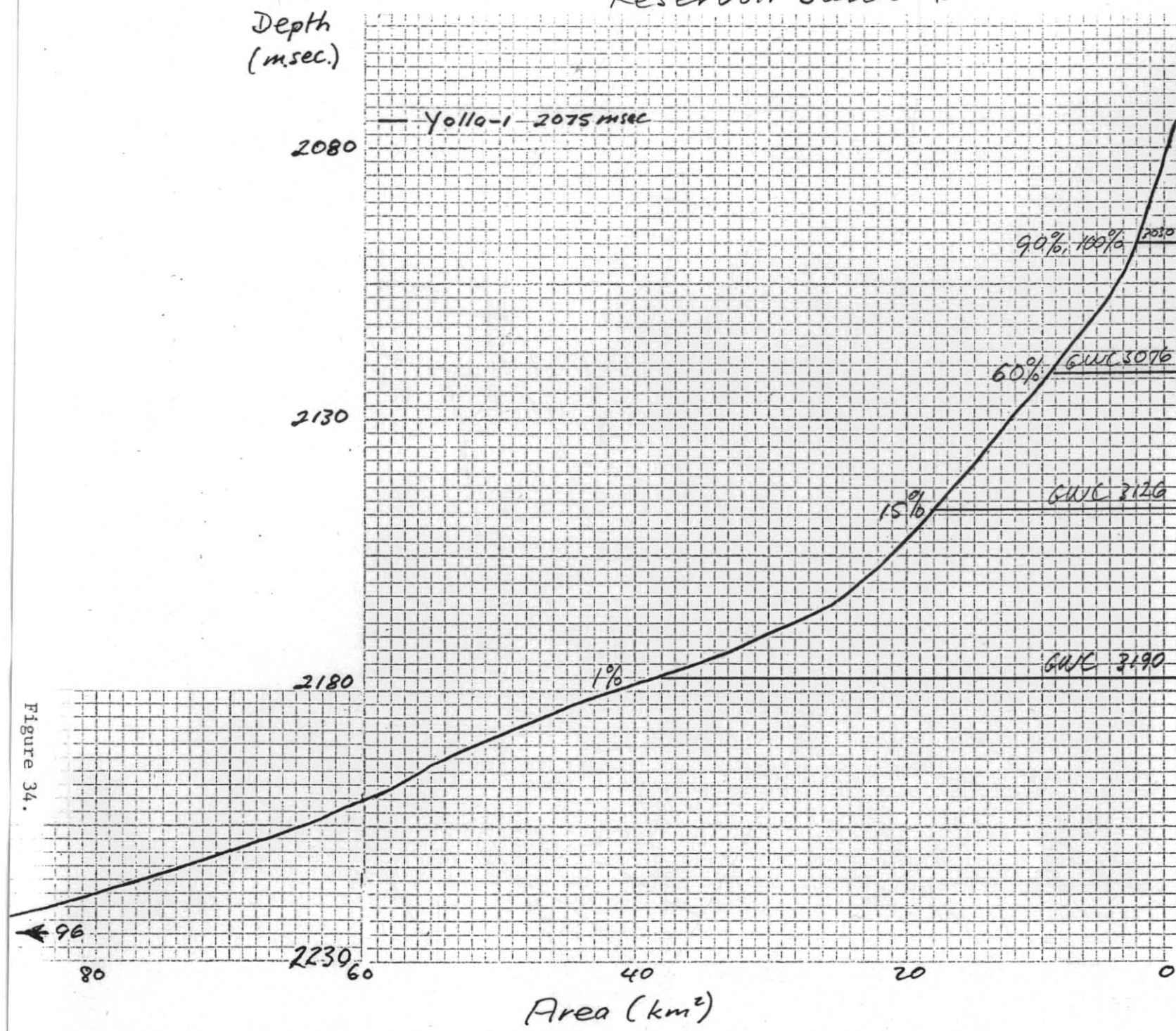
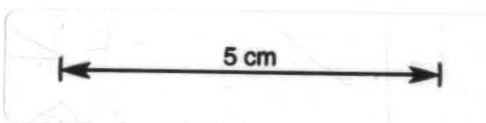


Figure 34.

499062



Reservoir Sands & other.

Depth
(msec.)

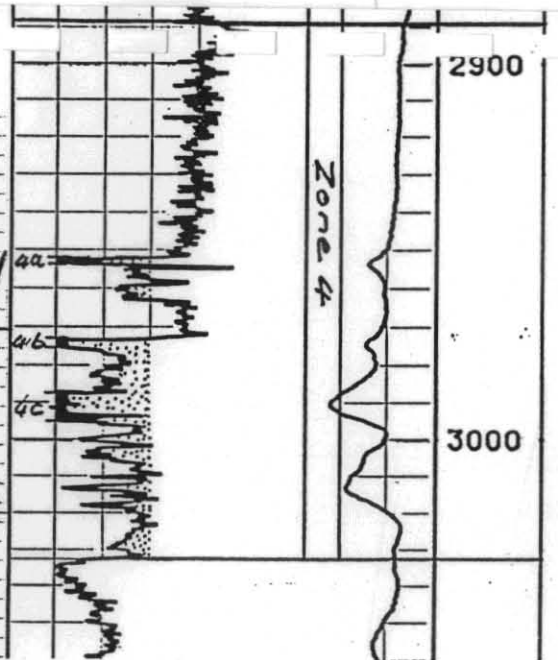
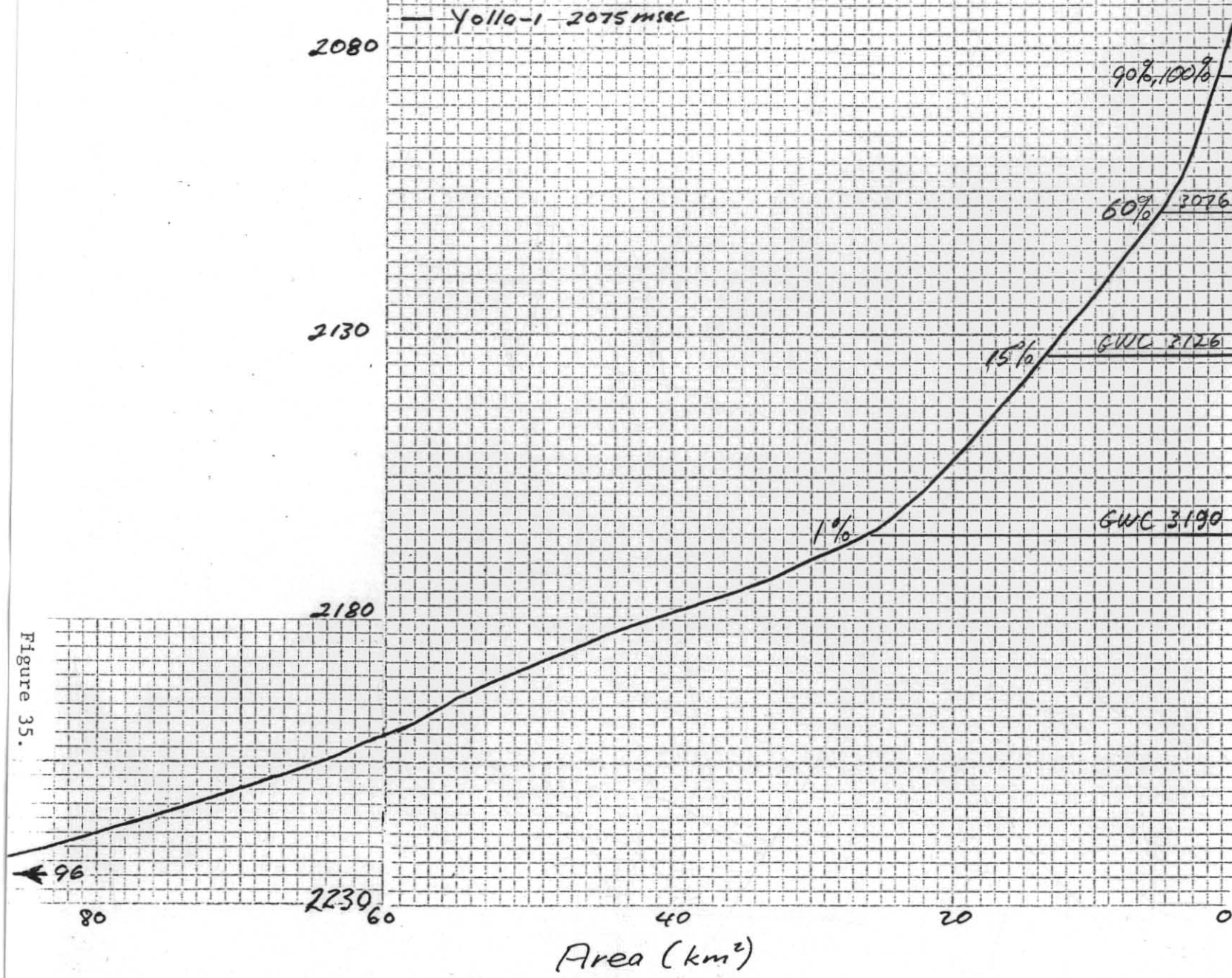
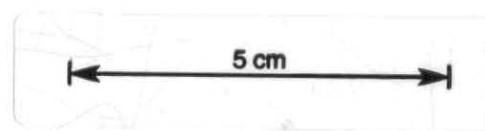


Figure 35.

499063



499064

<i>Reservoir Sand</i>	Depth Interval	Area	Net	Porosity,	Water	Gas	Gas-
	(m KB)	A (km ²)	Thickness h(m)	phi (%)	satura- tion, Sw (%)	Expan- sion Fac- tor, E (scf/rcf)	in-place GIP (x10 ⁹ m ³) (BCF)
1.	2718.0 to 2728.5		10.5	15	33	237	
2a.	2758.0 to 2764.0		6.0	18	28	238	
2b.	2809.0 to 2813.5		4.5	17	29	238	
2c.	2818.0 to 2825.0		8.0	20	25	238	
<i>Other</i> 3.	2873.0 to 2875.0		2.0	18	39	241	
4a.	2952.0 to 2954.0		2.0	18	14	248	
4b.	2973.0 to 2975.5		2.5	17	21	248	
4c. <i>Other</i>	2987.0 to 2995.0		8.0	20	18	248	

Probability 100%

Reservoir Sand	Depth Interval (m KB)	Area $A(\text{km}^2)$	Net Thick- ness h(m)	Poro- sity, phi (%)	Water satura- tion, Sw (%)	Gas Expan- sion Fac- tor, E (scf/rcf)	Gas- in-place GIP _g ($\times 10^9 \text{m}^3$)	(BCF)
	1.	2718.0 to 2728.5	20	10.5	15	33	237	5.002
2a.	2758.0 to 2764.0	13	6.0	18	28	238	2.406	84.93
2b.	2809.0 to 2813.5	4	4.5	17	29	238	0.517	18.253
2C.	2818.0 to 2825.0	3	8.0	20	25	238	0.857	30.245
Other		2	10.0	15	33	238	0.478	16.887
3.	2873.0 to 2875.0	4	2.0	18	39	241	0.212	7.473
Other		4	2.0	15	33	241	0.194	6.40
4a.	2952.0 to 2954.0	7	2.0	18	14	248	0.537	18.973
4b.	2973.0 to 2975.5	4.5	2.5	17	21	248	0.375	13.227
4C.	2987.0 to 2995.0	3	8.0	20	18	248	0.976	34.457
Other		1	10.0	15	33	248	0.249	8.798
							11.803	416.6

499066

Probability 90%

Reservoir Sand	Depth Interval (m KB)	Area A (km ²)	Net Thick- ness h(m)	Porosity, phi (%)	Water satura- tion, Sw (%)	Gas Expan- sion Fac- tor, E (scf/rcf)	Gas- in-place GIP (x10 ⁹ m ³) (BCF)
	1.	2718.0 to 2728.5	27	10.5	15	33	237
2a.	2758.0 to 2764.0	18	6.0	18	28	238	3.331 117.59
2b.	2809.0 to 2813.5	9	4.5	17	29	238	1.666 58.796
2c.	2818.0 to 2825.0	7	8.0	20	25	238	1.999 70.571
Other		4	10.0	15	33	238	0.957 33.774
3.	2873.0 to 2875.0	5	2.0	18	39	241	0.265 9.341
Other		5	2.0	15	33	241	0.242 8.55
4a.	2952.0 to 2954.0	7	2.0	18	14	248	0.537 18.973
4b.	2973.0 to 2975.5	4.5	2.5	17	21	248	0.375 13.22
4c.	2987.0 to 2995.0	3	8.0	20	18	248	0.976 34.457
Other		1	10.0	15	33	248	0.249 8.798
							17.349 612.42

Figure 38.

499067

Probability 60%

Reservoir Sand	Depth Interval (m KB)	Area $A(km^2)$	Net Thick- ness h(m)	Poro- sity, phi (%)	Water satura- tion, Sw (%)	Gas Expan- sion Fac- tor, E (scf/rcf)	Gas- in-place GIP _g ($\times 10^9 m^3$)	(BCF)
	1.	2718.0 to 2728.5	40	10.5	15	33	237	10.003
2a.	2758.0 to 2764.0	22.5	6.0	18	28	238	4.164	146.991
2b.	2809.0 to 2813.5	13	4.5	17	29	238	1.681	59.322
2C.	2818.0 to 2825.0	11	8.0	20	25	238	3.142	110.899
Other		8	10.0	15	33	238	1.914	67.547
3.	2873.0 to 2875.0	11.5	2.0	18	39	241	.609	21.484
Other		10	2.0	15	33	241	.484	17.100
4a.	2952.0 to 2954.0	15	2.0	18	14	248	1.152	40.658
4b.	2973.0 to 2975.5	12	2.5	17	21	248	.833	29.393
4C.	2987.0 to 2995.0	9	8.0	20	18	248	2.928	103.372
Other		5	10.0	15	33	248	1.246	43.991
							28.156	993.91

Figure 39.

Probability 15%

Reservoir Sand	Depth Interval (m KB)	Area A (km ²)	Net Thick- ness h(m)	Porosity, phi (%)	Water satura- tion, Sw (%)	Gas Expan- sion Fac- tor, E (scf/rcf)	Gas- in-place GIP _g (x10 ⁹ m ³)	(BCF)
	1.	2718.0 to 2728.5	65	10.5	15	33	237	16.256
2a.	2758.0 to 2764.0	48	6.0	18	28	238	8.883	313.58
2b.	2809.0 to 2813.5	22	4.5	17	29	238	2.484	100.39
2c.	2818.0 to 2825.0	20.5	8.0	20	25	238	5.855	206.67
Other		17	10.0	15	33	238	4.066	143.54
3.	2873.0 to 2875.0	20	2.0	18	39	241	1.059	37.36
Other		19	2.0	15	33	241	0.920	32.49
4a.	2952.0 to 2954.0	25	2.0	18	14	248	1.920	67.76
4b.	2973.0 to 2975.5	20	2.5	17	21	248	1.665	58.79
4c.	2987.0 to 2995.0	18	8.0	20	18	248	5.857	206.74
Other		13	10.0	15	33	248	3.24	114.38
							52.205	1,843.0

Figure 40.

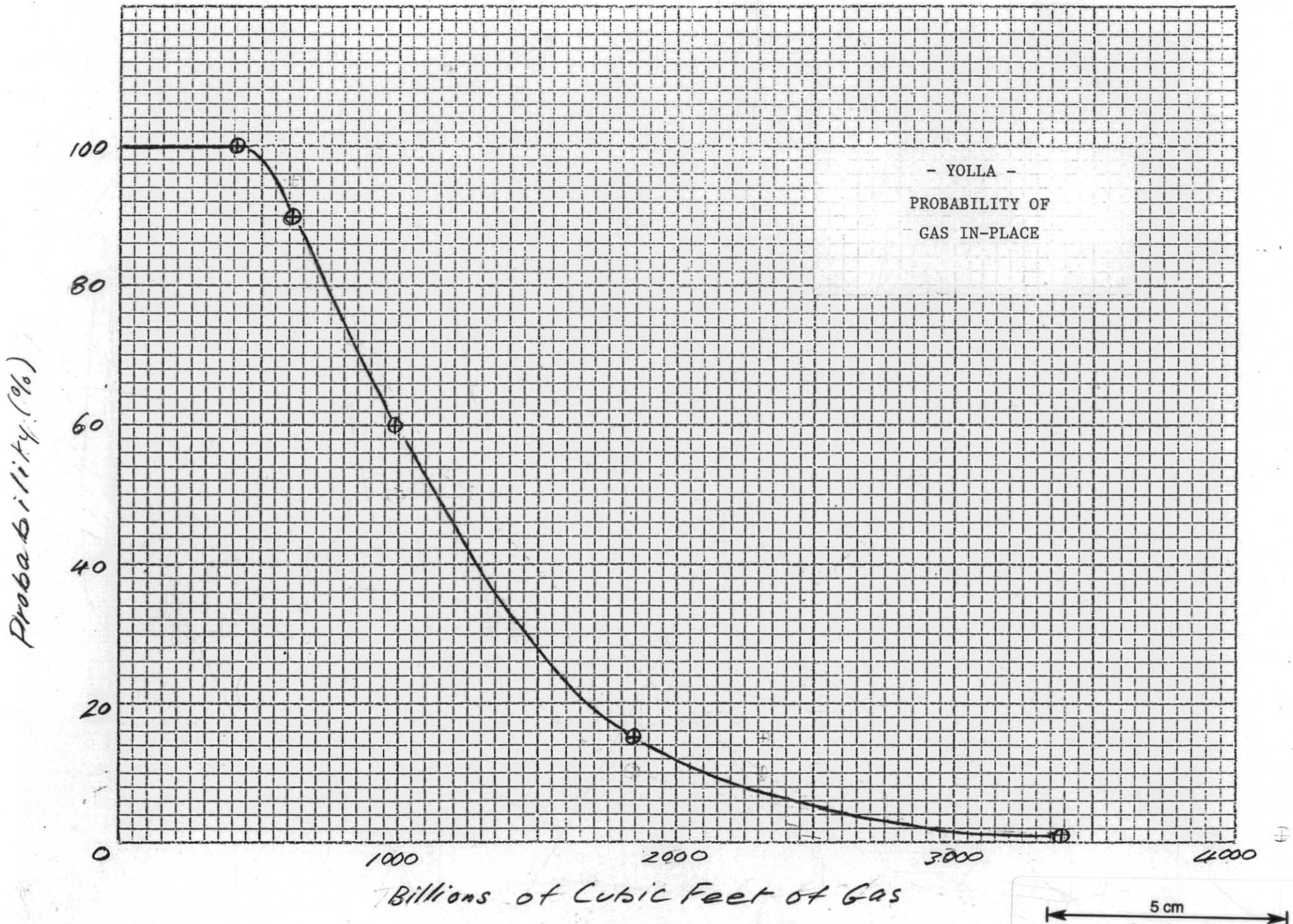


Figure 42.

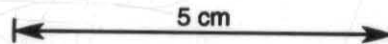
YUGLA #1
DST SUMMARY

499070

DST#	AVG FLOW			AVG FTP	AVG FBHP	SIBHP	SGR	API GR	COMMENTS
	MMCFD	BOPD	BWPD	PSIG	PSIG	PSIG			
1 (FLOW#1) 2809M- 2824.5M	10.2	420	TSTM	2716	4106	4197	.86	50.5	24285 GOR (41.2 BBLS/MMCF)/ CONDENSATE YELLOW/8-16% CO ₂ / 9214-9230' & 9243'-9264' PERF. 30/64" CHOKE.
1 (FLOW#2) 2809M- 2824M	15.1	580	TSTM	2533	4038	4197	.86	51.2	26034 GOR (38.4 BBLS/MMCF)/10- 25% CO ₂ /CONDENSATE YELLOW/40/ 64" CHOKE/SAME PERFS AS ABOVE
2 (FLOW#1) 1830M- 1835M	3.4	TSTM	-	957	2086	2690	-	-	MAKING TOO MUCH WATER ON 46/64" CHOKE/COULD NOT GET AN OIL LEVEL - CHOKE BACK/ PERF 5947'-6019' (1830-1835M)
2 (FLOW#2) 1830M- 1835M	2.2	TSTM	1675	1198	2412	2690	.81	48 -43.7	COULD NOT CHOKE BACK WATER ON A 32/64" CHOKE/CONDENSATE WAS A THIN LIGHT CRUDE COLOR LIQUID THAT TURNED TO WAX AT 60 F/PERFS SAME AS ABOVE.
2-A 1833.1M- 1833.7M	1.02	302	TSTM	1170	1984	2690	.87	45.5	PERFS 6013'-6015' (1833.1-1833.7M)/16/64" CHOKE/ 3376 GOR (296 BBLS/MMCF)/OIL WAS CARMEL IN COLOR AND TURNED TO WAX AT 68 F.
3 1813M- 1833.7M	11.8	892	0	950	1444	2690	.79	50.6	PERFS 5947'-6019' (1813-1831M)/80/64" CHOKE/GOR 13,229 (76 BBLS/MMCF)/OIL WAS DARK BROWN IN COLOR BUT DID NOT WAX UP.

Figure 43.

RJB011/JCW



Well-Stream Gas

Component	Mol Percent	Molecular Weight (lb/Mol)	Weight (pounds - lb)	Liquid Density (lb/U.S. gallons)	Liquid Volume (U.S. gallons)	Liquid Volume (STB)
Hydrogen Sulphide	0.00	34.08	0.00	6.553	0.00	0.000
Carbon Dioxide	18.86	44.01	830.03	6.808	121.92	2.903
Nitrogen	0.20	28.01	5.60	6.748	0.83	0.020
Methane	63.87	16.04	1024.47	2.500	409.79	9.757
Ethane	7.64	30.07	229.73	2.960	77.61	1.848
Propane	3.75	44.10	165.38	4.221	39.18	0.933
iso-Butane	0.65	58.12	37.78	4.684	8.07	0.192
n-Butane	1.04	58.12	60.44	4.861	12.43	0.296
iso-Pentane	0.38	72.15	27.42	5.196	5.28	0.126
n-Pentane	0.39	72.15	28.14	5.252	5.36	0.128
Hexanes	0.54	86.18	46.54	5.527	8.42	0.200
Heptanes+	2.68	100.21	268.56	5.729	46.88	1.116
		Average		TOTAL		
TOTAL MOLES	100.00	M.W.	- 27.24	VOLUME	- 735.77	17.519

Sales Gas to Raw Gas Ratio = 0.7151

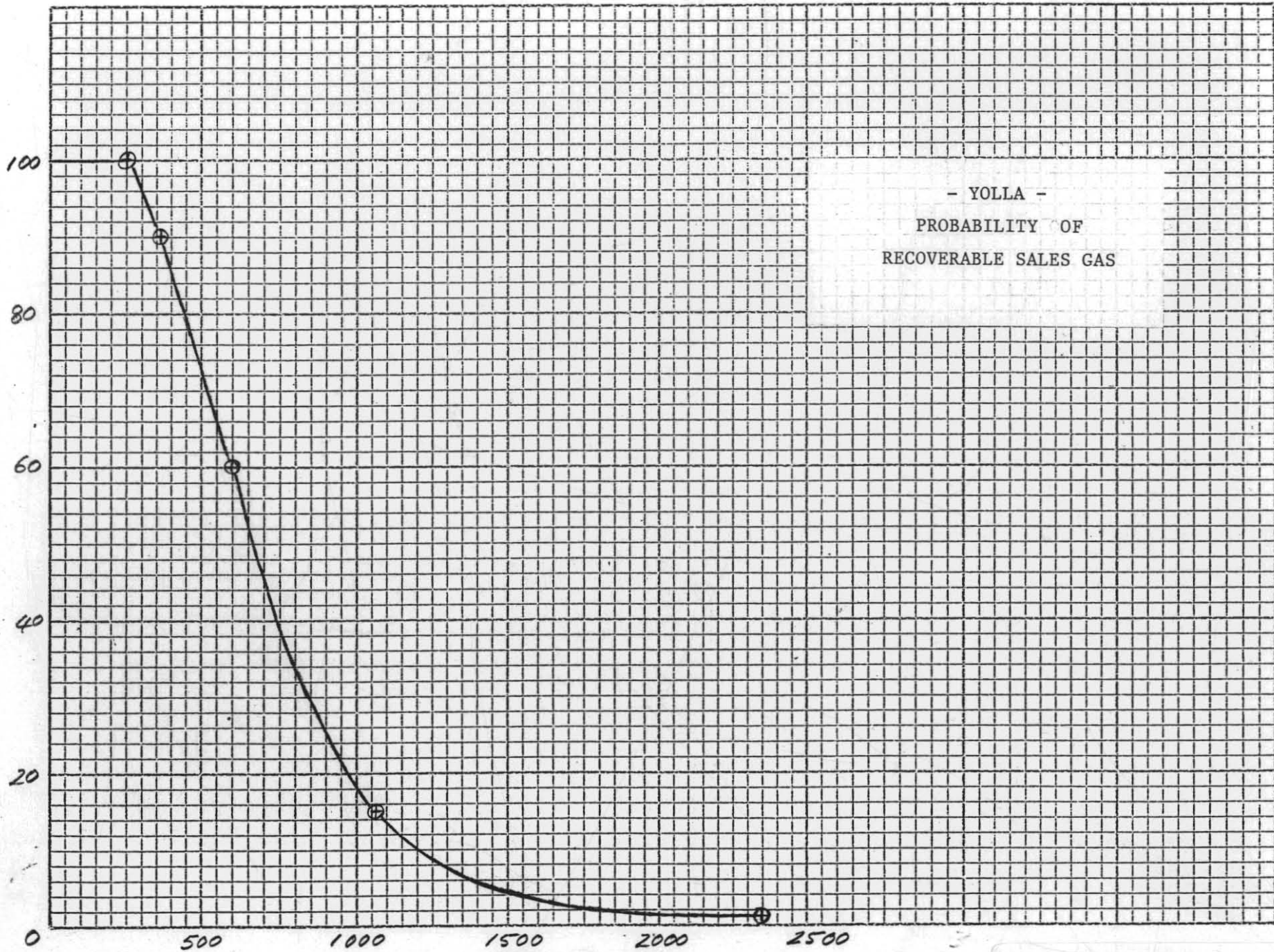
Volume occupied by 100 moles of well-stream gas = 37970 SCF

Gas Deviation Factor = 0.907 (source: DST-1 Reservoir Fluid Study)

LPG yield per million SCF of Raw Gas = 37.42 STB

Condensate yield per million SCF of Raw Gas = 41.35 STB

Probability (%)



- YOLLA -
PROBABILITY OF
RECOVERABLE SALES GAS

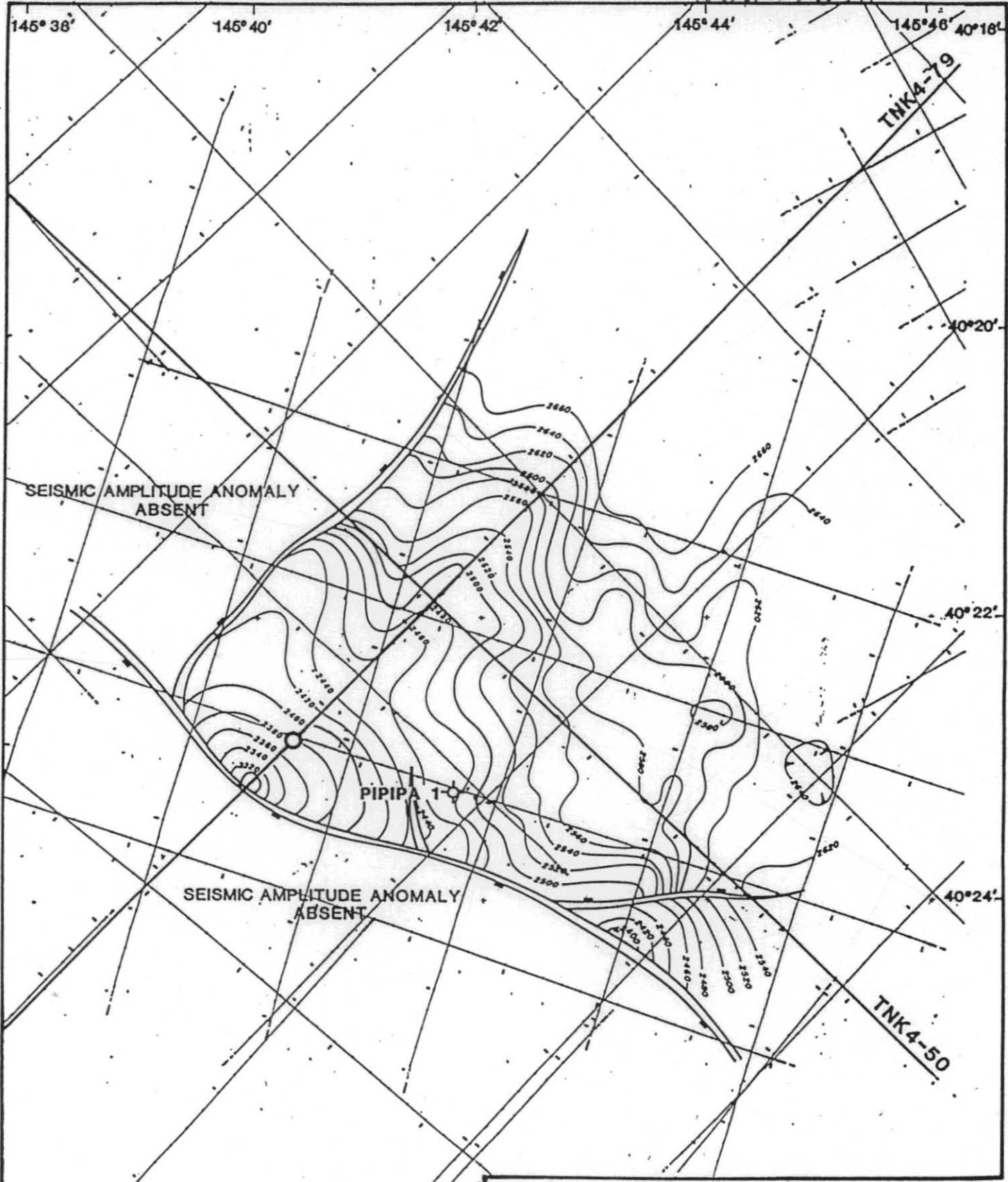
Billions of Cubic Feet of Gas

5 cm

Figure 45.

499072

499073



SAGASCO Resources Ltd.

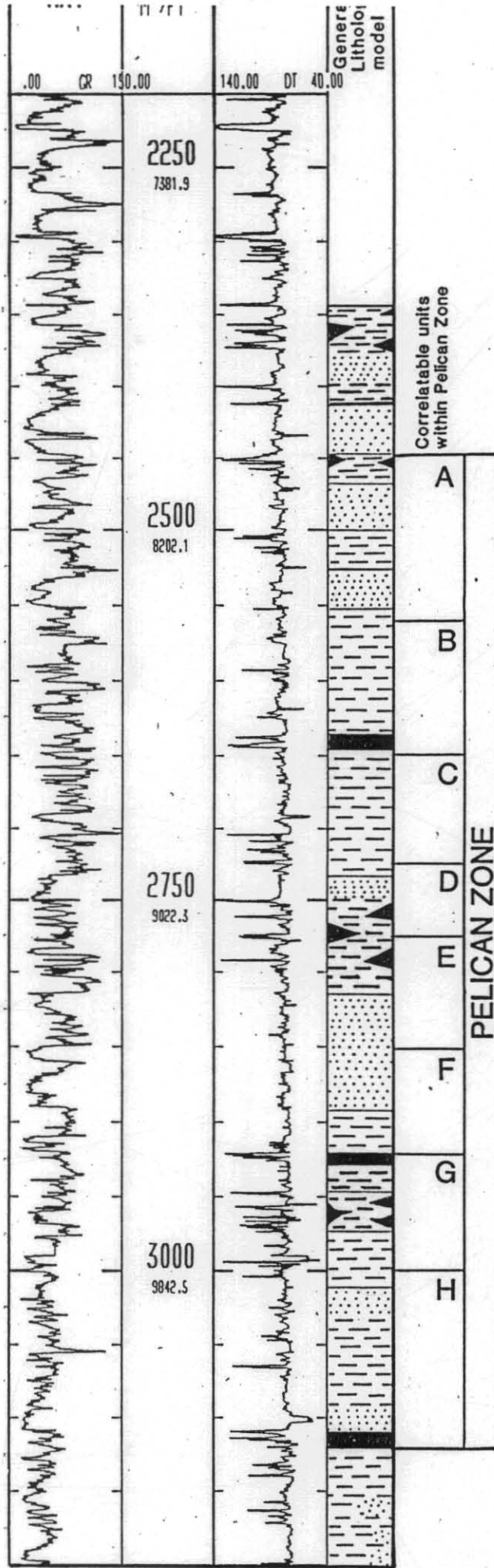
BASS BASIN - SOUTH AUSTRALIA
T-22-P BLOCK

**PIPIPA DEEP PROSPECT
TOP SEISMIC AMPLITUDE
ANOMALY-DEPTH STRUCTURE**

AUTHOR A. Waldron	DATE June 1990	PLAN PIP00.7677
DRAWN P. Oldham	DATUM M.S.L.	CHECKED
SCALE As shown	CONTOUR INTERVAL	

Figure 46.

499074



5 cm

Figure 47.

5 cm

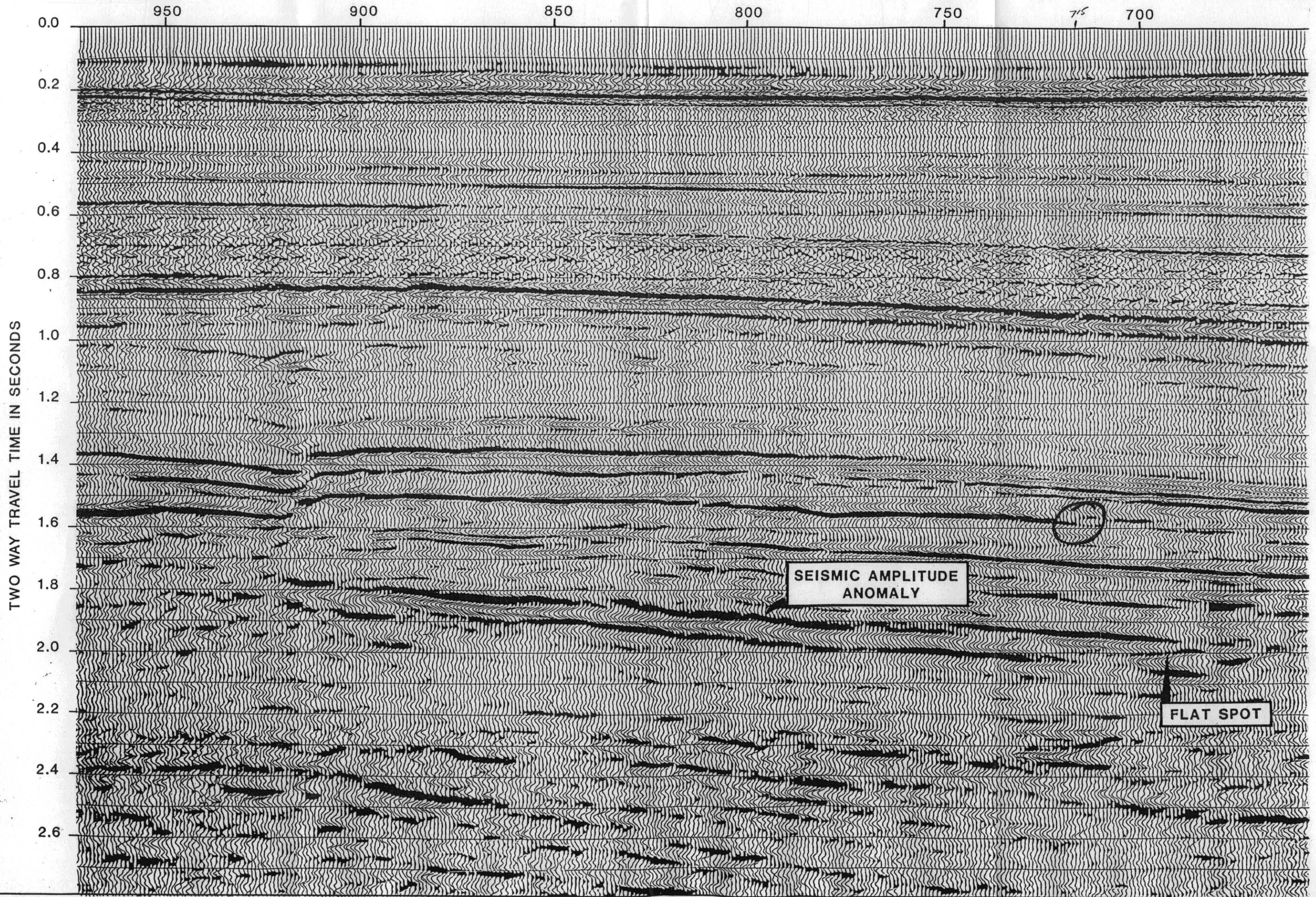
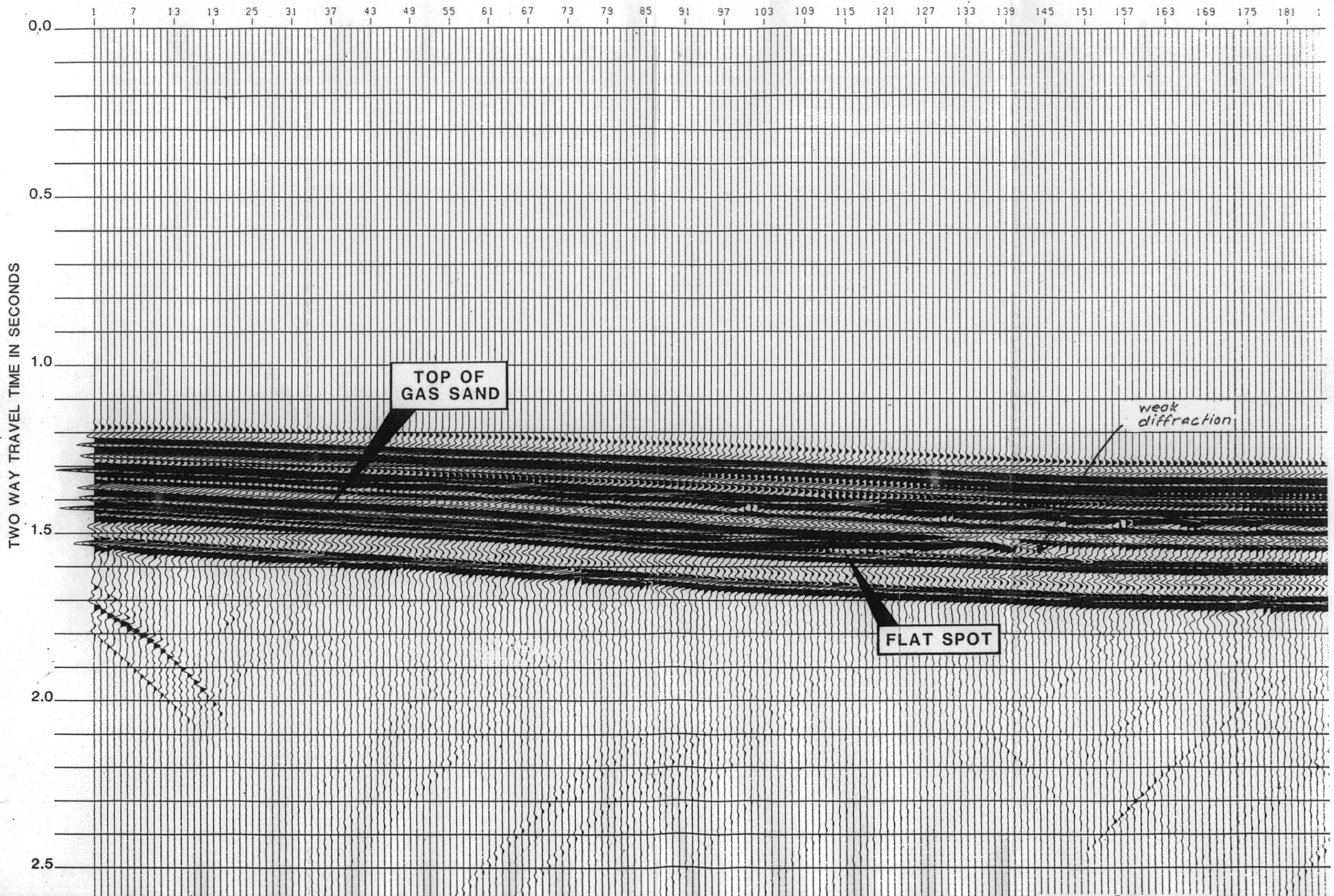


Figure 48.

SOURCE COORD. 2500 2900 3300 3700 4100 4500 4900 5300 5700 6100 6500 6900 7300 7700 8100 8500 8900 9300 9700 10100 10500 10900 11300 1170



TWO WAY TRAVEL TIME IN SECONDS

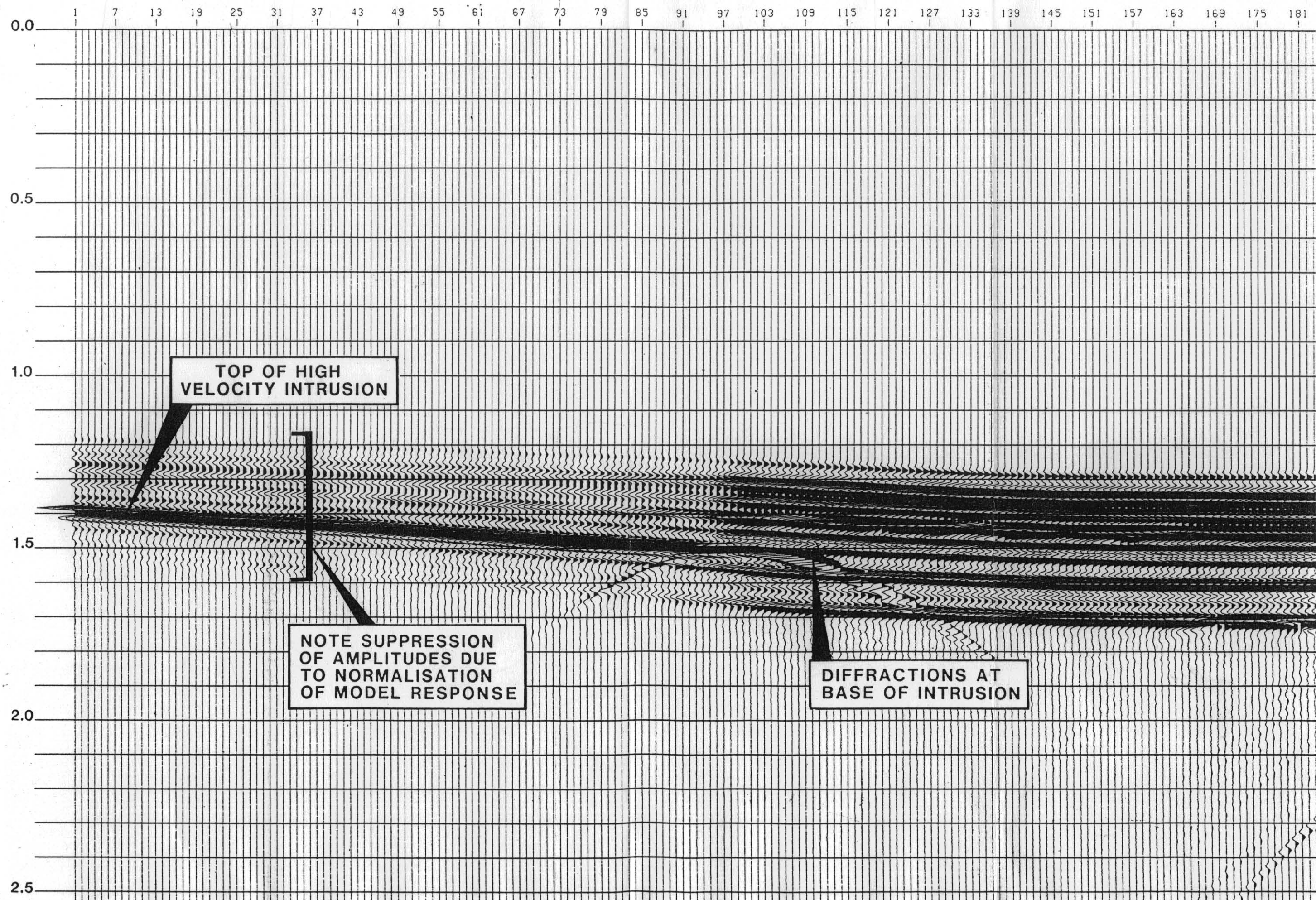
5 cm

Figure 49.

SHOT NO. 115 117 119 121 123 125 127 129 131 133 135 137 139 141 143 145 147 149 151 153 155 157 159
 SOURCE COORD. 2500 2900 3300 3700 4100 4500 4900 5300 5700 6100 6500 6900 7300 7700 8100 8500 8900 9300 9700 10100 10500 10900 11300

499077

TWO WAY TRAVEL TIME IN SECONDS



5 cm

Figure 50.

- PIPPA -
PROBABILITY OF
RECOVERABLE SALES GAS

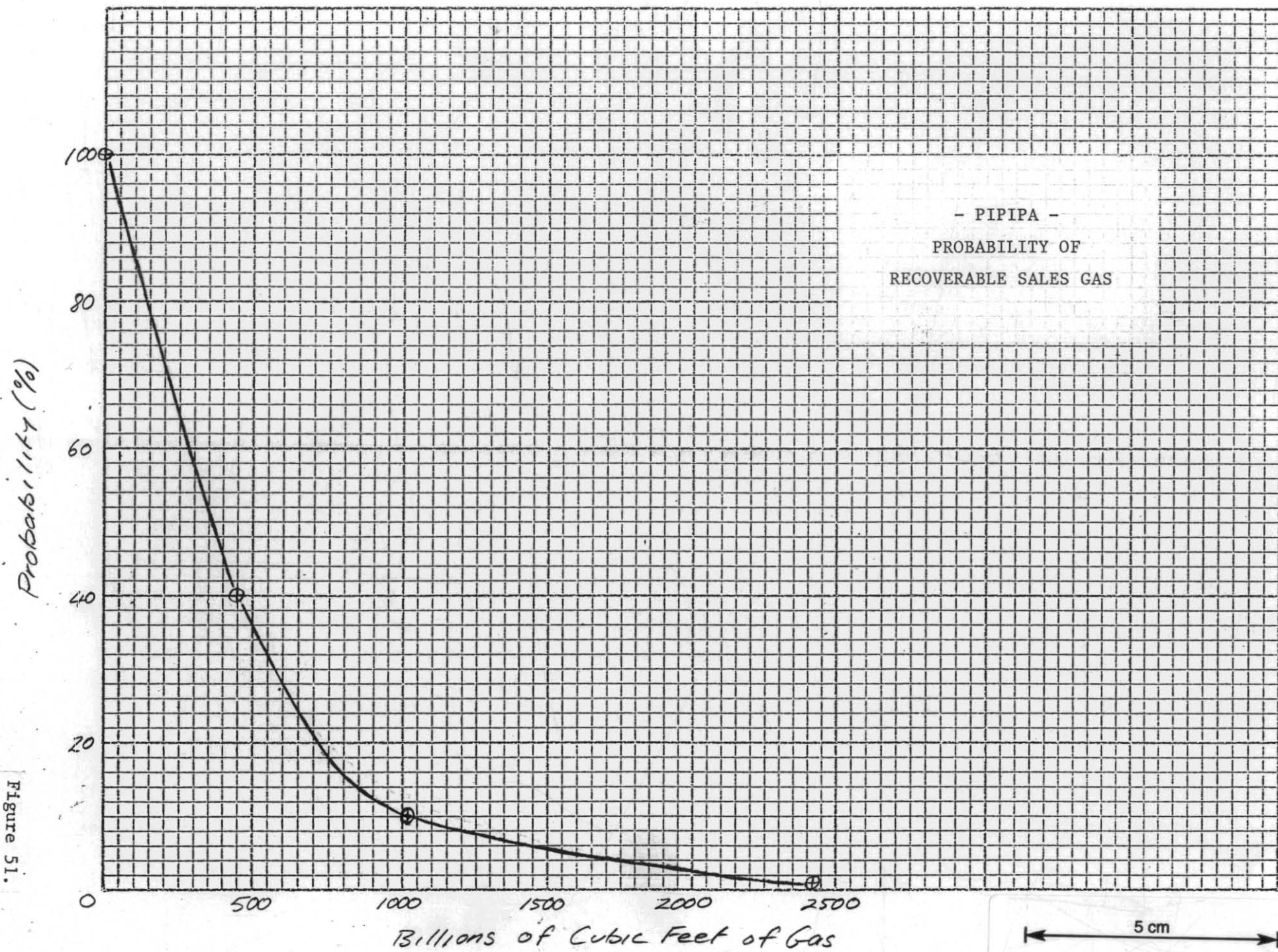


Figure 51.

499078

499079

DURROON-1

5 cm

69 69 69 68 67 66 750
450 500 550 600 650 700

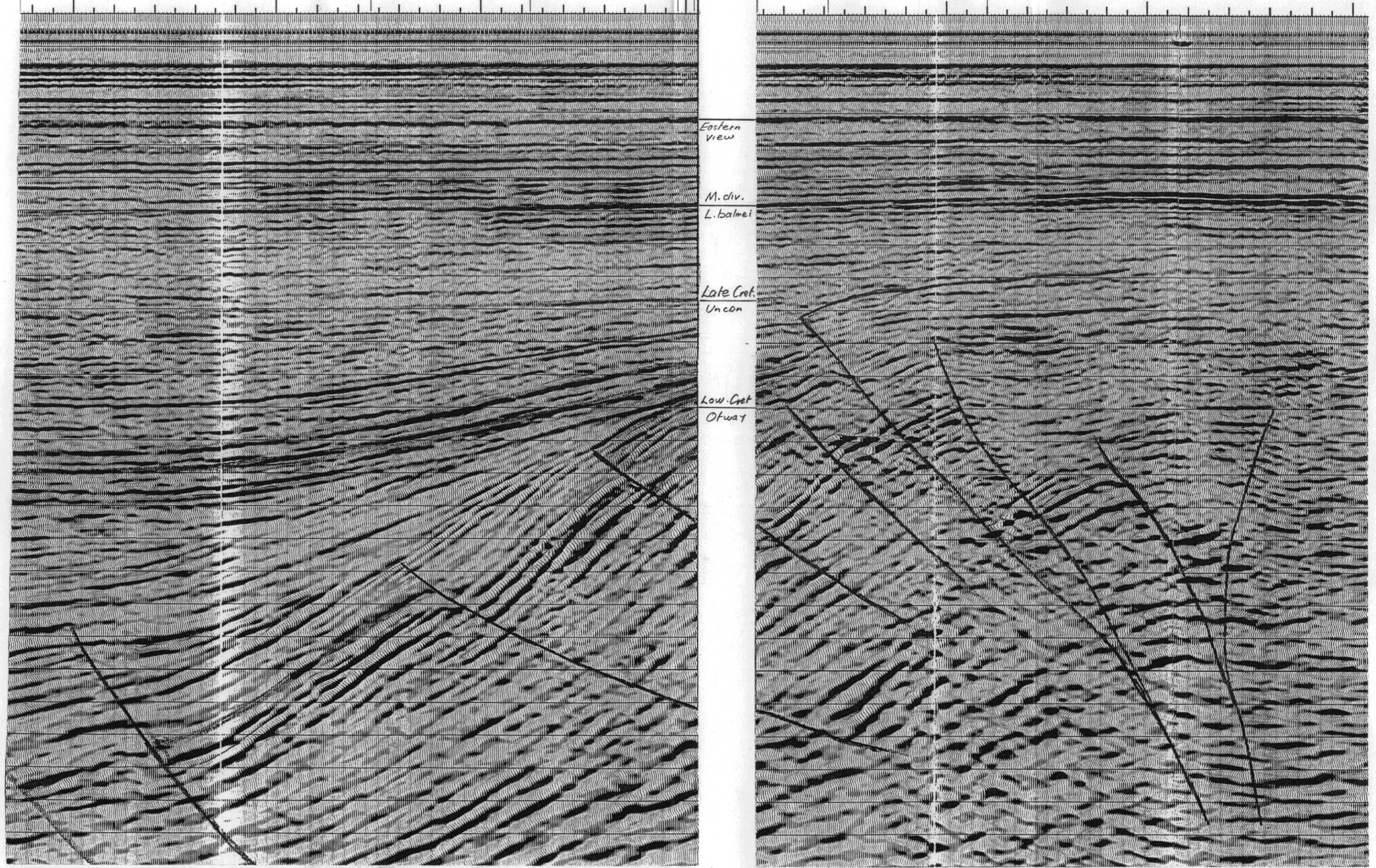


Figure 52.

499080

5 cm

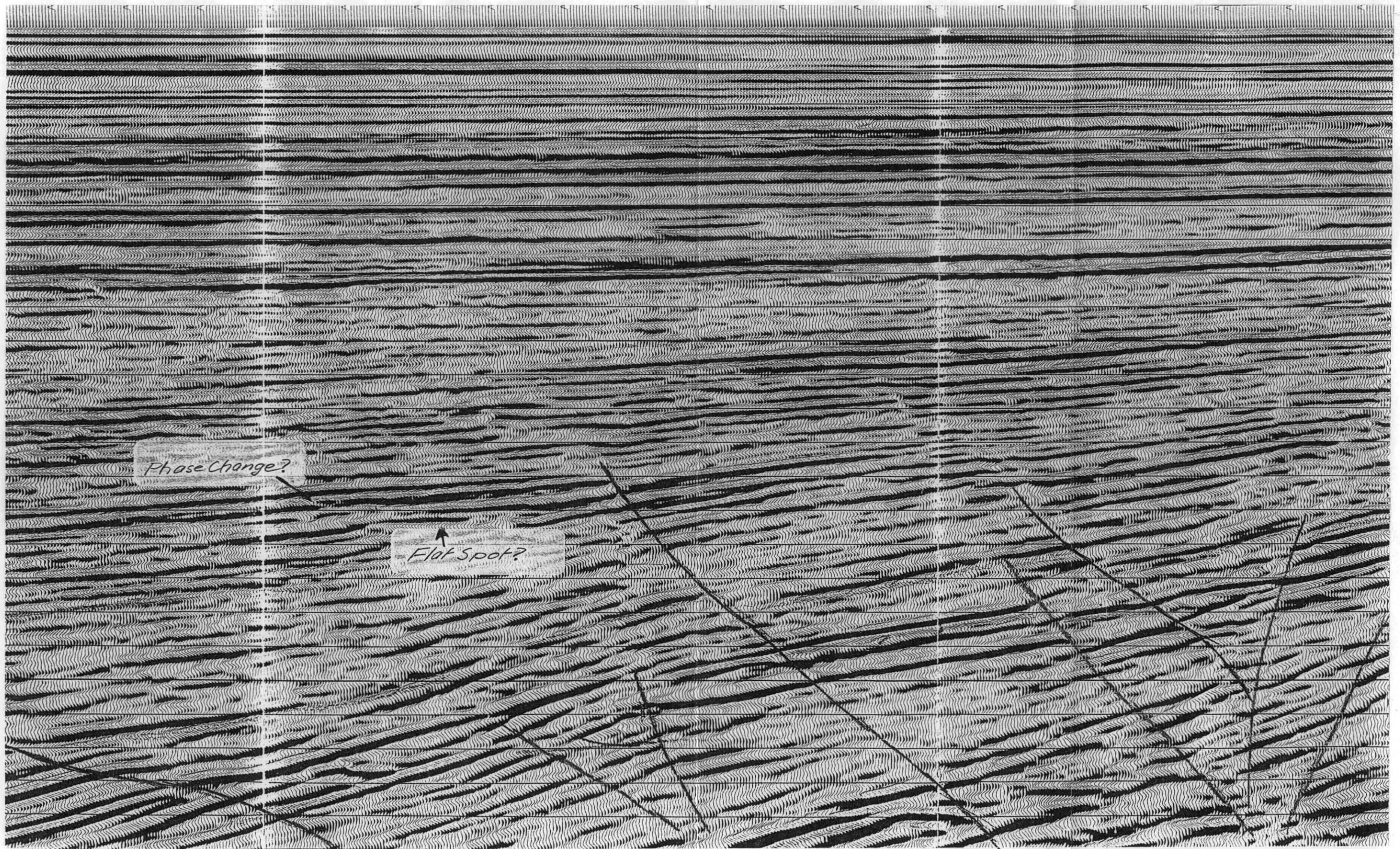


Figure 53.

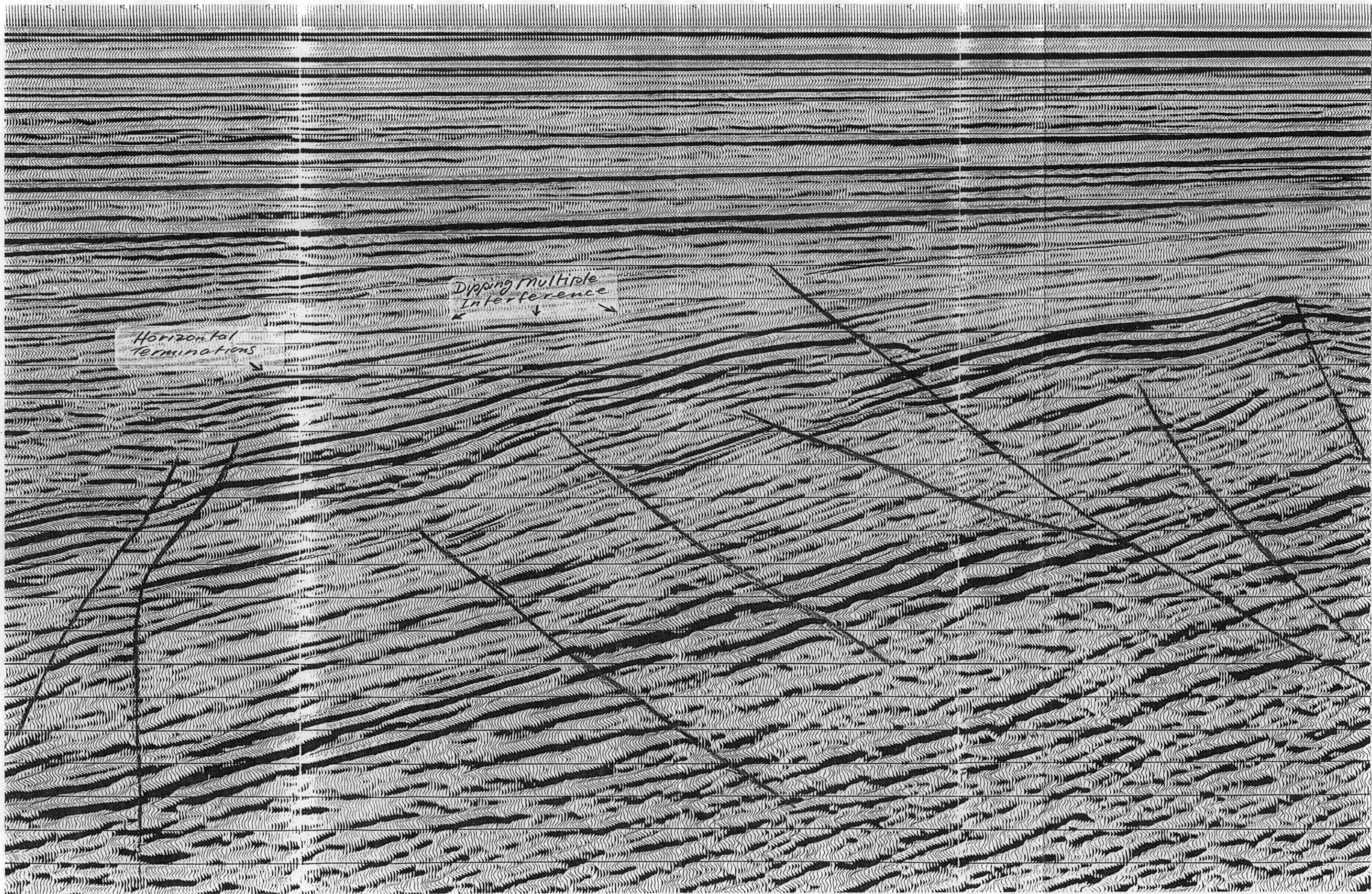


Figure 54.

1-0

499082

2-0

3-0

TOP EASTERN VIEW GROUP

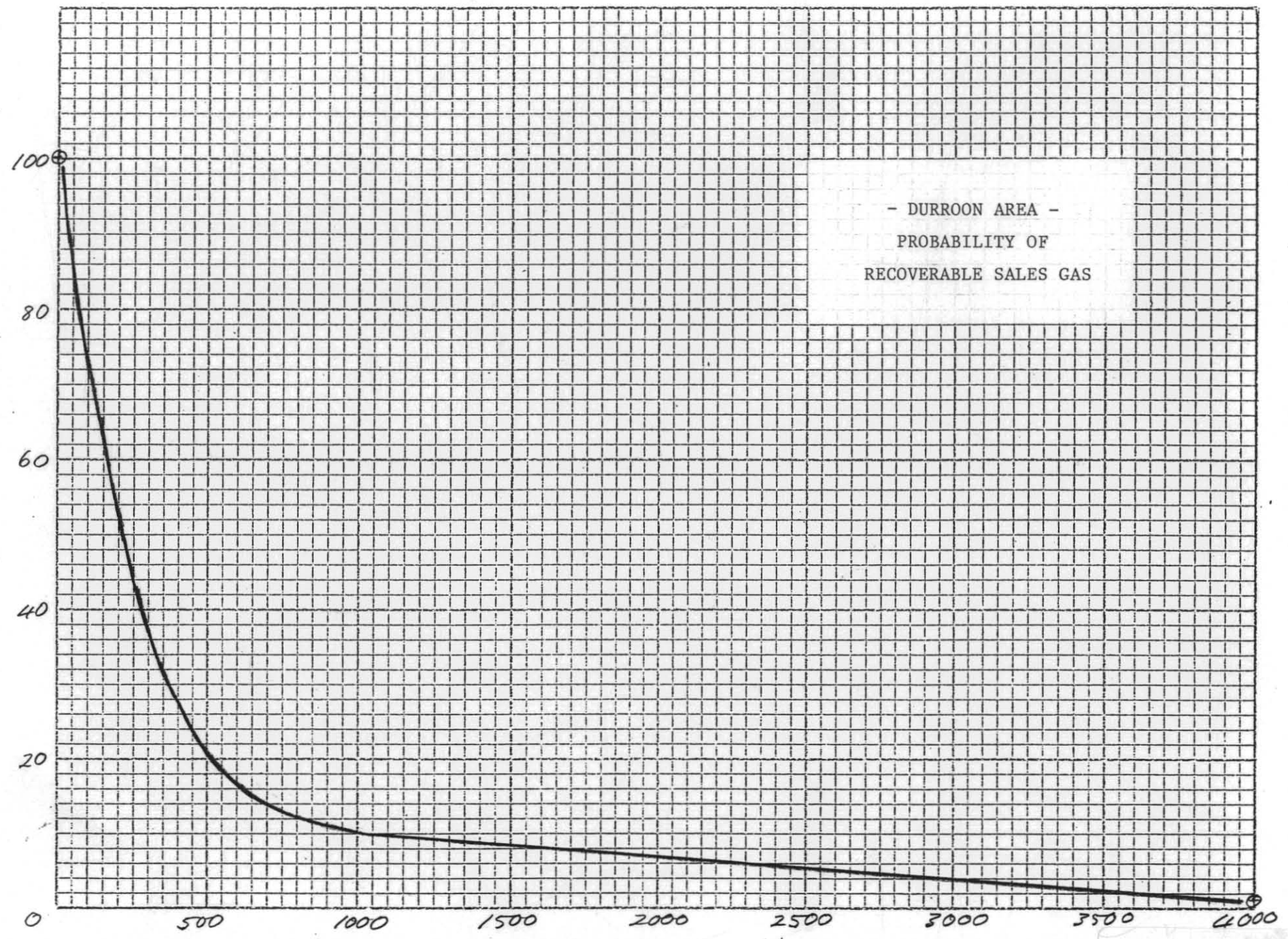
Top Eastern View
OVC

L. balmei
GUC

M. diversus UNCONFORMITY

5 cm





499083

Figure 56.

Billions of Cubic Feet of Gas

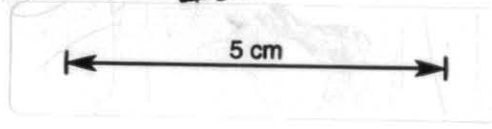
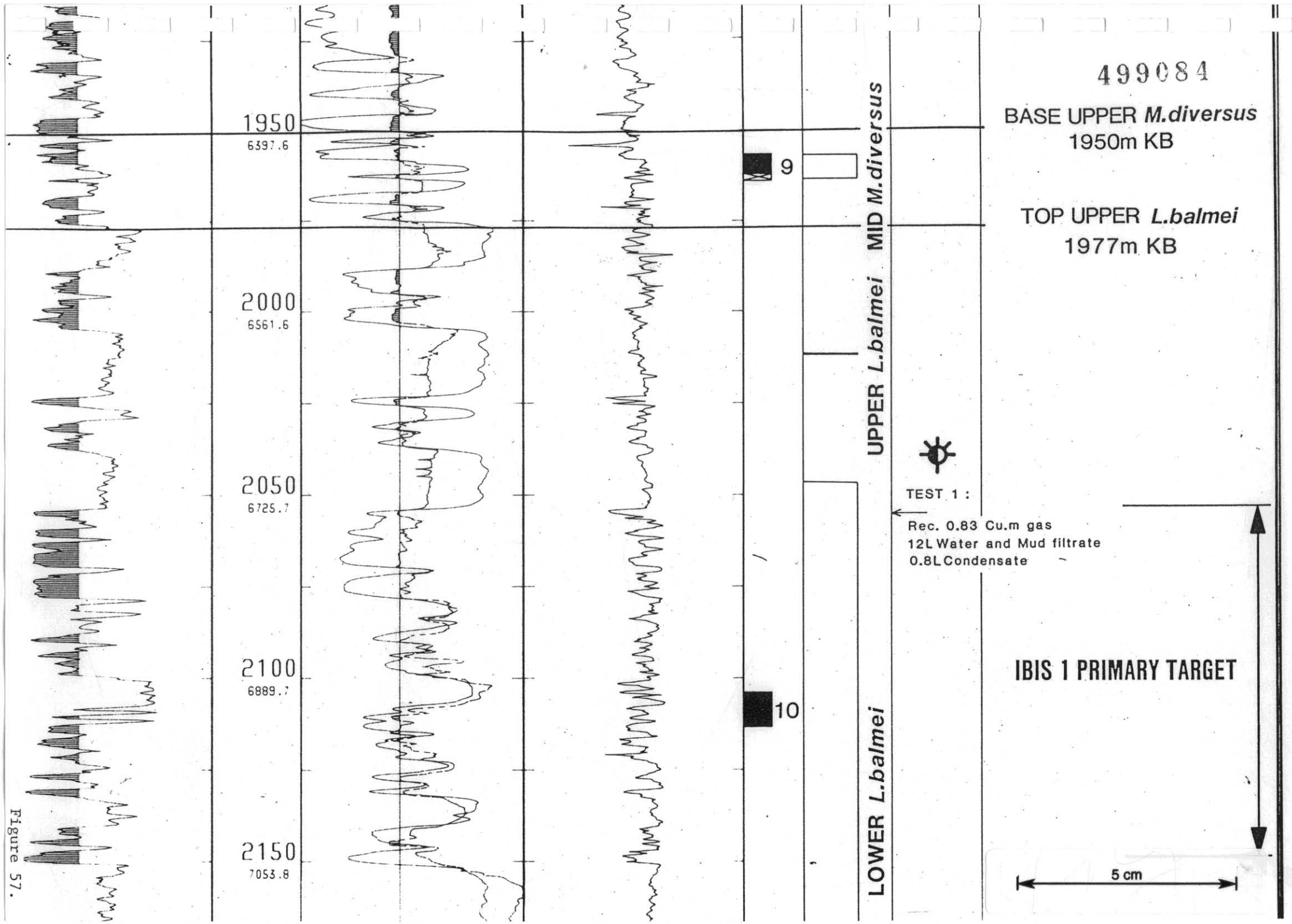


Figure 57.



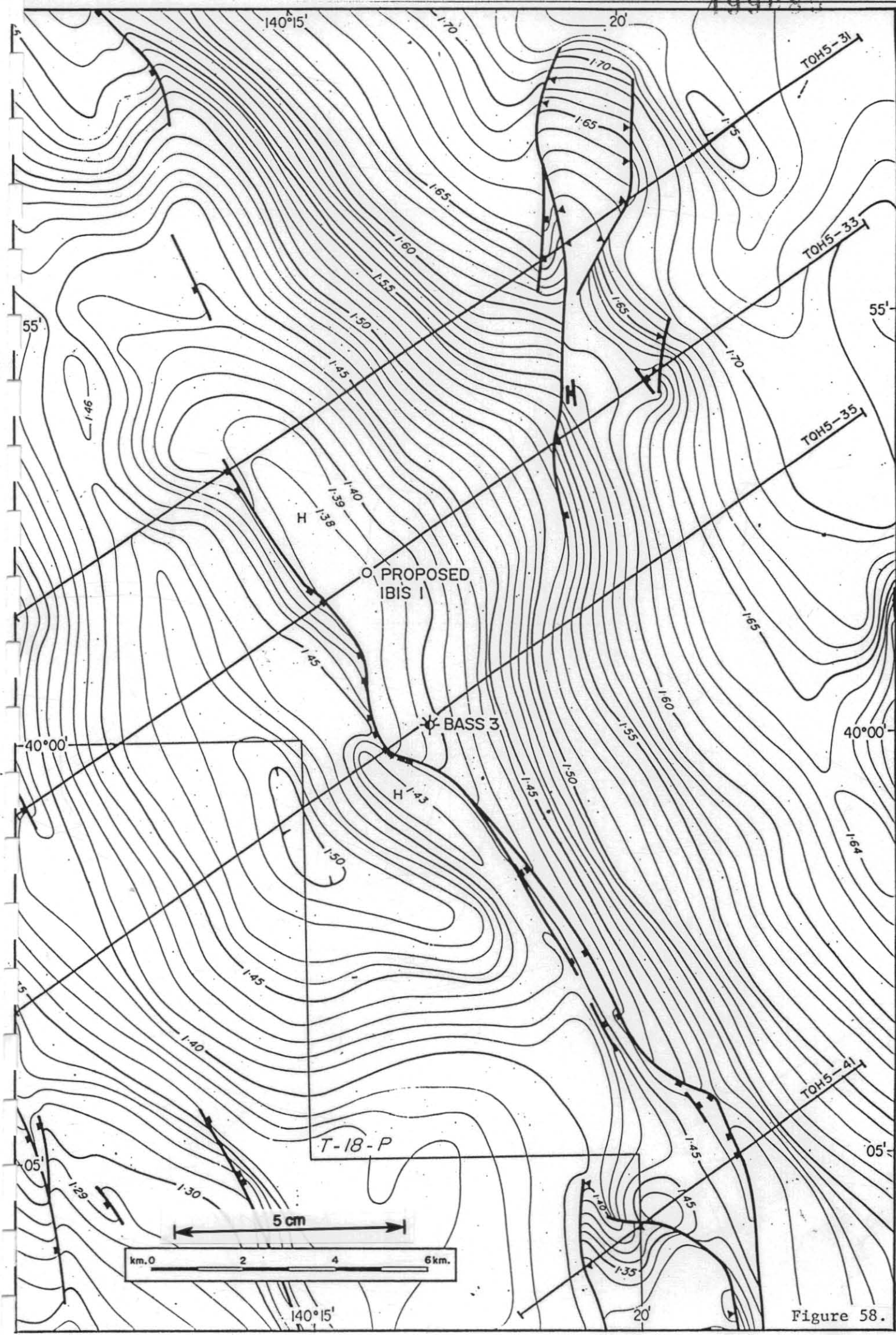


Figure 58.

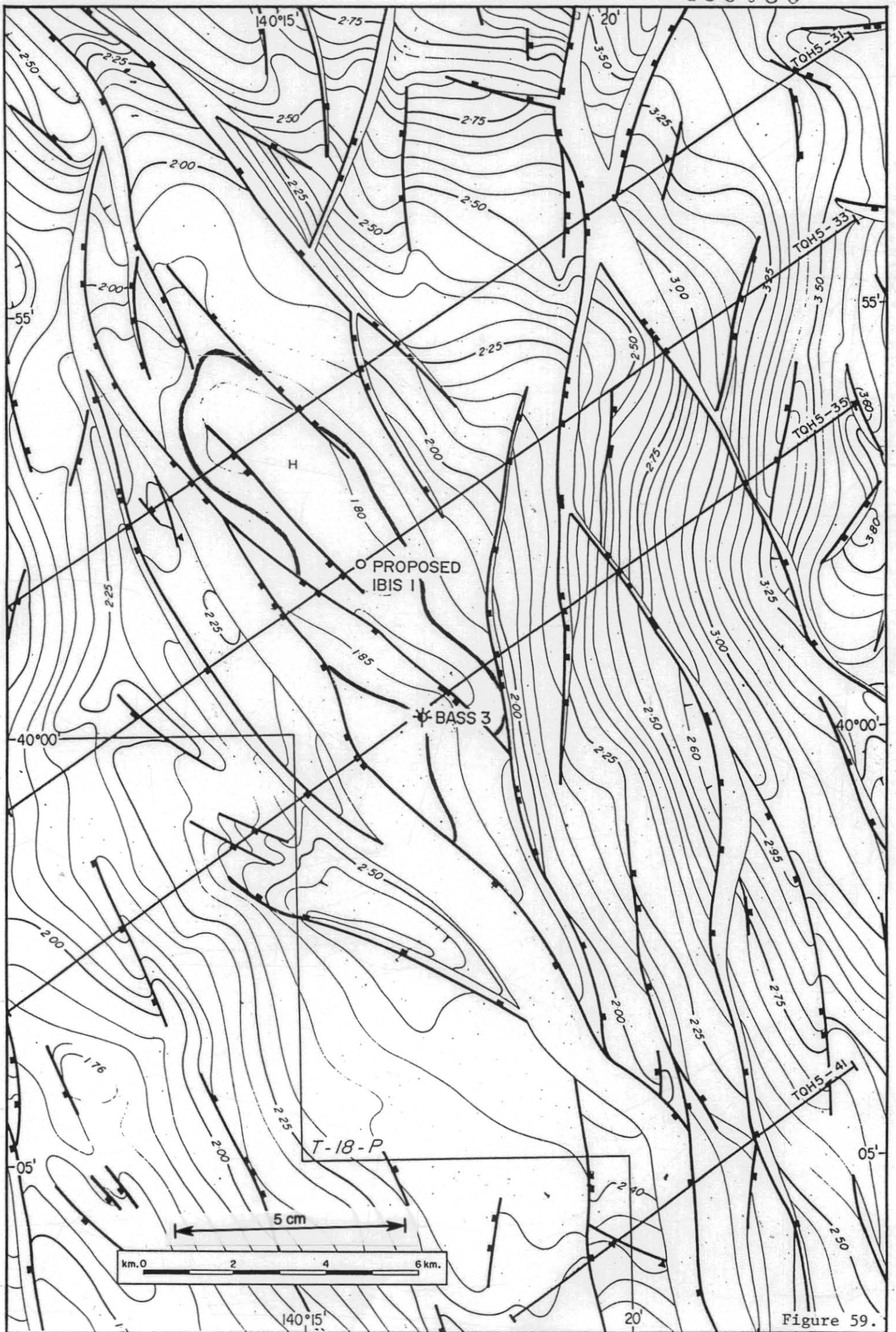
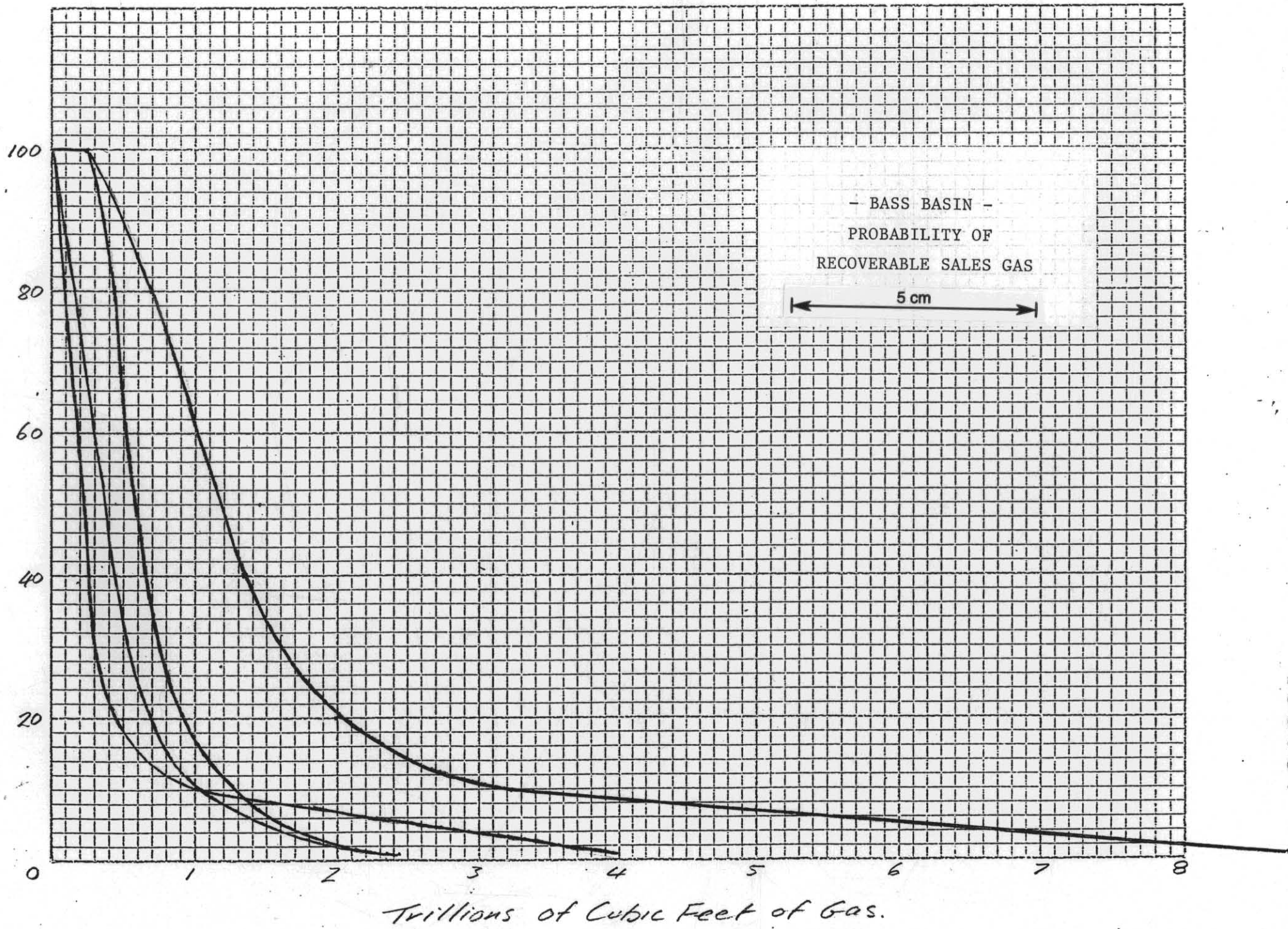


Figure 59.

Probability (%)

Figure 60.



499087